

Electronic Thesis and Dissertation Repository

4-23-2015 12:00 AM

Investigating the role of ephrins and their receptors in mouse folliculogenesis and ovulation

Adrian Buensuceso
The University of Western Ontario

Supervisor
Dr. Bonnie Deroo
The University of Western Ontario

Graduate Program in Biochemistry
A thesis submitted in partial fulfillment of the requirements for the degree in Doctor of Philosophy
© Adrian Buensuceso 2015

Follow this and additional works at: <https://ir.lib.uwo.ca/etd>



Part of the [Endocrinology Commons](#)

Recommended Citation

Buensuceso, Adrian, "Investigating the role of ephrins and their receptors in mouse folliculogenesis and ovulation" (2015). *Electronic Thesis and Dissertation Repository*. 2780.
<https://ir.lib.uwo.ca/etd/2780>

This Dissertation/Thesis is brought to you for free and open access by Scholarship@Western. It has been accepted for inclusion in Electronic Thesis and Dissertation Repository by an authorized administrator of Scholarship@Western. For more information, please contact wlsadmin@uwo.ca.

INVESTIGATING THE ROLE OF EPHRINS AND THEIR RECEPTORS IN
MOUSE FOLLICULOGENESIS AND OVULATION

(Thesis format: Integrated-Article)

by

Adrian Vincent Carlos Buensuceso

Graduate Program in Biochemistry

A thesis submitted in partial fulfillment
of the requirements for the degree of
Doctor of Philosophy

The School of Graduate and Postdoctoral Studies
The University of Western Ontario
London, Ontario, Canada

© Adrian Buensuceso 2015

Abstract

Follicle stimulating hormone (FSH) promotes granulosa cell (GC) proliferation, differentiation, and steroidogenesis. This series of events is critical for female fertility, and culminates in the formation of mature follicles responsive to the surge of luteinizing hormone (LH) that triggers ovulation. Ephrins (*Efn* genes) and Eph receptors (*Eph* genes) are membrane-associated signaling molecules that mediate communication at sites of cell-cell contact, and have been extensively studied in the context of embryonic development. The published literature contains several reports of ovarian *Eph* and *Efn* expression, although their precise roles in the ovary are unknown. Dysregulation of *Efna5* in GCs of the subfertile *Esr2*^{-/-} mouse suggests a role for Eph-ephrin signaling in ovarian function. We sought to investigate Eph receptors and ephrins in the mouse ovary using gonadotropin-stimulated animal models and cultured GCs. We identified several *Efn* and *Eph* genes for which expression is enhanced in GCs of the gonadotropin-stimulated mouse. Furthermore, we determined that cultured GCs stimulated with recombinant ephrin-A5 or EphA5 exhibit reduced cell spreading or adhesion, respectively, indicating a cell-autonomous response to Eph-ephrin stimulation. In order to ascertain the importance of ephrin-A5 in female fertility, we performed a reproductive assessment of females lacking *Efna5*, the sole ephrin-encoding gene upregulated by FSH in GCs. *Efna5*^{-/-} females are subfertile and exhibit an impaired response to LH, displaying attenuated ovulatory potential, reduced ovarian expression of *Pgr*, *Ptgs2*, and *Adamts4*, as well as abnormal follicle rupture. We also found an increased incidence of multi-oocyte follicles in adult, but not juvenile, *Efna5*^{-/-} females, indicating follicle merging. Finally, we determined that the mouse genomic region upstream of *Epha5* is transcriptionally activated by cAMP in a protein kinase A-dependent manner. Transcriptional activation of *Efna5*, *Epha3*, *Epha5*, *Epha8*, and *Ephb2* is reduced in GCs of eCG-treated *Esr2*^{-/-} females, which exhibit impaired cAMP production. These results suggest that cAMP is a novel transcriptional regulator for several *Eph* and *Efn* genes. Our findings establish a place for ephrins and their receptors within the current model of gonadotropin-dependent follicle growth and ovulation, and identify cAMP as a novel transcriptional regulator of *Epha5* and possibly other *Efn* and *Eph* genes.

Keywords

Eph receptor, ephrin, mouse, granulosa cell, follicle, ovary, folliculogenesis, ovulation, follicle rupture, gonadotropin

Co-authorship statement

Chapter 2: Buensuceso AV, Deroo BJ. The ephrin signaling pathway regulates morphology and adhesion of mouse granulosa cells in vitro. *Biol Reprod.* 2013;88(1):25. Dr. Bonnie Deroo conceived the project and co-wrote the manuscript.

Chapter 3: Dr. Alexander Son and Dr. Renping Zhou (Rutgers University, NJ, USA) provided *Efna5^{+/+}* and *Efna5^{-/-}* ovaries used for multi-oocyte follicle counts as well as founder mice for our mouse colony. Marilène Paquet performed histological examination of *Efna5^{+/+}* and *Efna5^{-/-}* ovaries. Benjamin M. Withers performed counts of follicles containing expanded COCs and corpora lutea, and performed histological archiving. Dr. Bonnie Deroo conceived the project and co-wrote the manuscript which was submitted to *Endocrinology*, ID# EN-15-1216.

Chapter 4: Erin Parker conducted genotyping for some *Esr2^{+/+}* and *Esr2^{-/-}* mice. Dr. Bonnie Deroo conceived the project.

Acknowledgements

First, I would like to thank my supervisor and mentor, Dr. Bonnie Deroo, for her excellent mentorship. She has guided my development as a scientist, providing me with constructive criticism and encouragement all along the way. She has always made time for me, and has built a research environment where I could flourish. I enjoy science now more than ever, and I credit her with that.

I would like to thank my supervisory committee members, Dr. Gabriel DiMattia and Dr. Eric Ball. Their guidance has played a major role in the development of my research.

I would also like to acknowledge my colleagues in the Deroo Lab: Caitie O’Flynn, Ola Carrier, and Dr. Macarena Pampillo. I value their insight and advice, and have very much enjoyed working with them. Furthermore, Dr. Gabriel DiMattia, Dr. Trevor Shepherd, Dr. Tom Drysdale, and Dr. Chris Pin, as well as their trainees and technicians, have given me valuable advice during our big group lab meetings. Many thanks as well to Robert Gauthier and Penny Smithers-Fortnum for helping to care for our mice.

Lastly, I would like to express my appreciation to my colleagues in the Victoria Research Labs and London Cancer Research Centre: Mateusz Rytelowski, Jessica Tong, Colin Way, Dr. Saman Maleki Vareki, Rene Figueredo, Dr. Julio Masabanda, and Dr. Pete Ferguson.

These people have all helped me to grow as a scientist and as a person during my time as a graduate student.

Ethics Approval

Experiments were performed in compliance with the guidelines set by the Canadian Council for Animal Care, and the policies and procedures approved by the University of Western Ontario Council on Animal Care (Protocol Number: 2008-042).

Table of Contents

Abstract.....	ii
Keywords	iii
Co-authorship statement	iv
Acknowledgements.....	v
Ethics Approval	vi
Table of Contents.....	vii
List of Figures	xiv
List of Tables	xvi
List of Abbreviations	xvii
1 Chapter 1: Introduction	1
1.1 Stages of Ovarian Follicle Growth.....	1
1.1.1 Introduction to Folliculogenesis	1
1.1.2 Formation of primordial follicles.....	1
1.1.3 Follicle-stimulating hormone-independent follicle growth	2
1.1.4 FSH-dependent follicle growth.....	3
1.1.5 LH-dependent oocyte maturation, cumulus expansion, ovulation, and corpus luteum formation	4
1.2 The hypothalamic-pituitary-gonadal axis.....	10
1.3 Eph receptors and Ephrins.....	12
1.3.1 Overview.....	12
1.3.2 Ephrins	14
1.3.3 Eph receptors	15
1.3.4 Initiation of Eph-Ephrin Signaling.....	17

1.3.5	Eph-ephrin Signal Transduction	17
1.3.6	Termination of Eph-ephrin Signaling	19
1.4	Rationale.....	21
1.5	Hypothesis	22
1.6	Objectives.....	22
1.7	Bibliography.....	23
2	Chapter 2: The ephrin signaling pathway regulates morphology and adhesion of mouse granulosa cells in vitro.....	33
2.1	Introduction	33
2.2	Materials and Methods	37
2.2.1	Cell Culture.....	37
2.2.2	Mice and Treatments.....	37
2.2.3	Isolation of GCs	37
2.2.4	RNA Isolation and qRT-PCR	38
2.2.5	Immunofluorescence.....	41
2.2.6	Cell Spreading and Adhesion Assays	41
2.2.7	Human Phospho-Kinase Array	43
2.2.8	Immunoblot Analysis: Beta-Catenin.....	44
2.3	Results	45
2.3.1	Identification of FSH-Regulated Ephrin Ligands and Eph Receptors in Mouse GCs	45
2.3.2	FSH and cAMP Regulate <i>Efna5</i> and <i>Epha5</i> Expression in a Rat GC Line	49
2.3.3	Localization of EFNA5 and EPHA5 in the Mouse Ovary.....	51
2.3.4	Inhibition of GC Spreading by EFNA5/Fc	55
2.3.5	Inhibition of GC-Substrate Adhesion by EPHA5.....	56

2.3.6	Beta-Catenin Is a Downstream Target of EFNA5-Induced Signaling in GCs	61
2.4	Discussion	63
2.4.1	Eph-Ephrin Gene Expression Is Regulated by FSH via the cAMP/PKA Pathway in GCs.....	63
2.4.2	EFNA5 and EPHA5 Localization During Folliculogenesis	64
2.4.3	EFNA5 Inhibits Spreading and Increases Rounding of GCs.....	65
2.4.4	EPHA5 Inhibits Adhesion of GCs	66
2.4.5	EFNA5 Reduces Beta-Catenin Protein Levels in GCs	68
2.5	Bibliography.....	70
3	Chapter 3: Ephrin-A5 is required for optimal fertility and a complete ovulatory response to gonadotropins in the mouse	75
3.1	Introduction	75
3.2	Materials and Methods.....	76
3.2.1	Mice and treatments	76
3.2.2	Continuous breeding study	77
3.2.3	Assessment of ovulatory potential in response to gonadotropin treatment	77
3.2.4	Assessment of serum steroid levels	77
3.2.5	RNA isolation and quantitative RT-PCR.....	78
3.2.6	Fixation, sectioning, and preparation of ovaries for histological examination	81
3.2.7	Histological quantitation of COCs, corpora lutea, and multi-oocyte follicles	81
3.3	Results	81
3.3.1	Ephrin-A5 is required for normal female fertility.....	81

3.3.2	<i>Efna5</i> ^{-/-} females ovulate fewer oocytes than controls	82
3.3.3	Serum estradiol and progesterone levels are unaffected by loss of ephrin-A5	82
3.3.4	Ovary to body weight ratio is unaffected by loss of ephrin-A5.....	82
3.3.5	Ovarian gene expression is altered in <i>Efna5</i> ^{-/-} females after gonadotropin stimulation	86
3.3.6	<i>Efna5</i> ^{-/-} ovaries exhibit increased numbers of expanded COCs after gonadotropin stimulation	87
3.3.7	Abnormal follicle rupture, hemorrhaging, and fibrin thrombus formation in <i>Efna5</i> ^{-/-} ovaries after gonadotropin stimulation	87
3.3.8	Increased number of multi-oocyte follicles in adult <i>Efna5</i> ^{-/-} mice	88
3.4	Discussion	95
3.4.1	<i>Efna5</i> ^{-/-} females produce smaller litters and release fewer oocytes than controls	95
3.4.2	<i>Efna5</i> ^{-/-} females exhibit an attenuated response to hCG but not eCG	95
3.4.3	<i>Efna5</i> ^{-/-} ovaries exhibit numerous histological abnormalities.....	95
3.4.4	Progesterone receptor (<i>Pgr</i>).....	96
3.4.5	Prostaglandin-endoperoxide synthase 2 (<i>Ptgs2</i>).....	96
3.4.6	ADAM metallopeptidase with thrombospondin type 1 motif, 4 (<i>Adamts4</i>)	97
3.4.7	Relating LH, <i>Pgr</i> , <i>Ptgs2</i> , and <i>Adamts4</i> to <i>Efna5</i> ^{-/-} reproductive and ovarian defects	97
3.4.8	Hemorrhaging, fibrin thrombi, and GCs in blood vessel lumina.....	98
3.4.9	How does loss of ephrin-A5 result in reduced expression of <i>Pgr</i> , <i>Ptgs2</i> , and <i>Adamts4</i> ?	99
3.4.10	<i>Efna5</i> is one of many neuronal guidance genes expressed in the mouse ovary	101

3.4.11	Experimental Considerations	101
3.4.12	Unexpected findings	102
3.5	Conclusion.....	102
3.6	Bibliography.....	103
4	Chapter 4: Cyclic AMP stimulates PKA-dependent transcriptional activation of the mouse <i>Epha5</i> upstream genomic region in the KGN granulosa cell line	107
4.1	Introduction	107
4.2	Materials and Methods.....	110
4.2.1	Cell culture and transfections.....	110
4.2.2	Mice	111
4.2.3	Isolation of GCs	111
4.2.4	RNA isolation and qRT-PCR.....	112
4.2.5	Immunoblotting.....	114
4.2.6	Generation of the <i>Epha5</i> -Luc luciferase reporter plasmid.....	114
4.2.7	Generation of the mut <i>Epha5</i> -Luc luciferase reporter plasmid by site-directed mutagenesis.....	115
4.2.8	Dual-luciferase assays.....	115
4.3	Results	115
4.3.1	Induction of FSH-responsive <i>Efn</i> and <i>Eph</i> genes is reduced in GCs of <i>Esr2</i> ^{-/-} mice	115
4.3.2	<i>Epha5</i> -Luc is transcriptionally activated by cAMP in KGN cells	119
4.3.3	cAMP-stimulated activation of <i>Epha5</i> -Luc is reduced by co-treatment with H-89	119
4.4	Discussion	124

4.4.1	hCG-stimulated induction of <i>Efna5</i> , <i>Epha3</i> , <i>Epha5</i> , and <i>Ephb2</i> is significantly reduced in GCs of <i>Esr2^{-/-}</i> mice	124
4.4.2	The 1589 bp region upstream of <i>Epha5</i> is transcriptionally activated by cAMP in a PKA-dependent manner in KGN cells	125
4.4.3	Conclusion	128
4.5	Bibliography.....	129
5	Chapter 5: Discussion.....	133
5.1	Summary	133
5.2	Expression of <i>Efna5</i> , <i>Epha3</i> , <i>Epha5</i> , <i>Epha8</i> , and <i>Ephb2</i> is enhanced in GCs of mice stimulated with equine chorionic gonadotropin (FSH).....	134
5.3	<i>Efna5</i> is required for a complete response to human chorionic gonadotropin (LH)	135
5.3.1	Morphological and adhesive responses in the context of the <i>Efna5^{-/-}</i> phenotype	135
5.3.2	A possible role for <i>Efna5</i> in follicle atresia.....	137
5.3.3	Putative Eph-ephrin signaling mechanisms in GCs.....	138
5.3.4	A potential link between abnormal follicle rupture and multi-oocyte follicle formation	142
5.3.5	cAMP-dependent pathways regulate <i>Epha5</i> expression in GCs.....	143
5.4	Experimental Considerations	144
5.4.1	Germline <i>Efna5^{-/-}</i> mouse model.....	144
5.5	Future Directions.....	145
5.5.1	Delineating Eph-ephrin signaling pathways in GCs.....	145
5.6	Conclusion.....	145
5.7	Bibliography.....	148
6	Appendix	152

6.1	Supplementary Material, Chapter 2	152
6.2	Supplementary Material, Chapter 3	161
	Curriculum Vitae	163

List of Figures

Figure 1-1: Histology of an antral follicle.	8
Figure 1-2: Stages of ovarian follicle growth.	9
Figure 1-3: Ephrin and Eph receptor domains.	16
Figure 2-1: Expression of a subset of ephrin ligands and Eph receptors is stimulated by FSH in mouse GCs.	47
Figure 2-2: FSH and forskolin increase <i>Efna5</i> and <i>Epha5</i> mRNA levels in the immortalized rat GC line GFSHR-17.	50
Figure 2-3: Localization of EFNA5 and EPHA5 in the mouse ovary.	53
Figure 2-4: EFNA5 inhibits spreading and induces rounding of immortalized rat GCs. .	57
Figure 2-5: EFNA5 inhibits spreading and increases rounding of primary mouse GCs. .	58
Figure 2-6: EPHA5 receptor inhibits adhesion of immortalized rat GCs to cell culture surfaces.	59
Figure 2-7: EPHA5 inhibits substrate adhesion of mouse primary GCs.	60
Figure 2-8: Beta-catenin protein levels in GFSHR-17 cells are reduced in response to EFNA5.	62
Figure 3-1: Reproductive assessment of <i>Efna5</i> ^{-/-} females.	83
Figure 3-2: Serum estradiol and progesterone concentrations are unaffected by loss of ephrin-A5.	84
Figure 3-3: Ovary/body weight ratio is normal in <i>Efna5</i> ^{-/-} females at PND 23, 60, and 120.	85
Figure 3-4: hCG-stimulated ovarian expression of <i>Pgr</i> , <i>Ptgs2</i> , and <i>Adamts4</i> is attenuated in <i>Efna5</i> ^{-/-} mice.	89
Figure 3-5: Follicles containing expanded COCs and retained oocytes are more numerous in superovulated <i>Efna5</i> ^{-/-} mice.	91

Figure 3-6: Superovulated <i>Efna5</i> ^{-/-} mice exhibit non-apical follicle rupture and an increased incidence of oocytes trapped within luteinized follicles.....	92
Figure 3-7: <i>Efna5</i> ^{-/-} adult females exhibit more multi-oocyte follicles than juveniles.	94
Figure 4-1: Induction of FSH-responsive <i>Efn</i> and <i>Eph</i> genes by eCG is significantly reduced in <i>Esr2</i> ^{-/-} GCs.....	117
Figure 4-2: A putative consensus CRE half-site upstream of <i>Epha5</i> is conserved across several species.....	120
Figure 4-3: Generation of the Epha5-Luc luciferase reporter construct.	121
Figure 4-4: Endogenous <i>EPHA5</i> is induced by FSH, and Epha5-Luc is activated by dbcAMP in KGN cells.....	122
Figure 4-5: Activation of Epha5-Luc by dibutyryl-cAMP is reduced by co-treatment with the PKA inhibitor H-89.....	123
Figure 5-1: Putative model for Eph-ephrin involvement in gonadotropin-stimulated gene expression in mouse granulosa cells.	147
Supplemental Figure 6-1: Screening study to determine mRNA levels of all known mouse ephrin (<i>Efn</i>) genes in granulosa cells isolated from immature female mice in response to FSH.	152
Supplemental Figure 6-2: Screening study to determine mRNA levels of all known mouse ephrin receptor (<i>Eph</i>) genes in granulosa cells isolated from immature female mice in response to FSH.	153
Supplemental Figure 6-3: Proteome Profiler Phospho-Kinase Arrays.	154
Supplemental Figure 6-4: EPHRIN-A5 protein levels are lower in granulosa cells of <i>Esr2</i> ^{-/-} mice compared to <i>Esr2</i> ^{+/+}	161
Supplemental Figure 6-5: Stimulation of KGN cells transfected with Epha5-Luc and mutEpha5-Luc with dibutyryl cAMP.	162

List of Tables

Table 2-1: The Ephrin receptors and their ephrin ligand specificities.....	35
Table 2-2: Primer sequences used for quantitative RT-PCR.....	39
Table 3-1: Primer sequences used for quantitative RT-PCR.....	79
Table 3-2: Taqman probe sets used for quantitative RT-PCR in Figure 3-4.....	80
Table 4-1: Primers used for qRT-PCR in Figure 4-1 and Figure 4-4.....	113
Supplemental Table 6-1: Human Phospho-Kinase Array capture antibodies	155
Supplemental Table 6-2: Phosphorylation of intracellular kinase targets in response to ephrinA5-Fc, 15 min post-seeding.....	157
Supplemental Table 6-3: Phosphorylation of intracellular kinase targets in response to ephrinA5-Fc, 20 min post-seeding.....	159

List of Abbreviations

%	per cent
°C	degrees celsius
µg	micrograms
µL	microlitres
µM	micromolar
<i>Adamts1</i>	gene encoding <u>a disintegrin and metalloproteinase with thrombospondin-like repeats 1</u>
<i>Adamts4</i>	gene encoding <u>a disintegrin and metalloproteinase with thrombospondin-like repeats 4</u>
ANOVA	analysis of variance
ATP	adenosine triphosphate
bp	base pairs
cAMP	cyclic adenosine monophosphate
<i>Cbfl</i>	Gene encoding Chick brain factor 1
CBL	Cbl proto-oncogene, E3 ubiquitin protein ligase protein
cDNA	complementary deoxyribonucleic acid
CK	casein kinase protein
CL	corpus luteum
CO ₂	carbon dioxide
COC	cumulus oocyte complex
CREB	cAMP response element-binding protein
CRK	V-Crk Avian Sarcoma Virus CT10 Oncogene Homolog protein
CYP11A1	cytochrome P450, family 11, subfamily A, polypeptide 1 protein
CYP17A1	cytochrome P450, family 17, subfamily A, polypeptide 1 protein
CYP19A1	cytochrome P450, family 19, subfamily A, polypeptide 1 protein

d	days
DAPI	4',6-diamidino-2-phenylindole
dbcAMP	dibutyryl cyclic adenosine monophosphate
DMEM	Dulbecco's Modified Eagle's Medium
DMSO	dimethyl sulfoxide
DNA	deoxyribonucleic acid
DNaseI	deoxyribonuclease I
eCG	equine chorionic gonadotropin
EGF	epidermal growth factor
<i>Efna5</i>	gene encoding ephrin-A5
<i>Epha3</i>	gene encoding Eph receptor A3
<i>Epha5</i>	gene encoding Eph receptor A5
<i>Epha8</i>	gene encoding Eph receptor A8
<i>Ephb2</i>	gene encoding Eph receptor B2
EphA	Eph receptor A protein
EphB	Eph receptor B protein
Ephrin-A	Ephrin A protein
Ephrin-B	Ephrin B protein
ERbeta	estrogen receptor beta
ERK	extracellular regulated kinase protein
FGF	fibroblast growth factor
FN1	fibronectin 1 protein
<i>Foxl2</i>	gene encoding forkhead box L2
FSH	follicle-stimulating hormone protein
FSHR	follicle-stimulating hormone receptor protein
GC	granulosa cell
GDF9	growth differentiation factor 9 protein
GNRH	gonadotropin-releasing hormone protein
GNRHR	gonadotropin-releasing hormone receptor protein
GPI	glycosylphosphatidylinositol
GSK3	glycogen synthase kinase 3 protein

h	hours
<i>Has2</i>	gene encoding hyaluronan synthase 2
hCG	human chorionic gonadotropin
HSD3B	hydroxy-delta-5-steroid dehydrogenase, 3 beta- and steroid delta-isomerase protein
IgG	immunoglobulin G
IOI	interovulatory interval
IU	international units
JM	juxtamembrane
KD	kinase domain
kDa	kiloDaltons
KISS1	kisspeptin protein
<i>Kiss1r</i>	gene encoding kisspeptin receptor
LBD	ligand-binding domain
LEF	Lymphoid enhancer-binding factor 1
<i>Lhcgr</i>	Gene encoding luteinizing hormone receptor
LH	luteinizing hormone
LHR	luteinizing hormone receptor
Luc	luciferase
<i>Mapk1</i>	gene encoding mitogen-associated kinase 1 protein (ERK2)
<i>Mapk3</i>	gene encoding mitogen-associated kinase 3 protein (ERK1)
mg	milligrams
min	minutes
mm	millimeters
mM	millimolar
MMP	matrix metalloproteinase
MOF	multi-oocyte follicle
mRNA	messenger ribonucleic acid
n	sample size
NaCl	sodium chloride
NCK4	NCK adaptor protein 2 protein

ng	nanograms
NGFR	nerve growth factor receptor protein
NTRK2	neurotrophic tyrosine kinase, receptor, type 2 protein
p	p-value
PBS	phosphate-buffered saline
PCR	polymerase chain reaction
PDZ	postsynaptic density protein 95/disks large homolog 4/zona occludens protein 1
pg	picogram
PGC	primordial germ cell
PI3K	phosphoinositide 3-kinase
PKA	protein kinase A
PKB	protein kinase B
PND	post-natal day
<i>Pgr</i>	gene encoding progesterone receptor
<i>Pten</i>	gene encoding Phosphatase and tensin homolog
<i>Ptgs2</i>	gene encoding prostaglandin synthase 2
<i>Ptx3</i>	gene encoding pentraxin 3
qRT-PCR	quantitative reverse transcription polymerase chain reaction
RAC1	ras-related C3 botulinum toxin substrate 1
RAPGEF	Rap Guanine Nucleotide Exchange Factor
RBD	receptor-binding domain
RET	ret proto-oncogene protein
RGS3	regulator of G-protein signaling 3 protein
RHOA	Ras homolog family member A protein
RNA	ribonucleic acid
<i>Rpl7</i>	gene encoding Ribosomal protein L7
rt	room temperature
RTK	receptor tyrosine kinase
SAM	sterile alpha motif

sc	sub-cutaneous
SDS	sodium dodecyl sulfate
SEM	standard error of the mean
SHC	Src homology 2 domain containing
SMAD	Mothers against decapentaplegic homolog protein
SRC	v-src avian sarcoma (Schmidt-Ruppin A-2) viral oncogene homolog
TNFAIP6	tumor necrosis factor-inducible gene 6 protein
UTR	untranslated region
V	volt
v/v	volume/volume
VCAN	versican protein
VEGF	vascular endothelial growth factor

1 Chapter 1: Introduction

1.1 Stages of Ovarian Follicle Growth

1.1.1 Introduction to Folliculogenesis

In female mammals, the ovary has two primary functions. The first is the synthesis of steroid hormones such as testosterone, 17β -estradiol, and progesterone. These hormones are necessary for the development of secondary sex characteristics, communication with the neuroendocrine components of the reproductive system, and communication with the uterus to induce changes that are necessary for establishing and maintaining pregnancy. The second function is the ovulation of a healthy and fertilizable oocyte. Both functions are performed by the functional unit of the ovary, the follicle. The ovarian follicle is an aggregate unit of a germ cell and its associated somatic cells, consisting of an oocyte, surrounded by granulosa cells (GCs), which are in turn surrounded by a basement membrane and thecal cells (**Figure 1-1**). The formation and maturation of the follicle, known as folliculogenesis, begins in the developing embryo. This process culminates in the generation of one or more mature follicles that are competent to ovulate and produce a fertilizable oocyte.

1.1.2 Formation of primordial follicles

In female mammals, folliculogenesis begins during embryonic development. Within the embryo, mitotic division of primordial germ cells (PGCs) gives rise to clusters of germ cells, known as “oocyte nests” (1). Prior to birth in humans and at birth in rodents (2), these clusters break down into individual germ cells called oogonia. Oogonia are then enclosed by a single layer of flat pre-granulosa cells derived from the ovarian stroma, forming a primordial follicle (3) (**Figure 1-2**). The mechanisms underlying these events are not fully understood, but loss-of-function studies have identified some factors that are required for this process (4). After formation, primordial follicles remain dormant and will not mature until they are activated at puberty. It is thought that this pool of primordial follicles will provide all of the oocytes required for the duration of the female’s reproductive life (5). However, some evidence indicates that adult mouse and human ovaries contain small numbers of stem cells that have the capacity to give rise to

oocytes in culture and *in vivo* (6). Whether this population of stem cells contributes to and/or replenishes the pool of primordial follicles in adults is not known.

1.1.3 Follicle-stimulating hormone-independent follicle growth

Once a female mammal reaches sexual maturity, cohorts of quiescent primordial follicles are selected for activation, acquiring the potential to grow, mature, and ovulate. The current body of evidence suggests that primordial follicles are maintained in a state of dormancy by inhibitory pathways within the follicle. One primordial follicle may remain dormant while the follicle adjacent to it is recruited for activation, suggesting inhibition by intra-ovarian factors (7). Deletion of the *Amh* gene in mice, which encodes the anti-mullerian hormone, results in decreased numbers of primordial follicles and increased numbers of growing follicles (8). Furthermore, oocyte-specific deletion of the phosphoinositide 3-kinase (PI3K) pathway inhibitor gene *Pten* in mice results in recruitment and activation of all primordial follicles, depletion of the ovarian reserve and infertility (9). Therefore, recruitment of primordial follicles likely involves relief of these and possibly other pathways that suppress activation.

Once a primordial follicle has been recruited, a series of events is initiated that results in the formation of primary and then secondary follicles (**Figure 1-2**), which occurs independently of gonadotropins. This is supported by histological observations in ovaries from *Fshb*^{-/-} mice, which lack the follicle-stimulating hormone (FSH) beta subunit and therefore do not produce FSH. Ovaries from these mice contain follicles at the primordial, primary, and secondary stages, indicating that FSH is not required for growth up to the secondary stage (10). During the transition from the primordial to the primary stage, the morphology of the single layer of pre-granulosa cells changes from flat to cuboidal, followed by *Foxl2* (forkhead box L2)-dependent granulosa cell proliferation (11). Progression to the secondary stage involves continued proliferation of GCs and recruitment of cells from the ovarian stroma to the outer periphery of the follicle. These cells differentiate into thecal cells (12). This stage of growth is dependent on GDF9 (growth differentiation factor 9), an oocyte-secreted protein and member of the TGFB (transforming growth factor beta) family. The requirement for GDF9 is supported by the observations that *Gdf9*^{-/-} female mice are infertile, have ovaries that contain only follicles

at the primordial and primary stages (13), and lack markers for thecal cells (14). Importantly, it is generally accepted that the secondary follicle stage is also the stage at which GCs begin to express *Fshr*, which encodes the FSH receptor (FSHR) (15), although some evidence suggests that primordial follicles respond to FSH (16). This permits the follicle to acquire responsiveness to FSH, the gonadotropin that promotes continued follicle growth.

1.1.4 FSH-dependent follicle growth

In contrast to growth of primordial and primary follicles, growth of secondary follicles to the antral stage is dependent on FSH, an idea supported by the observation that ovaries from *Fshb*^{-/-} female mice contain primordial, primary, and secondary follicles but lack antral follicles (10). Acting through FSHR, its cognate G protein coupled receptor in GCs, FSH initiates a number of changes in the secondary follicle, including increased proliferation of GCs, differentiation of GCs into more specialized cell types, increased production of autocrine, paracrine and endocrine messengers, formation of a fluid-filled antrum, and acquisition of responsiveness to LH (17).

As GCs continue to proliferate, they differentiate into two specialized subtypes: mural GCs and cumulus cells. These GC subtypes comprise distinct populations that are spatially segregated and serve different purposes in the follicle. Spatially, they are separated by the formation of a fluid-filled antrum, or cavity. The fluid within the antrum has a composition similar to that of serum, but with much lower concentrations of plasma proteins that have molecular weights greater than 100 kDa (18).

Several layers of mural GCs line the interior periphery of the follicle and are the primary site of estradiol synthesis in the ovary, producing increasing amounts of estradiol as the follicle grows. During early FSH-dependent follicle growth, estradiol output from the follicle is low and has a suppressive effect on hypothalamic GNRH (gonadotropin-releasing hormone) secretion. In this way, GNRH secretion is reduced but pulse frequency is unaltered, resulting in reduced pituitary FSH secretion (19). As follicle growth proceeds, estradiol production rises due to the increasing number of GCs and increased expression of steroidogenic genes (20). In contrast to low serum estradiol

concentration, high concentrations have the effect of increasing GNRH production and frequency, favouring production of LH (21). In addition to estradiol, mural GCs also produce the peptide hormones activin, inhibin, and follistatin, which are members of the TGF β family. These hormones were named based on their effect on FSH production, with activins having a stimulatory effect and inhibins having an inhibitory effect (22). Follistatin, which is present in serum, binds to activins with high affinity (23) and “neutralizes” them by preventing their interaction with activin receptors (24). Ovarian production of inhibins increases during FSH-dependent follicle growth (25), and acts to suppress FSH secretion (26). Therefore, mural GCs are responsible for producing the endocrine messengers that feed back on the hypothalamus and anterior pituitary.

In contrast to mural GCs, cumulus cells surround and are closely associated with the oocyte. Cumulus cells exhibit different patterns of gene expression compared to mural GCs, thought to be caused by a currently unidentified oocyte-secreted factor that establishes opposing gradients of FSH- and SMAD2/3-dependent signaling in the follicle, such that expression of FSH-responsive genes is strong in mural granulosa cells and weak in cumulus cells (27). During FSH-dependent follicle growth, the primary purpose of cumulus cells is to provide nutrients to the oocyte via gap junctions (28). Later in folliculogenesis, cumulus cells play crucial roles in the events leading to ovulation.

1.1.5 LH-dependent oocyte maturation, cumulus expansion, ovulation, and corpus luteum formation

Once the follicle reaches the preovulatory stage, estradiol levels are sufficiently high to trigger an acute release of LH from the anterior pituitary, known as the LH surge. Within the follicle, LH acts primarily on mural GCs, which express high levels of LH receptor (LHR). In cumulus cells, expression of *Lhcgr* is much lower than in mural GCs (29). LH promotes secretion of epidermal growth factor (EGF) and EGF-like factors from mural GCs, which are delivered to cumulus cells via the follicular fluid. These factors, which include amphiregulin, epiregulin, and betacellulin, activate EGF receptors expressed by cumulus cells (30). Therefore, the LH response in cumulus cells is mediated largely by these mural granulosa cell-derived, EGF-like factors. These and other factors

initiate several events that are critical for fertility: resumption of oocyte meiosis, cumulus expansion, follicle rupture, and formation of the corpus luteum.

1.1.5.1 Resumption of meiosis

During primordial follicle formation, oocytes are arrested during meiosis I (31), and resumption only occurs following the LH surge. Meiotic resumption is necessary for the production of a fertilizable oocyte, although the exact mechanism by which meiotic resumption is initiated has not been elucidated. The current body of evidence indicates that follicle-derived factors maintain the oocyte in a state of meiotic arrest. Arrested oocytes removed from the follicle and placed in culture resume meiosis spontaneously, suggesting that a follicle-derived factor inhibits meiotic resumption in oocytes (32,33). Presumably, the LH surge inhibits the production or activity of this factor, resulting in meiotic resumption. While this factor has not been identified, there is evidence suggesting that its action on the oocyte is dependent on GPR3 (G-protein coupled receptor 3) (34-36), since oocytes from mice lacking GPR3 undergo meiotic resumption within antral follicles independently of LH, indicating that oocyte-expressed GPR3 is required for suppression of meiotic resumption (37). In addition, mouse oocytes cultured in the presence of the GPR3 ligands sphingosylphosphorylcholine or sphingosine-1-phosphate exhibit delayed meiotic resumption (38).

1.1.5.2 Cumulus expansion

Cumulus expansion involves the production of an extracellular matrix by the cumulus cells, resulting in increased COC volume (39). This matrix is rich in hyaluronan and hyaluronan-binding proteins including TNFAIP6 (tumor necrosis factor-inducible gene 6 protein) (40), VCAN (versican) (41), as well as laminins and FN1 (fibronectin) (42). Cumulus expansion is critical for ovulation. Pharmacological blockade of hyaluronan precursor synthesis during expansion in mice reduces ovulation and fertility (43). Furthermore, knockout mouse studies have revealed that many genes critical for ovulation are involved in cumulus expansion (44), including *Has2* (hyaluronan synthase 2), *Tnfaip6*, *Ptx3* (pentraxin 3), and *Ptgs2* (Prostaglandin-endoperoxide synthase 2). Cumulus expansion also requires the presence of oocyte-derived factors. Removal of the

oocyte from COCs blocks cumulus expansion in culture (45). More recent evidence suggests that the role of the oocyte in promoting cumulus expansion is dependent on SMAD2/3 signaling in cumulus cells (46). This finding is consistent with evidence indicating that a gradient of SMAD2/3 signaling occurs in GCs of the antral follicle, with SMAD2/3 phosphorylation highest near the oocyte and lowest at the periphery of the follicle near the basement membrane (27). The cumulus matrix has been proposed to facilitate extrusion from the follicle and its capture by oviductal fimbria (47). This idea is supported by evidence indicating an association between cumulus expansion and a transient increase in COC invasiveness and motility, properties that may be necessary for oocyte release from the follicle (48).

1.1.5.3 Follicle rupture

Successful ovulation requires release of the oocyte and its associated somatic cells to the exterior of the follicle, necessitating rupture of the follicle wall at a location adjacent to the exterior periphery of the ovary (the apical follicle surface). Degradation of the ECM at the site of rupture results in the formation of a rounded protuberance known as the stigma, which ruptures and releases the oocyte. This event is mediated by proteases that are expressed in the follicle in response to LH, including members of the MMP (matrix metalloproteinase) and ADAMTS (a disintegrin and metalloproteinase with thrombospondin-like repeats) families. Several members of these families are upregulated during follicle rupture in rhesus macaques, and injection of the dominant follicle with an MMP inhibitor blocks ovulation (49). The observation that multiple proteases are upregulated suggests that all are involved in follicle rupture, however only one protease knockout model has been reported to exhibit a reproductive phenotype. *Adamts1*^{-/-} female mice are subfertile and exhibit reduced ovulation and fertilization rates, indicating that this protease is critical for ovulation (50). Knockout mouse models lacking other LH-induced MMP- and ADAMTS-encoding genes do not exhibit reproductive phenotypes (51-55), suggesting that other proteases may compensate for their loss.

1.1.5.4 Luteinization and formation of the corpus luteum

Following ovulation, the remaining cells of the follicle form a structure known as the corpus luteum (CL). The CL contains two types of steroid-producing luteal cells: those derived from mural GCs (granulosa-luteal cells), and those derived from thecal cells (thecal-luteal cells). Like the parental cells from which these luteal cells arise, they play different roles in the CL. Granulosa-luteal, but not from thecal-luteal cells, exhibit strong immunoreactivity against CYP19A1, suggesting that granulosa-luteal cells are the primary sites of estradiol synthesis in the CL. In the macaque CL, luteal cells derived from thecal cells exhibit strong immunoreactivity against CYP17A1 (cytochrome P450, family 17, subfamily A, polypeptide 1), suggesting that thecal-luteal cells are the primary sites of androgen synthesis. Both luteal cell types exhibited immunoreactivity against CYP11A1 (cytochrome P450, family 11, subfamily A, polypeptide 1) and HSD3B (hydroxy-delta-5-steroid dehydrogenase, 3 beta- and steroid delta-isomerase), indicating that both cell types produce progesterone (56). Progesterone produced by the CL is required for the initiation and maintenance of pregnancy, while estradiol and inhibins produced in the CL suppress FSH secretion. As a result, FSH-dependent follicle growth is generally inhibited until the CL regresses and its endocrine influence diminishes.

In addition to producing endocrine messengers, the CL also undergoes extensive neovascularization. This is driven primarily by an increase in both VEGF (vascular endothelial growth factor) and FGF (fibroblast growth factor), which is stimulated by the LH surge (57-59). This provides the CL with a direct interface to the circulation, allowing efficient access to cholesterol for steroid synthesis and release of endocrine messengers into the blood.

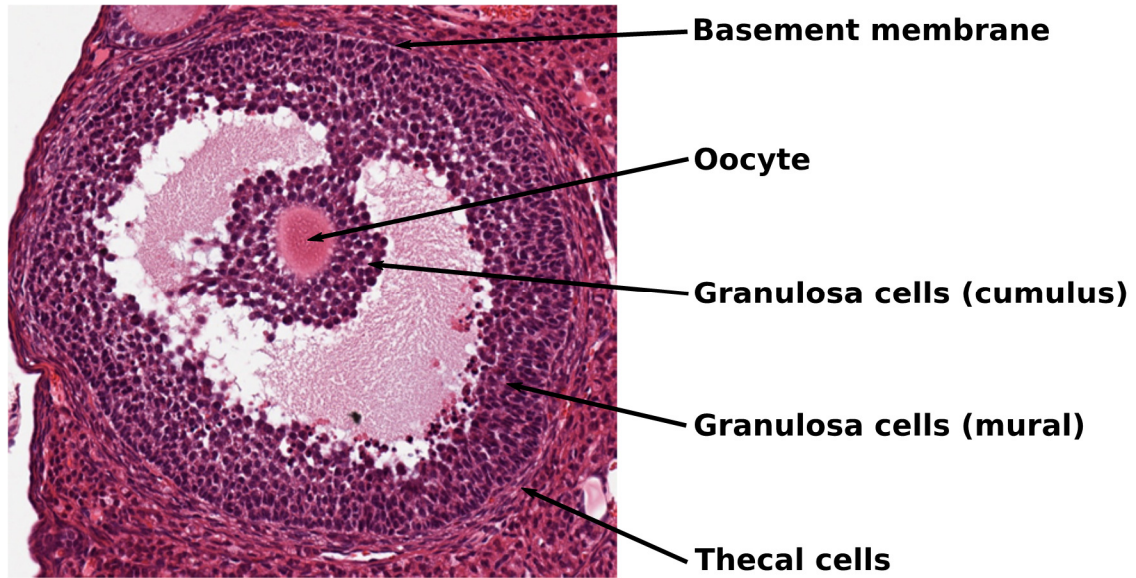


Figure 1-1: Histology of an antral follicle.

The antral follicle consists of an oocyte, surrounded by granulosa cells, a basement membrane, and thecal cells. Under the influence of FSH, granulosa cells that are in close proximity to the oocyte differentiate into cumulus cells. Granulosa cells that line the interior periphery of the follicle differentiate into mural granulosa cells.

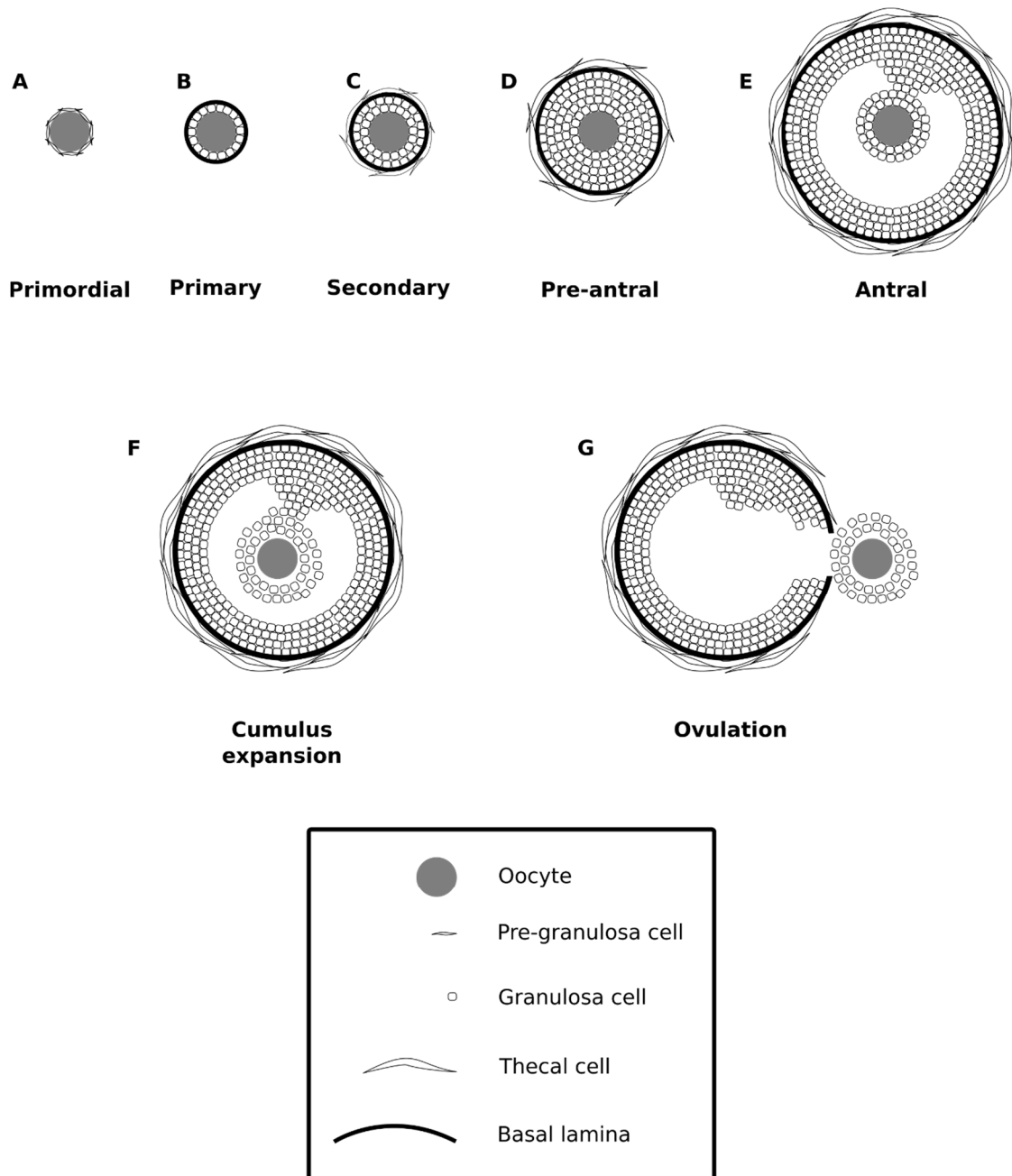


Figure 1-2: Stages of ovarian follicle growth.

Primordial follicles undergo FSH-independent growth (A-C), becoming responsive to FSH at the secondary stage. FSH-dependent growth (D-E) results in the formation of a large follicle responsive to LH. Under the influence of LH (F-G), cumulus expansion occurs, followed by ovulation.

1.2 The hypothalamic-pituitary-gonadal axis

In all reproductively mature, non-pregnant female mammals, follicle growth and ovulation are controlled by communication between the hypothalamus, the anterior pituitary, and the ovaries. In general, communication between these organs is mediated by GNRH, FSH, LH, and steroid hormones including estradiol and progesterone. The hypothalamus is the “master regulator” of female reproductive function, and may thus serve as a control point to integrate external information about stress and resource availability in order to modulate reproductive function. This integration of information may allow fertility to be limited during times of physiological stress or poor nutrition (60).

At the onset of puberty, a subset of cells within the hypothalamus called GNRH neurons begin to secrete GNRH into the circulation in a pulsatile manner, with the frequency of release determining the gonadotropin secreted. Pulsatile GNRH secretion is dependent on KISS1 (kisspeptin), a hormone that is secreted by kisspeptin neurons also located in the hypothalamus and acts on GNRH neurons which express *Kiss1r* (KISS1 receptor). Engineered mice with a GNRH neuron-specific depletion of *Kiss1r* fail to undergo puberty (61). GNRH secreted from the hypothalamus reaches the anterior pituitary and stimulates gonadotrope cells that express *Gnrhr* (gonadotropin-releasing hormone receptor). Upon stimulation, these gonadotrope cells synthesize and secrete gonadotropins into the circulation. Low GNRH pulsatile frequency favours secretion of FSH and high frequency favours secretion of LH.

When FSH reaches the ovaries via the circulation, growth of several preantral follicles is initiated, which may vary with respect to size and responsiveness to FSH. The exact number is species specific, with a range of 4-14 preantral follicles recruited in humans (62). Ultimately, most of these follicles will undergo apoptosis during a process known as atresia. These are known as subordinate follicles. Only a small subset of recruited follicles, and in some species only one, will reach the preovulatory stage. These are known as dominant follicles. These follicles are likely to be the ones that were the largest and/or most mature when FSH levels began to rise.

Once growth of preantral follicles has been initiated, proliferation of GCs and expression of *Cyp19a1* (cytochrome P450, family 19, subfamily A, polypeptide 1) is enhanced. CYP19A1, commonly referred to as aromatase, catalyzes the aromatization of testosterone and is the rate-limiting step in estradiol biosynthesis. The combination of increased numbers of GCs and increased expression of *Cyp19a1* results in elevated serum estradiol, which serves as a messenger to the hypothalamus to secrete GNRH at a higher frequency. Increased frequency of GNRH secretion serves two purposes: suppression of FSH secretion and promotion of LH production, causing a switch in the gonadotropin output of the anterior pituitary. FSH levels then begin to fall, which has important consequences for growing follicles. During the early stages of FSH-driven follicle growth, survival of the follicle is dependent on elevated serum concentration of FSH. Once the follicle reaches a threshold size, such elevated FSH levels are no longer required for survival (63). Subordinate follicles still require elevated FSH levels for survival, and the decline in FSH triggers atresia in these follicles. However, follicles that were initially more mature and responsive to FSH, the dominant follicle(s), no longer require such elevated FSH for survival. Therefore, as FSH levels fall, subordinate follicles die, leaving the dominant follicle(s) to reach the preovulatory stage. Furthermore, dominant follicles also produce large quantities of estradiol and inhibin. In fact, production of inhibin-B peaks during the follicular phase in humans (64). These endocrine messengers act together to suppress FSH secretion, and in this way the dominant follicles hasten the demise of subordinates (65).

In some cases, none of the preantral follicles that were initially recruited for growth by FSH become dominant, and all undergo atresia. In this case, another cohort of preantral follicles is recruited for growth, constituting a second “wave” of follicle growth. This process may repeat, with the recruitment of additional waves, until a dominant follicle arises. Evidence for waves of follicle growth came from transvaginal ultrasound data, which demonstrated that two thirds of women experience 2 waves per interovulatory interval (IOI) and one-third experience 3 waves per IOI (66).

As growth of the dominant follicles continue, expression of LHR in mural GCs increases and estradiol production continues to rise. Once a threshold concentration of

serum estradiol is met, an acute release of LH is triggered from the anterior pituitary. This “LH surge” acts on the preovulatory follicle to trigger resumption of meiosis, cumulus expansion, ovulation and formation of the CL. The CL produces large quantities of estradiol, progesterone, and inhibin A, which all suppress FSH secretion (67). This is when the follicular phase ends, and the luteal phase, characterized by the dominating influence of CL, begins. It should be noted that basal levels of FSH continue to recruit cohorts of preantral follicles for growth during the luteal phase. However, until the influence of the CL is diminished, FSH levels do not reach levels sufficient for a dominant follicle to arise, and the likely outcome for these follicles is atresia.

If pregnancy is not initiated, the CL undergoes a process known as luteolysis, which involves apoptosis of luteal cells, regression of the CL, and a corresponding decline in steroid and inhibin A production. As serum levels of these endocrine messengers decline, their suppressive effect on FSH production is relieved. As the CL regresses further and is reabsorbed into the ovary, rising FSH levels once again initiate growth of the next cohort of preantral follicles. Thus, the luteal phase gives way to the follicular phase, and the ovarian cycle begins again.

On the other hand, if the ovulated oocyte is fertilized and pregnancy is initiated, the CL is rescued from luteolysis by chorionic gonadotropin (CG) produced in the placenta, and then maintained by other factors of placental origin (68). For the remainder of pregnancy, the CL continues to produce endocrine messengers that suppress FSH secretion.

1.3 Eph receptors and Ephrins

1.3.1 Overview

The first Eph receptor was discovered and characterized during a human genomic library screen for novel receptor tyrosine kinases (RTKs). Probing for sequences homologous to the tyrosine kinase domain of v-fps, a viral oncogene, revealed a novel, highly-conserved gene that is highly expressed in the erythropoietin-producing human hepatocellular carcinoma cell line ETL-1. The novel gene was termed *eph*, after the cell type in which it was initially discovered (69). Since then, the family of identified Eph

receptors has expanded and now comprises the largest known family of receptor tyrosine kinases (RTKs) in vertebrates. In vertebrates, 16 receptors (encoded by *Eph* genes) and 9 ephrin ligands (encoded by *Efn* genes) have been identified. These can be further classified into two classes each of receptor and ligand, designated A and B based on sequence similarity and receptor-ligand affinity. In general, Eph receptors and ephrins have higher binding affinity for partners of the same class, and bind within these classes promiscuously.

Eph receptors and their ephrin ligands exhibit a number of features that distinguish them from other RTK families and their ligands. For example, all Eph receptors and ephrin ligands are associated with the cell membrane by either a transmembrane domain or a glycosylphosphatidylinositol (GPI) linkage. As such, Eph-ephrin signaling is initiated exclusively at points of cell-cell contact.

Another unique aspect of Eph-ephrin signaling is that it is bidirectional, allowing signaling cascades to propagate into both receptor-bearing (forward signaling) and ligand-bearing (reverse signaling) cells. Forward signaling is mediated by Eph tyrosine kinase activity and adaptor proteins that enable crosstalk with downstream signaling pathways. Reverse signaling via B-class ephrins occurs in a similar manner, where the receptor-bound ligand can interact with intracellular signaling elements via adaptor proteins. Much less is known about reverse signaling via A-class ephrins, which are associated with the cell membrane but lack a transmembrane domain. It has been proposed that clustering of A-class ephrins into higher-order signaling clusters favours the recruitment of transmembrane proteins, which in turn interact with intracellular signaling elements. To date, several such partners have been identified (70-72) .

Eph-ephrin signaling has been characterized primarily in the context of developmental processes and other functions in complex animals. However, it is likely that Eph-ephrin signaling played important roles in much more primitive organisms, as suggested by the identification of an Eph receptor in the sponge (73). This suggests that Eph receptors were present prior to the divergence of parazoans and eumetazoans (74), which is estimated to have occurred roughly 940 million years ago (75). Evidence from a

recent phylogenetic analysis of Eph receptors and ephrins indicates that ancient chordates had one A-class ephrin, one B-class ephrin, and one Eph receptor that was capable of binding both classes of ligand. Since then, duplication and diversification has likely resulted in the large families of Eph receptors and ephrins that are expressed in modern organisms (76).

1.3.2 Ephrins

Like Eph receptors, all ephrins are membrane-associated signaling elements and can be classified into two subtypes, A and B, based on sequence similarity. However, the inter-class structural differences are greater for ephrins than for Eph receptors. A-class ephrins consist of one extracellular receptor-binding domain (RBD) that contains a hydrophobic pocket, which serves as an acceptor site for a G-H loop present in the ligand-binding domain (LBD) of cognate Eph receptors. This RBD is linked to the plasma membrane via a glycosylphosphatidylinositol (GPI) linkage; A-class ephrins do not possess transmembrane or cytoplasmic domains (). The lack of a cytoplasmic domain means that cytoplasmic signaling partners could not be inferred based on known interacting motifs. However, a growing body of evidence indicates that A-class ephrins transmit downstream signals via cis interactions of A-class ephrins with partners that contain transmembrane domains. This occurs during the formation of signaling clusters, and such partners include NTRK2 (neurotrophic tyrosine kinase, receptor, type 2) (71), NGFR (nerve growth factor receptor) (70), and RET (ret proto-oncogene) (72).

Like A-class ephrins, B-class ephrins also contain a RBD, which interacts with the LBD of cognate Eph receptors in a manner similar to that of A-class ephrins. However, in B-class ephrins the RBD is linked to a transmembrane helix, which is in turn linked to the cytoplasmic region of the ligand. The intracellular region contains several conserved tyrosine residues as well as a PDZ (postsynaptic density protein 95/disk large homolog 4/zona occludens protein 1) domain. Upon activation and formation of signaling clusters, the ephrin-B PDZ domain is phosphorylated by SRC (*v-src* avian sarcoma (Schmidt-Ruppin A-2) viral oncogene homolog) kinases. The phosphorylated PDZ domain recognizes and binds adaptor proteins that facilitate downstream signaling. Such adaptor proteins include RGS3 (regulator of G-protein signaling 3) (77) and NCK2 (NCK adaptor

protein 2) (78). Disruption of the ephrin-B PDZ domain in mice results in lymphatic defects (79) and defective formation of the corpus callosum (80).

1.3.3 Eph receptors

Like classic RTKs, Eph receptors have an ectodomain (a region that extends into the extracellular space), a transmembrane region spanning the cell membrane, and an intracellular region involved in propagation of downstream signals. The ectodomain contains residues that serve to interact with ephrin ligands as well as other Eph receptors. The LBD of the Eph receptor contains a hydrophobic pocket that interacts with a hydrophobic loop in the RBD of cognate ephrin ligands. This high-affinity interaction is believed to be the primary thermodynamic driver for complex formation (81). The cysteine-rich region is important for cis-interactions with other Eph receptors during the formation of higher-order signaling clusters (82). To date, no functions have been assigned to the two fibronectin type-III domains of the ectodomain.

The membrane-spanning region consists of a transmembrane helix that links the ectodomain to the cytoplasmic region. The cytoplasmic region consists of a juxtamembrane domain (JM) proximal to the interior of the cell membrane, a kinase domain (KD), and two regions that bind downstream signaling proteins: a sterile-alpha motif (SAM) and a PDZ domain. In the inactive Eph receptor monomer, the JM occludes the KD, suppressing kinase activity. Activation of the Eph receptor by a cognate ligand favours recruitment of another receptor-ligand pair, forming a heterotetramer. Autophosphorylation of the JM results in phosphorylation at two conserved tyrosine residues, which in turn initiates a conformational change that disrupts the JM-KD interaction (83).

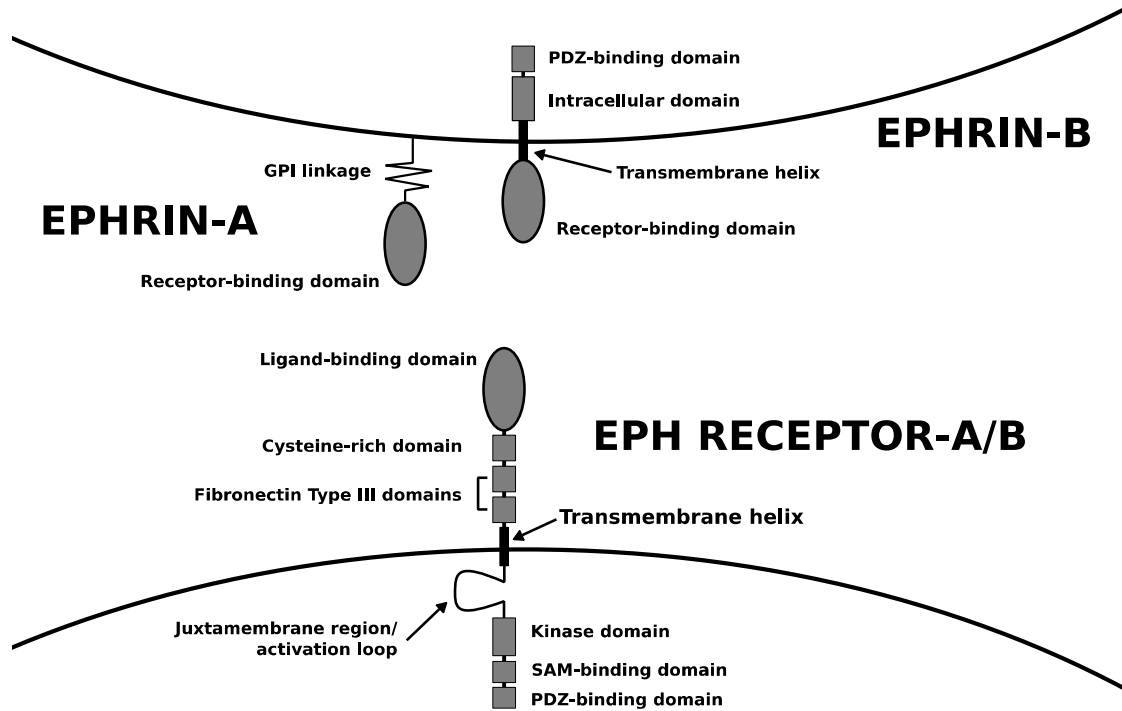


Figure 1-3: Ephrin and Eph receptor domains.

Eph receptors and ephrins are classified into 2 subtypes, A and B, based on receptor-ligand affinity and sequence similarity. Eph receptors of both A and B subtypes consist of a ligand-binding domain, a cysteine-rich domain, 2 fibronectin type III domains, a transmembrane helix, a juxtamembrane region, a kinase domain, a sterile-alpha motif (SAM), and a PDZ-binding domain. A-class ephrins consist of a receptor-binding domain associated with the cell membrane via a GPI-linkage. B-class ephrins consist of a receptor-binding domain, a transmembrane helix, an intracellular domain, and a PDZ-binding domain.

1.3.4 Initiation of Eph-Ephrin Signaling

All Eph receptors and ephrin ligands are membrane-associated, and as such, signaling is initiated from points of cell-cell contact. Initiation of signaling begins with the thermodynamically favourable insertion of the ephrin receptor-binding domain G-H loop into a hydrophobic pocket present in the ligand-binding domain of the cognate Eph receptor (84). The conformational flexibility of this hydrophobic pocket varies amongst different Eph receptors, which contributes to the promiscuity and variable affinities of Eph-ephrin pairs (85-88).

These heterodimers then combine resulting in the formation of heterotetramers. Heterotetramer formation is facilitated by interactions between the LBDs of the Eph receptor from each heterodimer. Interactions at this interface are mostly polar, consisting of van der Waals contacts, hydrogen bonds, and ionic interactions (89). Heterotetramers also comprise the fundamental unit of ephrin signaling, due to the nature of RTK activation. The Eph receptor KD is autoinhibited by the receptor's own activation loop. This loop obstructs the KD active site, preventing access to ATP and tyrosine substrates. Ligand-induced Eph receptor dimerization initiates autophosphorylation, and promotes phosphorylation of conserved tyrosine residues in the JM and activation loop of one Eph receptor by its partner (90). This results in relief of the autoinhibitory activation loop-KD interaction, allowing the KD to enter an "active" conformation and to access ATP and tyrosine substrates (91).

Oligomerization of active heterotetramers into higher-order signaling clusters is facilitated by interactions in cis between the LBD and cysteine-rich domains of Eph receptors. Interactions at the LBD-cysteine-rich domain interface are also mostly polar, consisting of van der Waals contacts, hydrogen bonds, and ionic interactions (88). Continued recruitment of heterotetramers enlarges the heterooligomer, resulting in the formation of higher-order Eph-ephrin signaling clusters that also behave as adhesive contacts between cells. The size of these signaling clusters is not currently known, and is a subject of continued investigation (89).

1.3.5 Eph-ephrin Signal Transduction

Transduction of Eph-ephrin signaling begins at points of cell-cell contact, and is notable for its bidirectionality, with signaling cascades propagating via receptors as well as ligands. Signal transduction via Eph receptors is termed “forward signaling” while transduction via ephrins is termed “reverse signaling”.

Forward signaling is mediated primarily by conserved tyrosine residues in the intracellular regions of the activated Eph receptor. Upon activation by ephrin ligands and formation of heterotetramers, autophosphorylation by the Eph kinase domain results in phosphorylation of these tyrosine residues. In addition to triggering conformational changes that enhance kinase domain activity, these residues also serve as docking sites for intracellular proteins that facilitate further signal propagation. These include Src family kinases, Abl family kinases, guanine-exchange factors, GTPase-activating proteins, as well as adaptor proteins that facilitate recruitment of additional kinases and GTPase-modulating proteins. Recruitment of these cytoplasmic signaling elements permits the activated Eph receptor to impinge on intracellular signaling pathways that control cytoskeletal remodeling, migration, adhesion, proliferation, and gene expression. For example, stimulation of *EPHA2* in MDA-MB-231 breast cancer cells with recombinant ephrin-A1 results in recruitment of the adaptor proteins SHC (Src homology 2 domain containing) and GRB2 (Growth factor receptor-bound protein 2), which enables phosphorylation of ERK (Extracellular regulated kinase) (92). In another example, stimulation of *EPHA3*-expressing human epithelial kidney 293T cells with recombinant ephrin-A5 promotes recruitment of the adaptor protein CRK (V-Crk Avian Sarcoma Virus CT10 Oncogene Homolog) and activation of the GTPase RHOA (Ras homolog family member A), which in turn induces membrane blebbing and retraction of cellular protrusions (93). These examples illustrate how Eph receptors can sense physical contact with another cell and trigger various cellular responses. Some are transient, such as cytoskeletal rearrangement, while others, such as ERK activation, may have lasting effects via phosphorylation of ERK substrate proteins that regulate gene expression.

In addition to kinase domain-dependent signaling, some evidence supports kinase domain-independent signaling. These studies involved mice that express Eph receptors which lack cytoplasmic domains (94,95) or possess KD-inactivating mutations (96), but

are capable of rescuing the phenotype of the full-Eph receptor knockout. It has been proposed that in such cases, the extracellular Eph domains may potentiate signaling activity of other membrane-associated receptors (95), or that induction of reverse signaling via ephrins in adjacent cells was sufficient for phenotype rescue (94,96).

Reverse signaling is less understood. Little is known about the mechanisms underlying signal transduction via A-class ephrins, which are associated with the cell membrane via a GPI-linkage. Since these ephrins lack transmembrane domains, it was proposed that the formation of large signaling clusters resulted in recruitment of transmembrane signaling proteins that facilitate signal transduction. This was confirmed with the discovery that the transmembrane protein NGFR (p75 neurotrophin receptor) co-localizes and physically interacts with ephrin-A5 in mouse retinal axons. The same study found that retinal axons from mice lacking NGFR did not exhibit a response to EphA7, indicating that this transmembrane receptor is required for reverse signaling via ephrin-A5 in mouse retinal axons (70).

Signaling via B-class ephrins is better understood. In contrast to A-class ephrins, the B-class ephrin extracellular domain is associated with the cell membrane via a transmembrane helix, which is in turn linked to a cytoplasmic region that contains a PDZ domain. As is the case with Eph receptors, the intracellular domains of B-class ephrins contain conserved tyrosine residues that are phosphorylated by SRC kinases upon receptor binding. These residues serve as docking sites for adaptor proteins that facilitate downstream signaling.

In addition to forward and reverse signaling, which are initiated by Eph receptors and cognate ephrins interacting in trans, Eph-ephrin interactions in cis have also been reported. It has been proposed that these interactions suppress activation of Eph receptors that are co-expressed with ephrins, resulting in silencing of forward signaling (97). Interaction of ephrin-B2 and EPHA3 in cis has also been reported in H226 and A549 lung cancer cells, resulting in attenuation of EPHA3 activation. This suggests that Eph-ephrin interactions in cis do not necessarily require a cognate ligand-receptor pair (98).

1.3.6 Termination of Eph-ephrin Signaling

In many biological systems in which Eph-ephrin signaling has been studied, the main roles of Eph receptors and ephrins are to mediate adhesive and repulsive responses in order to control cell positioning. Eph-ephrin signaling clusters are adhesive structures that physically tether interacting cells, meaning that the initial interaction between cells bearing cognate Eph receptors and ephrins is adhesive in nature. Depending on the cell type, the outcome of this interaction may involve maintenance of adhesion or initiation of a repulsive response. This is especially relevant in biological processes such as axon guidance, tissue segmentation, and tissue remodeling, where repulsive responses are crucial in guiding cells to the correct position or maintaining boundaries between different populations of cells (99). In order for these repulsive responses to occur, the initial adhesive Eph-ephrin interaction must be terminated so that Eph-ephrin tethered cells can disengage and migration may proceed. So far, two disengagement mechanisms have been identified: proteolytic cleavage of Eph receptor or ephrin ectodomains, and endocytosis of the cell membrane region that contains the Eph-ephrin signaling cluster.

The first reported mechanism of disengagement involved proteolytic cleavage of ephrin-A2 by the ADAM10 metalloprotease (100). Further studies revealed that ADAM10 is constitutively associated with EphA3, interacting with this Eph receptor via its LBD. Formation of the Eph-ephrin heterodimer positions the protease domain of ADAM10 such that cleavage of the ephrin-A2 ectodomain occurs *in trans*, which severs the Eph-ephrin tether between cells (101,102). More recently, proteolytic cleavage of Eph receptor ectodomains has also been reported. In contrast to cleavage of ephrins, which is mediated by ADAM-family metalloproteases, cleavage of Eph receptors is mediated by gamma-secretase (103,104).

For B-class Eph-ephrin pairs, the current body of evidence suggests that the predominant mechanism for disengagement is endocytosis. ADAM13 has been reported to cleave the ephrin-B1 ectodomain in *Xenopus* embryos, although this may not be a general mechanism that is conserved across species (105). Disengagement via endocytosis has been reported for forebrain neurons expressing EphB2 and ephrin-B1, where immunofluorescence studies demonstrated that vesicles containing both receptor and ligand are transported into both cells (106). Another study published simultaneously

reported that adjacent Swiss 3T3 fibroblasts expressing EphB4 and ephrin-B2 exhibit endocytosis of vesicles containing both receptor and ligand into both cells. Small-molecule blockade of the RAC1 (ras-related C3 botulinum toxin substrate 1) pathway prevented endocytosis and retraction, indicating that endocytosis is RAC1-dependent in this model (107). Neither of these studies investigated the fate of endocytosed signaling elements. However, it was later reported that activation of EphB1 in Chinese hamster ovary cells results in phosphorylation of CBL (Cbl proto-oncogene, E3 ubiquitin protein ligase) and ubiquitination of EphB1, suggesting subsequent proteasomal degradation of EphB1 (108).

Thus, the mechanisms underlying termination of signaling for Eph-ephrin complexes is class-dependent. In general, A-class Eph-ephrin complexes are severed via cleavage of the ephrin ectodomain, while B-class Eph-ephrin complexes are endocytosed into adjacent cells and subsequently undergo ubiquitination and degradation. Future studies may identify additional mechanisms for termination of Eph-ephrin signaling.

1.4 Rationale

Since the first Eph receptor was identified in 1987, several reports have provided evidence that Eph-ephrin signaling occurs in the adult ovary. LacZ (beta-galactosidase) staining of ovarian sections from mice expressing an ephrin-B2-beta-galactosidase fusion protein revealed that ephrin-B2 is expressed by thecal cells of preovulatory ovarian follicles and blood vessels in the CL, suggesting that Eph-ephrin signaling is involved in ovarian angiogenesis (109). Subsequent RT-PCR studies detected transcripts for *EPHB1*, *EPHB2*, *EPHB3*, *EPHB4*, *EPHB6*, *EFNB1*, *EFNB2*, and *EFNB3* in the human CL, suggesting that these Eph receptors and ephrins are involved in CL formation (110). Lastly, transcripts for *Efna4*, *Efnb1*, *Efnb2*, *Epha2*, *Epha4*, and *Epha7* were detected in human GCs (111), suggesting a role for these Eph receptors and ephrins in the preovulatory follicle.

These reports indicated that Eph receptors and ephrins are expressed in the ovarian follicle and the CL. However, the first evidence suggesting their involvement in follicle growth came from microarray data indicating that *Efna5* expression is reduced in GCs

from eCG-treated *Esr2*^{-/-} mice (112). These mice lack estrogen receptor beta (ER β) and exhibit a severe reproductive phenotype, with females exhibiting impaired follicle growth and subfertility (113) due to impaired FSH-induced differentiation of GCs and an attenuated response to LH (114). Taken together, these reports indicate that *Efna5* expression is reduced in GCs of a mouse model that is subfertile and exhibits an impaired response to gonadotropins. Therefore, reduced expression of *Efna5* in GCs may be involved in the reproductive phenotype of this mouse.

Taken together, these reports suggest that Eph-ephrin signaling occurs in the ovary during follicle growth and formation of the CL. However, there have been no published investigations of Eph receptor and ephrin expression and/or function in a gonadotropin-stimulated animal model of follicle growth and ovulation. Understanding how Eph-ephrin signaling is involved in these critical events will define a novel role for Eph receptors and ephrins in ovarian function, a system outside the current scope of ephrin biology.

1.5 Hypothesis

The work presented in this thesis aims to test the hypothesis that ephrin-A5 is required for gonadotropin-dependent follicle growth and ovulation, as well as optimal fertility.

1.6 Objectives

In order to test this hypothesis, I pursued the following objectives:

1. Characterize expression of *Efn* and *Eph* genes in granulosa cells of an eCG-stimulated mouse model and a granulosa cell line, and determine whether cultured GCs respond to stimulation with Eph receptors and ephrins.
2. Perform a reproductive assessment of *Efna5*^{-/-} female mice to determine whether absence of ephrin-A5 alters fertility.
3. Characterize transcriptional regulation of *Epha5* by FSH and downstream cAMP-dependent pathways.

1.7 Bibliography

1. Pepling ME. From primordial germ cell to primordial follicle: mammalian female germ cell development. *Genesis*. 2006;44(12):622-632.
2. Tingen C, Kim A, Woodruff TK. The primordial pool of follicles and nest breakdown in mammalian ovaries. *Molecular human reproduction*. 2009;15(12):795-803.
3. Pepling ME, Spradling AC. Mouse ovarian germ cell cysts undergo programmed breakdown to form primordial follicles. *Dev Biol*. 2001;234(2):339-351.
4. Pepling ME. Follicular assembly: mechanisms of action. *Reproduction*. 2012;143(2):139-149.
5. Kezele P, Nilsson E, Skinner MK. Cell-cell interactions in primordial follicle assembly and development. *Frontiers in bioscience : a journal and virtual library*. 2002;7:d1990-1996.
6. White YA, Woods DC, Takai Y, Ishihara O, Seki H, Tilly JL. Oocyte formation by mitotically active germ cells purified from ovaries of reproductive-age women. *Nature medicine*. 2012;18(3):413-421.
7. McLaughlin EA, McIver SC. Awakening the oocyte: controlling primordial follicle development. *Reproduction*. 2009;137(1):1-11.
8. Durlinger AL, Kramer P, Karels B, de Jong FH, Uilenbroek JT, Grootegoed JA, Themmen AP. Control of primordial follicle recruitment by anti-Mullerian hormone in the mouse ovary. *Endocrinology*. 1999;140(12):5789-5796.
9. Reddy P, Liu L, Adhikari D, Jagarlamudi K, Rajareddy S, Shen Y, Du C, Tang W, Hamalainen T, Peng SL, Lan ZJ, Cooney AJ, Huhtaniemi I, Liu K. Oocyte-specific deletion of Pten causes premature activation of the primordial follicle pool. *Science*. 2008;319(5863):611-613.
10. Kumar TR, Wang Y, Lu N, Matzuk MM. Follicle stimulating hormone is required for ovarian follicle maturation but not male fertility. *Nature genetics*. 1997;15(2):201-204.
11. Schmidt D, Ovitt CE, Anlag K, Fehsenfeld S, Gredsted L, Treier AC, Treier M. The murine winged-helix transcription factor Foxl2 is required for granulosa cell differentiation and ovary maintenance. *Development*. 2004;131(4):933-942.
12. Parrott JA, Skinner MK. Kit ligand actions on ovarian stromal cells: effects on theca cell recruitment and steroid production. *Molecular reproduction and development*. 2000;55(1):55-64.
13. Dong J, Albertini DF, Nishimori K, Kumar TR, Lu N, Matzuk MM. Growth differentiation factor-9 is required during early ovarian folliculogenesis. *Nature*. 1996;383(6600):531-535.
14. Yan C, Wang P, DeMayo J, DeMayo FJ, Elvin JA, Carino C, Prasad SV, Skinner SS, Dunbar BS, Dube JL, Celeste AJ, Matzuk MM. Synergistic roles of bone

- morphogenetic protein 15 and growth differentiation factor 9 in ovarian function. *Molecular endocrinology*. 2001;15(6):854-866.
15. Bianchi E, Barbagallo F, Valeri C, Geremia R, Salustri A, De Felici M, Sette C. Ablation of the Sam68 gene impairs female fertility and gonadotropin-dependent follicle development. *Human molecular genetics*. 2010;19(24):4886-4894.
 16. Lei L, Jin S, Mayo KE, Woodruff TK. The interactions between the stimulatory effect of follicle-stimulating hormone and the inhibitory effect of estrogen on mouse primordial folliculogenesis. *Biol Reprod*. 2010;82(1):13-22.
 17. Hunzicker-Dunn M, Maizels ET. FSH signaling pathways in immature granulosa cells that regulate target gene expression: branching out from protein kinase A. *Cell Signal*. 2006;18(9):1351-1359.
 18. Rodgers RJ, Irving-Rodgers HF. Formation of the ovarian follicular antrum and follicular fluid. *Biol Reprod*. 2010;82(6):1021-1029.
 19. Chongthammakun S, Terasawa E. Negative feedback effects of estrogen on luteinizing hormone-releasing hormone release occur in pubertal, but not prepubertal, ovariectomized female rhesus monkeys. *Endocrinology*. 1993;132(2):735-743.
 20. Couse JF, Hewitt SC, Korach KS. Chapter 15 - Steroid Receptors in the Ovary and Uterus. In: Wassarman JDNMPWPRGCMdKSRM, ed. *Knobil and Neill's Physiology of Reproduction (Third Edition)*. St Louis: Academic Press; 2006:593-678.
 21. Thompson IR, Kaiser UB. GnRH pulse frequency-dependent differential regulation of LH and FSH gene expression. *Mol Cell Endocrinol*. 2014;385(1-2):28-35.
 22. Gregory SJ, Kaiser UB. Regulation of gonadotropins by inhibin and activin. *Seminars in reproductive medicine*. 2004;22(3):253-267.
 23. Nakamura T, Takio K, Eto Y, Shibai H, Titani K, Sugino H. Activin-binding protein from rat ovary is follistatin. *Science*. 1990;247(4944):836-838.
 24. de Winter JP, ten Dijke P, de Vries CJ, van Achterberg TA, Sugino H, de Waele P, Huylebroeck D, Verschueren K, van den Eijnden-van Raaij AJ. Follistatins neutralize activin bioactivity by inhibition of activin binding to its type II receptors. *Mol Cell Endocrinol*. 1996;116(1):105-114.
 25. Anderson RA. Predicting the menopause: the role of inhibin B. *Trends in Urology, Gynaecology & Sexual Health*. 2007;12(2):9-10.
 26. Culler MD. Inhibin suppresses luteinizing hormone (LH)-releasing hormone self-priming: direct action on follicle-stimulating hormone secretion and opposition of estradiol-enhanced LH secretion. *Endocrinology*. 1992;130(3):1605-1614.
 27. Diaz FJ, Wigglesworth K, Eppig JJ. Oocytes determine cumulus cell lineage in mouse ovarian follicles. *J Cell Sci*. 2007;120(Pt 8):1330-1340.

28. Kidder GM, Vanderhyden BC. Bidirectional communication between oocytes and follicle cells: ensuring oocyte developmental competence. *Canadian journal of physiology and pharmacology*. 2010;88(4):399-413.
29. Eppig JJ, Wigglesworth K, Pendola F, Hirao Y. Murine oocytes suppress expression of luteinizing hormone receptor messenger ribonucleic acid by granulosa cells. *Biol Reprod*. 1997;56(4):976-984.
30. Conti M, Hsieh M, Zamah AM, Oh JS. Novel signaling mechanisms in the ovary during oocyte maturation and ovulation. *Mol Cell Endocrinol*. 2012;356(1-2):65-73.
31. Strauss Iii JF, Williams CJ. Chapter 9 - The Ovarian Life Cycle. In: Barbieri JFSL, ed. *Yen & Jaffe's Reproductive Endocrinology (Seventh Edition)*. Philadelphia: W.B. Saunders; 2014:157-191.e158.
32. Pincus G, Enzmann EV. The Comparative Behavior of Mammalian Eggs in Vivo and in Vitro : I. The Activation of Ovarian Eggs. *The Journal of experimental medicine*. 1935;62(5):665-675.
33. Erickson GF, Sorensen RA. In vitro maturation of mouse oocytes isolated from late, middle, and pre-antral graafian follicles. *The Journal of experimental zoology*. 1974;190(1):123-127.
34. Eggerickx D, Deneff JF, Labbe O, Hayashi Y, Refetoff S, Vassart G, Parmentier M, Libert F. Molecular cloning of an orphan G-protein-coupled receptor that constitutively activates adenylate cyclase. *The Biochemical journal*. 1995;309 (Pt 3):837-843.
35. Uhlenbrock K, Gassenhuber H, Kostenis E. Sphingosine 1-phosphate is a ligand of the human gpr3, gpr6 and gpr12 family of constitutively active G protein-coupled receptors. *Cell Signal*. 2002;14(11):941-953.
36. Bresnick JN, Skynner HA, Chapman KL, Jack AD, Zamiara E, Negulescu P, Beaumont K, Patel S, McAllister G. Identification of signal transduction pathways used by orphan g protein-coupled receptors. *Assay and drug development technologies*. 2003;1(2):239-249.
37. Mehlmann LM, Saeki Y, Tanaka S, Brennan TJ, Evsikov AV, Pendola FL, Knowles BB, Eppig JJ, Jaffe LA. The Gs-linked receptor GPR3 maintains meiotic arrest in mammalian oocytes. *Science*. 2004;306(5703):1947-1950.
38. Hinckley M, Vaccari S, Horner K, Chen R, Conti M. The G-protein-coupled receptors GPR3 and GPR12 are involved in cAMP signaling and maintenance of meiotic arrest in rodent oocytes. *Dev Biol*. 2005;287(2):249-261.
39. D'Alessandris C, Canipari R, Di Giacomo M, Epifano O, Camaioni A, Siracusa G, Salustri A. Control of mouse cumulus cell-oocyte complex integrity before and after ovulation: plasminogen activator synthesis and matrix degradation. *Endocrinology*. 2001;142(7):3033-3040.

40. Ochsner SA, Day AJ, Rugg MS, Breyer RM, Gomer RH, Richards JS. Disrupted function of tumor necrosis factor-alpha-stimulated gene 6 blocks cumulus cell-oocyte complex expansion. *Endocrinology*. 2003;144(10):4376-4384.
41. Russell DL, Ochsner SA, Hsieh M, Mulders S, Richards JS. Hormone-regulated expression and localization of versican in the rodent ovary. *Endocrinology*. 2003;144(3):1020-1031.
42. Familiari G, Verlengia C, Nottola SA, Renda T, Micara G, Aragona C, Zardi L, Motta PM. Heterogeneous distribution of fibronectin, tenascin-C, and laminin immunoreactive material in the cumulus-corona cells surrounding mature human oocytes from IVF-ET protocols--evidence that they are composed of different subpopulations: an immunohistochemical study using scanning confocal laser and fluorescence microscopy. *Molecular reproduction and development*. 1996;43(3):392-402.
43. Chen L, Russell PT, Larsen WJ. Functional significance of cumulus expansion in the mouse: roles for the preovulatory synthesis of hyaluronic acid within the cumulus mass. *Molecular reproduction and development*. 1993;34(1):87-93.
44. Russell DL, Robker RL. Molecular mechanisms of ovulation: co-ordination through the cumulus complex. *Human reproduction update*. 2007;13(3):289-312.
45. Buccione R, Vanderhyden BC, Caron PJ, Eppig JJ. FSH-induced expansion of the mouse cumulus oophorus in vitro is dependent upon a specific factor(s) secreted by the oocyte. *Dev Biol*. 1990;138(1):16-25.
46. Dragovic RA, Ritter LJ, Schulz SJ, Amato F, Thompson JG, Armstrong DT, Gilchrist RB. Oocyte-secreted factor activation of SMAD 2/3 signaling enables initiation of mouse cumulus cell expansion. *Biol Reprod*. 2007;76(5):848-857.
47. Salustri A, Camaioni A, D'Alessandris C. Endocrine and paracrine regulation of cumulus expansion. *Zygote*. 1996;4(4):313-315.
48. Akison LK, Alvino ER, Dunning KR, Robker RL, Russell DL. Transient invasive migration in mouse cumulus oocyte complexes induced at ovulation by luteinizing hormone. *Biol Reprod*. 2012;86(4):125.
49. Peluffo MC, Murphy MJ, Baughman ST, Stouffer RL, Hennebold JD. Systematic analysis of protease gene expression in the rhesus macaque ovulatory follicle: metalloproteinase involvement in follicle rupture. *Endocrinology*. 2011;152(10):3963-3974.
50. Brown HM, Dunning KR, Robker RL, Boerboom D, Pritchard M, Lane M, Russell DL. ADAMTS1 cleavage of versican mediates essential structural remodeling of the ovarian follicle and cumulus-oocyte matrix during ovulation in mice. *Biol Reprod*. 2010;83(4):549-557.
51. Itoh T, Tanioka M, Matsuda H, Nishimoto H, Yoshioka T, Suzuki R, Uehira M. Experimental metastasis is suppressed in MMP-9-deficient mice. *Clinical & experimental metastasis*. 1999;17(2):177-181.

52. Boerboom D, Lafond JF, Zheng X, Lapointe E, Mittaz L, Boyer A, Pritchard MA, DeMayo FJ, Mort JS, Drolet R, Richards JS. Partially redundant functions of Adamts1 and Adamts4 in the perinatal development of the renal medulla. *Developmental dynamics : an official publication of the American Association of Anatomists*. 2011;240(7):1806-1814.
53. Zhao S, Zhao Y, Niu P, Wang N, Tang Z, Zan L, Li K. Molecular characterization of porcine MMP19 and MMP23B genes and its association with immune traits. *International journal of biological sciences*. 2011;7(8):1101-1113.
54. Fanjul-Fernandez M, Folgueras AR, Fueyo A, Balbin M, Suarez MF, Fernandez-Garcia MS, Shapiro SD, Freije JM, Lopez-Otin C. Matrix metalloproteinase Mmp-1a is dispensable for normal growth and fertility in mice and promotes lung cancer progression by modulating inflammatory responses. *The Journal of biological chemistry*. 2013;288(20):14647-14656.
55. Bobadilla M, Sainz N, Rodriguez JA, Abizanda G, Orbe J, de Martino A, Garcia Verdugo JM, Paramo JA, Prosper F, Perez-Ruiz A. MMP-10 is required for efficient muscle regeneration in mouse models of injury and muscular dystrophy. *Stem Cells*. 2014;32(2):447-461.
56. Sanders SL, Stouffer RL. Localization of steroidogenic enzymes in macaque luteal tissue during the menstrual cycle and simulated early pregnancy: immunohistochemical evidence supporting the two-cell model for estrogen production in the primate corpus luteum. *Biol Reprod*. 1997;56(5):1077-1087.
57. Geva E, Jaffe RB. Role of vascular endothelial growth factor in ovarian physiology and pathology. *Fertility and sterility*. 2000;74(3):429-438.
58. Wulff C, Wilson H, Lague P, Duncan WC, Armstrong DG, Fraser HM. Angiogenesis in the human corpus luteum: localization and changes in angiopoietins, tie-2, and vascular endothelial growth factor messenger ribonucleic acid. *The Journal of clinical endocrinology and metabolism*. 2000;85(11):4302-4309.
59. Wulff C, Wiegand SJ, Saunders PT, Scobie GA, Fraser HM. Angiogenesis during follicular development in the primate and its inhibition by treatment with truncated Flt-1-Fc (vascular endothelial growth factor Trap(A40)). *Endocrinology*. 2001;142(7):3244-3254.
60. McCartney CR, Marshall JC. Chapter 1 - Neuroendocrinology of Reproduction. In: Barbieri JFSL, ed. *Yen & Jaffe's Reproductive Endocrinology (Seventh Edition)*. Philadelphia: W.B. Saunders; 2014:3-26.e28.
61. Kirilov M, Clarkson J, Liu X, Roa J, Campos P, Porteous R, Schutz G, Herbison AE. Dependence of fertility on kisspeptin-Gpr54 signaling at the GnRH neuron. *Nature communications*. 2013;4:2492.
62. Baerwald AR, Adams GP, Pierson RA. Ovarian antral folliculogenesis during the human menstrual cycle: a review. *Human reproduction update*. 2012;18(1):73-91.

63. Brown JB. Pituitary control of ovarian function--concepts derived from gonadotrophin therapy. *The Australian & New Zealand journal of obstetrics & gynaecology*. 1978;18(1):46-54.
64. Groome NP, Illingworth PJ, O'Brien M, Cooke I, Ganesan TS, Baird DT, McNeilly AS. Detection of dimeric inhibin throughout the human menstrual cycle by two-site enzyme immunoassay. *Clinical endocrinology*. 1994;40(6):717-723.
65. Zeleznik AJ, Pohl CR. Chapter 45 - Control of Follicular Development, Corpus Luteum Function, the Maternal Recognition of Pregnancy, and the Neuroendocrine Regulation of the Menstrual Cycle in Higher Primates. In: Wassarman JDNMPWPRGCMdKSRM, ed. *Knobil and Neill's Physiology of Reproduction (Third Edition)*. St Louis: Academic Press; 2006:2449-2510.
66. Baerwald AR, Adams GP, Pierson RA. A new model for ovarian follicular development during the human menstrual cycle. *Fertility and sterility*. 2003;80(1):116-122.
67. Zeleznik AJ. The physiology of follicle selection. *Reprod Biol Endocrinol*. 2004;2:31.
68. Oon VJ, Johnson MR. The regulation of the human corpus luteum steroidogenesis: a hypothesis? *Human reproduction update*. 2000;6(5):519-529.
69. Hirai H, Maru Y, Hagiwara K, Nishida J, Takaku F. A novel putative tyrosine kinase receptor encoded by the eph gene. *Science*. 1987;238(4834):1717-1720.
70. Lim YS, McLaughlin T, Sung TC, Santiago A, Lee KF, O'Leary DD. p75(NTR) mediates ephrin-A reverse signaling required for axon repulsion and mapping. *Neuron*. 2008;59(5):746-758.
71. Marler KJ, Becker-Barroso E, Martinez A, Llovera M, Wentzel C, Poopalasundaram S, Hindges R, Soriano E, Comella J, Drescher U. A TrkB/EphrinA interaction controls retinal axon branching and synaptogenesis. *J Neurosci*. 2008;28(48):12700-12712.
72. Bonanomi D, Chivatakarn O, Bai G, Abdesselem H, Lettieri K, Marquardt T, Pierchala BA, Pfaff SL. Ret is a multifunctional coreceptor that integrates diffusible- and contact-axon guidance signals. *Cell*. 2012;148(3):568-582.
73. Suga H, Koyanagi M, Hoshiyama D, Ono K, Iwabe N, Kuma K, Miyata T. Extensive gene duplication in the early evolution of animals before the parazoan-eumetazoan split demonstrated by G proteins and protein tyrosine kinases from sponge and hydra. *Journal of molecular evolution*. 1999;48(6):646-653.
74. Drescher U. Eph family functions from an evolutionary perspective. *Current opinion in genetics & development*. 2002;12(4):397-402.
75. Nikoh N, Iwabe N, Kuma K, Ohno M, Sugiyama T, Watanabe Y, Yasui K, Shicui Z, Hori K, Shimura Y, Miyata T. An estimate of divergence time of Parazoa and Eumetazoa and that of Cephalochordata and Vertebrata by aldolase and triose phosphate isomerase clocks. *Journal of molecular evolution*. 1997;45(1):97-106.

76. Mellott DO, Burke RD. The molecular phylogeny of eph receptors and ephrin ligands. *BMC cell biology*. 2008;9:27.
77. Lu Q, Sun EE, Klein RS, Flanagan JG. Ephrin-B reverse signaling is mediated by a novel PDZ-RGS protein and selectively inhibits G protein-coupled chemoattraction. *Cell*. 2001;105(1):69-79.
78. Cowan CA, Henkemeyer M. The SH2/SH3 adaptor Grb4 transduces B-ephrin reverse signals. *Nature*. 2001;413(6852):174-179.
79. Makinen T, Adams RH, Bailey J, Lu Q, Ziemiecki A, Alitalo K, Klein R, Wilkinson GA. PDZ interaction site in ephrinB2 is required for the remodeling of lymphatic vasculature. *Genes & development*. 2005;19(3):397-410.
80. Bush JO, Soriano P. Ephrin-B1 regulates axon guidance by reverse signaling through a PDZ-dependent mechanism. *Genes & development*. 2009;23(13):1586-1599.
81. Himanen JP, Goldgur Y, Miao H, Myshkin E, Guo H, Buck M, Nguyen M, Rajashankar KR, Wang B, Nikolov DB. Ligand recognition by A-class Eph receptors: crystal structures of the EphA2 ligand-binding domain and the EphA2/ephrin-A1 complex. *EMBO reports*. 2009;10(7):722-728.
82. Lackmann M, Oates AC, Dottori M, Smith FM, Do C, Power M, Kravets L, Boyd AW. Distinct subdomains of the EphA3 receptor mediate ligand binding and receptor dimerization. *The Journal of biological chemistry*. 1998;273(32):20228-20237.
83. Singla N, Erdjument-Bromage H, Himanen JP, Muir TW, Nikolov DB. A semisynthetic Eph receptor tyrosine kinase provides insight into ligand-induced kinase activation. *Chemistry & biology*. 2011;18(3):361-371.
84. Himanen JP, Rajashankar KR, Lackmann M, Cowan CA, Henkemeyer M, Nikolov DB. Crystal structure of an Eph receptor-ephrin complex. *Nature*. 2001;414(6866):933-938.
85. Qin H, Shi J, Noberini R, Pasquale EB, Song J. Crystal structure and NMR binding reveal that two small molecule antagonists target the high affinity ephrin-binding channel of the EphA4 receptor. *The Journal of biological chemistry*. 2008;283(43):29473-29484.
86. Bowden TA, Aricescu AR, Nettleship JE, Siebold C, Rahman-Huq N, Owens RJ, Stuart DI, Jones EY. Structural plasticity of eph receptor A4 facilitates cross-class ephrin signaling. *Structure*. 2009;17(10):1386-1397.
87. Qin H, Noberini R, Huan X, Shi J, Pasquale EB, Song J. Structural characterization of the EphA4-Ephrin-B2 complex reveals new features enabling Eph-ephrin binding promiscuity. *The Journal of biological chemistry*. 2010;285(1):644-654.
88. Xu K, Tzvetkova-Robev D, Xu Y, Goldgur Y, Chan YP, Himanen JP, Nikolov DB. Insights into Eph receptor tyrosine kinase activation from crystal structures of the EphA4 ectodomain and its complex with ephrin-A5. *Proceedings of the*

National Academy of Sciences of the United States of America.
2013;110(36):14634-14639.

89. Himanen JP, Yermekbayeva L, Janes PW, Walker JR, Xu K, Atapattu L, Rajashankar KR, Mensinga A, Lackmann M, Nikolov DB, Dhe-Paganon S. Architecture of Eph receptor clusters. *Proceedings of the National Academy of Sciences of the United States of America.* 2010;107(24):10860-10865.
90. Binns KL, Taylor PP, Sicheri F, Pawson T, Holland SJ. Phosphorylation of tyrosine residues in the kinase domain and juxtamembrane region regulates the biological and catalytic activities of Eph receptors. *Molecular and cellular biology.* 2000;20(13):4791-4805.
91. Wybenga-Groot LE, Baskin B, Ong SH, Tong J, Pawson T, Sicheri F. Structural basis for autoinhibition of the Ephb2 receptor tyrosine kinase by the unphosphorylated juxtamembrane region. *Cell.* 2001;106(6):745-757.
92. Pratt RL, Kinch MS. Activation of the EphA2 tyrosine kinase stimulates the MAP/ERK kinase signaling cascade. *Oncogene.* 2002;21(50):7690-7699.
93. Lawrenson ID, Wimmer-Kleikamp SH, Lock P, Schoenwaelder SM, Down M, Boyd AW, Alewood PF, Lackmann M. Ephrin-A5 induces rounding, blebbing and de-adhesion of EphA3-expressing 293T and melanoma cells by CrkII and Rho-mediated signalling. *J Cell Sci.* 2002;115(Pt 5):1059-1072.
94. Birgbauer E, Cowan CA, Sretavan DW, Henkemeyer M. Kinase independent function of EphB receptors in retinal axon pathfinding to the optic disc from dorsal but not ventral retina. *Development.* 2000;127(6):1231-1241.
95. Grunwald IC, Korte M, Wolfer D, Wilkinson GA, Unsicker K, Lipp HP, Bonhoeffer T, Klein R. Kinase-independent requirement of EphB2 receptors in hippocampal synaptic plasticity. *Neuron.* 2001;32(6):1027-1040.
96. Kullander K, Mather NK, Diella F, Dottori M, Boyd AW, Klein R. Kinase-dependent and kinase-independent functions of EphA4 receptors in major axon tract formation in vivo. *Neuron.* 2001;29(1):73-84.
97. Carvalho RF, Beutler M, Marler KJ, Knoll B, Becker-Barroso E, Heintzmann R, Ng T, Drescher U. Silencing of EphA3 through a cis interaction with ephrinA5. *Nat Neurosci.* 2006;9(3):322-330.
98. Falivelli G, Lisabeth EM, Rubio de la Torre E, Perez-Tenorio G, Tosato G, Salvucci O, Pasquale EB. Attenuation of eph receptor kinase activation in cancer cells by coexpressed ephrin ligands. *PloS one.* 2013;8(11):e81445.
99. Cayuso J, Xu Q, Wilkinson DG. Mechanisms of boundary formation by Eph receptor and ephrin signaling. *Dev Biol.* 2014.
100. Hattori M, Osterfield M, Flanagan JG. Regulated cleavage of a contact-mediated axon repellent. *Science.* 2000;289(5483):1360-1365.
101. Janes PW, Saha N, Barton WA, Kolev MV, Wimmer-Kleikamp SH, Nievergall E, Blobel CP, Himanen JP, Lackmann M, Nikolov DB. Adam meets Eph: an ADAM

substrate recognition module acts as a molecular switch for ephrin cleavage in trans. *Cell*. 2005;123(2):291-304.

102. Janes PW, Wimmer-Kleikamp SH, Frangakis AS, Treble K, Griesshaber B, Sabet O, Grabenbauer M, Ting AY, Saftig P, Bastiaens PI, Lackmann M. Cytoplasmic relaxation of active Eph controls ephrin shedding by ADAM10. *PLoS Biol*. 2009;7(10):e1000215.
103. Litterst C, Georgakopoulos A, Shioi J, Ghersi E, Wisniewski T, Wang R, Ludwig A, Robakis NK. Ligand binding and calcium influx induce distinct ectodomain/gamma-secretase-processing pathways of EphB2 receptor. *The Journal of biological chemistry*. 2007;282(22):16155-16163.
104. Inoue E, Deguchi-Tawarada M, Togawa A, Matsui C, Arita K, Katahira-Tayama S, Sato T, Yamauchi E, Oda Y, Takai Y. Synaptic activity prompts gamma-secretase-mediated cleavage of EphA4 and dendritic spine formation. *The Journal of cell biology*. 2009;185(3):551-564.
105. Wei S, Xu G, Bridges LC, Williams P, White JM, DeSimone DW. ADAM13 induces cranial neural crest by cleaving class B Ephrins and regulating Wnt signaling. *Dev Cell*. 2010;19(2):345-352.
106. Zimmer M, Palmer A, Kohler J, Klein R. EphB-ephrinB bi-directional endocytosis terminates adhesion allowing contact mediated repulsion. *Nat Cell Biol*. 2003;5(10):869-878.
107. Marston DJ, Dickinson S, Nobes CD. Rac-dependent trans-endocytosis of ephrinBs regulates Eph-ephrin contact repulsion. *Nat Cell Biol*. 2003;5(10):879-888.
108. Fasen K, Cerretti DP, Huynh-Do U. Ligand binding induces Cbl-dependent EphB1 receptor degradation through the lysosomal pathway. *Traffic*. 2008;9(2):251-266.
109. Gale NW, Baluk P, Pan L, Kwan M, Holash J, DeChiara TM, McDonald DM, Yancopoulos GD. Ephrin-B2 selectively marks arterial vessels and neovascularization sites in the adult, with expression in both endothelial and smooth-muscle cells. *Dev Biol*. 2001;230(2):151-160.
110. Egawa M, Yoshioka S, Higuchi T, Sato Y, Tatsumi K, Fujiwara H, Fujii S. Ephrin B1 is expressed on human luteinizing granulosa cells in corpora lutea of the early luteal phase: the possible involvement of the B class Eph-ephrin system during corpus luteum formation. *The Journal of clinical endocrinology and metabolism*. 2003;88(9):4384-4392.
111. Xu Y, Zagoura D, Keck C, Pietrowski D. Expression of Eph receptor tyrosine kinases and their ligands in human Granulosa lutein cells and human umbilical vein endothelial cells. *Experimental and Clinical Endocrinology and Diabetes*. 2006;114(10):590-595.
112. Deroo BJ, Rodriguez KF, Couse JF, Hamilton KJ, Collins JB, Grissom SF, Korach KS. Estrogen receptor beta is required for optimal cAMP production in mouse granulosa cells. *Molecular endocrinology*. 2009;23(7):955-965.

- 113.** Krege JH, Hodgin JB, Couse JF, Enmark E, Warner M, Mahler JF, Sar M, Korach KS, Gustafsson JA, Smithies O. Generation and reproductive phenotypes of mice lacking estrogen receptor beta. *Proceedings of the National Academy of Sciences of the United States of America*. 1998;95(26):15677-15682.
- 114.** Couse JF, Yates MM, Deroo BJ, Korach KS. Estrogen receptor-beta is critical to granulosa cell differentiation and the ovulatory response to gonadotropins. *Endocrinology*. 2005;146(8):3247-3262.

2 Chapter 2: The ephrin signaling pathway regulates morphology and adhesion of mouse granulosa cells in vitro

This chapter is based on a peer-reviewed journal article:

Buensuceso AV, Deroo BJ. The ephrin signaling pathway regulates morphology and adhesion of mouse granulosa cells in vitro. *Biol Reprod.* 2013;88(1):25.

2.1 Introduction

The successful formation of a preovulatory follicle in response to follicle-stimulating hormone (FSH) requires dramatic changes in the follicle, including an increase in follicle size and granulosa cell (GC) number, GC differentiation, and formation of an antrum. FSH also induces changes in GC morphology and adhesion that are essential for preovulatory follicle development both in vivo and in vitro (1). Interestingly, changes in GC morphology and adhesion can also be induced by proteins of the extracellular matrix (ECM) during preovulatory follicle formation (1). Alterations in GC morphology are largely attributed to modifications of the cytoskeleton resulting from signals from the ECM or adherens junctions, whereas GC adhesion and contact are primarily mediated by gap junctions, tight junctions, and adherens junctions (1). However, few other mechanisms regulating GC morphology and contact have been identified. Recently, the Eph-ephrin family of molecules, a family that consists of ephrin ligands and their Ephrin (*Eph*) receptors, has been shown to regulate both cellular shape and adhesion during development, cancer, and the normal function of many different tissues (2,3). Although members of the Eph-ephrin family have been identified in the ovary, Eph-ephrin signaling and the role it may play during folliculogenesis have not been well-characterized.

Eph receptors comprise the largest known family of receptor tyrosine kinases (RTKs), with 16 Eph receptors (encoded by Eph genes) and 9 ephrin ligands (encoded by *Efn* genes) (**Table 2-1**) (2,4-6). Both Eph receptors and ligands are divided into either A-class or B-class, based on receptor-ligand affinity and sequence similarity. Eph receptors and their ephrin ligands are membrane-associated; thus, signaling is initiated exclusively

from points of cell-to-cell contact upon binding of the ephrin ligand of one cell to the Eph receptor of an adjacent cell. Ephrin signaling is bidirectional, with signals propagating into both the receptor-bearing cells (forward signaling) and ligand-bearing cells (reverse signaling) (2). Eph receptors and ephrins were initially implicated in cell positioning and migration during development, particularly of the nervous system; however, ephrins have since been shown to regulate cell positioning, migration, adhesion, and differentiation during the development of many other tissues, including the retina (7), thyroid (8), vasculature (9), and mammary gland (10,11). Eph-ephrin signaling also regulates keratinocyte adhesion and differentiation (12) and hematopoietic stem cell adhesion (13). Compelling evidence also suggests that Eph-ephrin signaling plays several important roles in cancer development and progression (3). Expression of ephrin ligands and receptors is often reduced in advanced-stage tumors, and Eph-ephrin signaling regulates tumor growth, metastasis, and angiogenesis by altering cell proliferation, motility, invasion, and migration (3). Given that FSH induces changes in GC morphology and adhesion during formation of a preovulatory follicle, we speculated that FSH may regulate Eph-ephrin gene expression, and that Eph-ephrin signaling may regulate GC function.

Table 2-1: The Ephrin receptors and their ephrin ligand specificities.

Ligands are listed in approximate order of decreasing affinity for each receptor.

Table adapted from (4) and updated (i (5), ii (6), and iii (6)).

Eph receptors	Ligands
EphA1	ephrin-A1
EphA2	ephrin-A3, ephrin-A1, ephrin-A5, ephrin-A4, ephrin-A2
EphA3	ephrin-A5, ephrin-A2, ephrin-A3, ephrin-A1, ephrin-A4, ephrin-B1
EphA4	ephrin-A5, ephrin-A1, ephrin-A3, ephrin-A2, ephrin-B2, ephrin-B3, ephrin-A4
EphA5	ephrin-A5, ephrin-A1, ephrin-A2, ephrin-A3, ephrin-A4
EphA6	ephrin-A2, ephrin-A1, ephrin-A3, ephrin-A4, ephrin-A5
EphA7	ephrin-A2, ephrin-A3, ephrin-A1, ephrin-A4, ephrin-A5
EphA8	ephrin-A5, ephrin-A3, ephrin-A2
EphB1	ephrin-B2, ephrin-B1, ephrin-A3
EphB2	ephrin-B1, ephrin-B2, ephrin-B3, ephrin-A5 ⁱ
EphB3	ephrin-B1, ephrin-B2, ephrin-B3
EphB4	ephrin-B2, ephrin-B1
EphB6	ephrin-B2 ⁱⁱ , ephrin-B3 ⁱⁱⁱ

To date, a limited number of reports have described Eph-ephrin gene expression in the mammalian ovary (14-16). Gale et al. (14) identified ephrin-B2 (EPHB2) in the endothelium of vessels surrounding and invading the theca interna of mouse preovulatory follicles and in the highly vascularized corpus luteum. Those authors suggested that EPHB2 regulates angiogenesis during the formation of preovulatory follicles and the corpus luteum. Egawa et al. (15) investigated the mRNA levels of all B-class ephrins in the human ovary during formation of the corpus luteum. They also demonstrated that EPHB1 localized to the theca interna and that EPHB2 bound to the surface of freshly isolated human GCs. Xu et al. (16) characterized the mRNA levels of ephrin A and B ligands and receptors in human GCs and detected expression of *EPHA2*, *EPHA4*, *EPHA7*, *EFNA4*, *EFNB1*, and *EFNB2*. This expression was unaffected by treatment of GCs with human chorionic gonadotropin (hCG) (16). Finally, expression of *EPHA4* has been detected in bovine theca cells (17).

None of these studies investigated whether FSH regulates the expression of Eph-ephrin genes in the ovary, nor did they demonstrate a functional or behavioral effect of Eph-ephrin signaling on follicular cells, such as changes in cell shape and adhesion. Therefore, given that changes in cell shape and contact occur during GC differentiation both in vitro and in vivo in response to FSH signaling, and given that a subset of ephrins has been identified in GCs, we hypothesized that Eph-ephrin signaling may be a novel mechanism by which GC shape and adhesion are regulated and that expression of ephrin family members may be regulated by gonadotropins.

To determine if FSH regulates Eph-ephrin gene expression in mouse GCs, we examined the expression of the entire family of Eph-ephrin genes after FSH treatment of primary mouse GCs and an immortalized, FSH-responsive rat GC line (GFSHR-17) (18). Using these models and recombinant ephrin ligands and receptors, we also investigated the functional effects of Eph-ephrin signaling on GC morphology and adhesion and identified beta-catenin as a potential downstream target of EFNA5 signaling in GCs.

2.2 Materials and Methods

2.2.1 Cell Culture

The GFSHR-17 cell line is an immortalized, gonadotropin-responsive rat GC line (18) that we obtained from Dr. Abraham Amsterdam (Weizmann Institute of Science). GFSHR-17 cells were maintained in Dulbecco modified Eagle medium/F12 (DMEM/F12; Wisent, Inc.) containing 5% fetal bovine serum (FBS; Wisent, Inc.) at 37°C in 5% CO₂ before use in experiments.

2.2.2 Mice and Treatments

Experiments were performed in compliance with the guidelines set by the Canadian Council for Animal Care and the policies and procedures approved by The University of Western Ontario Council on Animal Care. Investigations were conducted in accordance with the National Research Council's Guide for Care and Use of Laboratory Animals. C57BL/6 female mice (Postnatal Day [PND] 23–28) were used in all experiments. For quantitative RT-PCR (qRT-PCR) studies, mice were treated either with saline or with 3.25 or 5.0 IU of equine chorionic gonadotropin (eCG; Sigma Chemical Co.) for 48 h before isolation of GCs. For immunofluorescence studies, immature females were treated with either saline for 48 h, 5.0 IU of eCG for 48 h, or 5.0 IU of eCG for 48 h followed by 5.0 IU of hCG for 24 h (Sigma).

2.2.3 Isolation of GCs

Ovaries were removed and immediately transferred to a 100-mm cell-culture dish containing 15 mL of ice-cold M199 medium supplemented with 1 mg/mL of bovine serum albumin (BSA), 2.5 µg/mL of amphotericin B, and 50 µg/mL of gentamicin (all reagents from Invitrogen). Ovaries were pooled, and the GCs from each pool were then expressed by manual puncture with 25-gauge needles followed by pressure applied with a sterile spatula. Follicular debris was removed manually, and the GC suspension was filtered through a 150-µm Nitex nylon membrane (Sefar America, Inc.) mounted in a Swinnex filter (Millipore). The GCs were then pelleted by centrifugation at 250 × g for 5 min at 4°C followed by two washes in DMEM/F12 medium containing 1% penicillin/streptomycin solution (15070-063; Invitrogen). The final cell pellet was frozen

at -80°C for qRT-PCR studies or cultured in DMEM/F12 supplemented with 10% FBS for GC spreading and adhesion studies. For qRT-PCR studies, human recombinant FSH was obtained from Dr. A.F. Parlow (National Hormone and Peptide Program, National Institute of Diabetes and Digestive and Kidney Diseases). Forskolin was purchased from Sigma Chemical Co.

2.2.4 RNA Isolation and qRT-PCR

Frozen pellets of GCs were solubilized in TRIzol (Invitrogen), and RNA was isolated according to the manufacturer's protocol. RNA was further treated with DNase I, then reverse-transcribed using Superscript II (Invitrogen). Complementary DNA (cDNA) levels were detected using qRT-PCR with the ABI PRISM 7900 Sequence Detection System (Applied Biosystems) and SYBR Green I dye (Applied Biosystems). Primers were generated using Primer Express Software (Version 2.0; Applied Biosystems) (). Fold-changes in gene expression were determined by quantitation of cDNA from target (treated) samples relative to a calibrator sample (vehicle). The gene for ribosomal protein L7 (*Rpl7*) was used as the endogenous control for normalization of initial RNA levels. Expression ratios were calculated according to the mathematical model described by Pfaffl (19), where $\text{ratio} = (E_{\text{target}})^{\Delta\text{Ct}(\text{target})} / (E_{\text{control}})^{\Delta\text{Ct}(\text{control})}$ and E = efficiency of the primer set, calculated from the slope of a standard curve of $\log(\text{ng of cDNA})$ versus cycle threshold (Ct) for a sample that contains the target according to the formula $E = 10^{-(1/\text{slope})}$ and $\Delta\text{Ct} = \text{Ct}_{(\text{vehicle})} - \text{Ct}_{(\text{treated sample})}$. Three independent experiments were carried out, and the results were averaged for statistical analysis by a one-way ANOVA followed by a Tukey multiple comparison post-hoc test (**Figure 2-1**) or by a two-tailed unpaired Student t-test (**Figure 2-2**).

Table 2-2: Primer sequences used for quantitative RT-PCR.

Gene	Forward Primer	Reverse Primer
<i>MOUSE</i>		
<i>Rpl7</i>	5' – AGCTGGCCTTTGTCATCAGAA – 3'	5' – GACGAAGGAGCTGCAGAACCT – 3'
<i>Epha1</i>	5' – CCTGGAGGGAATCTGAGCTATG – 3'	5' – CCTGGGTTCCAACACCATCT – 3'
<i>Epha2</i>	5' – CCAGGAAGGCTACGAGAAGG – 3'	5' – TCAGATGCCTCAGACTTGAAG – 3'
<i>Epha3</i>	5' – CCGCAGTCAGCATCACAACT – 3'	5' – TTCTGGAAGTCCGATCTTCTTAA – 3'
<i>Epha4</i>	5' – GACAACGATGCAGCCTCCAT – 3'	5' – TCTCGTTGACATTAGAAATCAA – 3'
<i>Epha5</i>	5' – GCTGGTCCCATTGGGAAAT – 3'	5' – CACATTGGTGACTGGAGAAGGA – 3'
<i>Epha6</i>	5' – CTCCCAAGCCATTCACAGCTAT – 3'	5' – GCCCAGTCCTTCTCATCATAACC – 3'
<i>Epha7</i>	5' – TCTTCGCTGCTGTTAGCATCA – 3'	5' – GCAGTACTCGCTCCTTCATGACT – 3'
<i>Epha8</i>	5' – CTCGGATGAAGAGAAGATGCATT – 3'	5' – TGGTTCAAGGGCAAGAAGACA – 3'
<i>Ephb1</i>	5' – CAAGATGTGTTTCCAGACTCTGACA – 3'	5' – TGCCGAGCCAGCAATCA – 3'
<i>Ephb2</i>	5' – ACCTCAGTTCGCCTCTGTGAA – 3'	5' – GGCTCACCTGGTGCATGAT – 3'
<i>Ephb3</i>	5' – AGCGGGTTACGGACAGTATAGC – 3'	5' – AGCTGCTGGGCACCTGAA – 3'
<i>Ephb4</i>	5' – GATCCTCACGGAATTCATGGA – 3'	5' – ACTGTGAACTGCCCGTCGTT – 3'
<i>Ephb6</i>	5' – GGCAGCAGCCATCAATGTC – 3'	5' – GGCTCACCTGGTGCATCAC – 3'
<i>Efna1</i>	5' – AGTGCTTGAAGCTGAAGGTGA – 3'	5' – TCTTCTCCTGTGGGTTGACAT – 3'
<i>Efna2</i>	5' – TTTTCCCTGGGCTTTGAGTTC – 3'	5' – GGGTCGGTCCACGAGGTT – 3'
<i>Efna3</i>	5' – TGCCGGCCAAGAATACTACTACA – 3'	5' – ACCTTCATCCTCAGACACTTCCA – 3'
<i>Efna4</i>	5' – GGCCGGTGCCTGAGACT – 3'	5' – CCCGGACGTACCGCTTT – 3'
<i>Efna5</i>	5' – TCTGCAATCCCAGACAACGGAAGA – 3'	5' – TCATGTACGGTGTTCATCTGCTGGT – 3'
<i>Efnb1</i>	5' – TCGCACCCGCACTATGAA – 3'	5' – TCAACTGCTCGGGTGTGACA – 3'
<i>Efnb2</i>	5' – CAGACAAGAGCCATGAAGATCCT – 3'	5' – GACCGTGATTCTGGCTGAT – 3'
<i>Efnb3</i>	5' – CAGAGGCATGAAGGTGCTTCT – 3'	5' – GCATTTTCAGACACAGGTTTTTCG – 3'

RAT

<i>Rpl7</i>	5' – CGCTGCGCCAGGAACCCTTA – 3'	5' – GCCTTTCGCAGTGTCTTCAGGGC – 3'
<i>Epha5</i>	5' – TCCTTGCTCACACAAACTATACCT – 3'	5' – TACATTTACAGACACATACTGCCG – 3'
<i>Ejma5</i>	5' – TGGAAGAAGATCCTGCCTAAAGC – 3'	5' – CGATCACGAACACCTATAGTTTTCA – 3'

2.2.5 Immunofluorescence

Dissected ovaries were immediately embedded in Cryomatrix (Fisher Scientific, Inc.) and frozen using liquid nitrogen. Tissues were cut into sections (section thickness, 6 μm), mounted onto slides (Fisher), and stored at -20°C until use. Sections were fixed with 4% formaldehyde for 10 min, rinsed three times with PBS, then permeabilized with 0.1% Triton X-100 for 15 min. Sections were again rinsed three times with PBS, blocked for 30 min with blocking solution (5% BSA in 0.1% Triton X-100), then rinsed three times with blocking solution. The tissue was then incubated for 1 h with primary antibody specific to each target—namely, rabbit anti-EFNA5 (1:50; sc-20722; Santa Cruz Biotechnology, Inc.), rabbit anti-EPHA5 (1:50; ab5397-100; Abcam), and rabbit anti-pan-cadherin (1:100; ab6529; Abcam). Sections were then rinsed three times in blocking solution and incubated in secondary antibody (fluorescein isothiocyanate-conjugated goat anti-rabbit secondary antibody, 1:250; F9887; Sigma). The tissue was then rinsed twice in PBS followed by a 5 min incubation in 4',6-diamidino-2-phenylindole (1:1000; Sigma), and slides were mounted with VECTASHIELD (Vector Laboratories). Slides were stored at 4°C and visualized the following day with an AX70 Provis upright microscope (Olympus). Images were captured using Image-Pro 6.2 software (Media Cybernetics).

2.2.6 Cell Spreading and Adhesion Assays

Cell spreading and adhesion assays were based on similar assays used by others (20-23) to study the effects of Eph-ephrin interactions on cell rounding, spreading, and adhesion. In these assays, recombinant ephrin ligand or Eph receptor protein is spotted onto tissue-culture plastic, after which cells are seeded onto the plates and allowed to attach. Rounding or adhesion is then quantified within the spotted area. In the present experiments, both primary mouse GCs and GFSHR-17 cells were used.

In these assays, recombinant human EFNA5/human Fc (immunoglobulin [Ig] G) chimera (374-EA; R&D Systems), rat EPHA5/human Fc chimera (541-A5; R&D Systems), or human Fc (IgG; 009-000-008; Jackson ImmunoResearch) was used. (Eph-ephrin recombinant proteins are commercially available only as Fc-fusion proteins, which

interact with the preclustering antibodies.) Each of these recombinant proteins was first preclustered before application to tissue-culture surfaces by combining Fc with F(ab')₂ fragment rabbit anti-human IgG antibody (Fc γ fragment specific; 309-006-008; Jackson ImmunoResearch) at a 5:1 molar ratio followed by gentle agitation at room temperature for 2 h. Preclustering of recombinant Eph receptor and ephrin fusion proteins is necessary to activate either the ephrin ligands or the Eph receptors, because this mimics the membrane Eph receptor or ephrin ligand clustering that occurs in vivo upon activation (24-26). Serial dilutions in PBS were then prepared as follows: EFNA5/Fc at 74, 37, 18.5, and 9.25 $\mu\text{g}/\text{mL}$ for the cell rounding/spreading assay and EPHA5/Fc at 83, 42, 21, and 10 $\mu\text{g}/\text{mL}$ for the cell adhesion assay. These concentrations were chosen based on those used by Yin et al. (23) in similar experiments and resulted in equimolar amounts of EFNA5 and EPHA5 in each dilution. Droplets (3.5 μl) of preclustered Fc or EFNA5/Fc or EPHA5/Fc were placed onto a 60-mm tissue-culture dish (Sarstedt) and incubated at 37°C for 1.5 h to allow the protein to adsorb to the tissue-culture surface. For both assays, serial dilutions of the Fc (IgG) fragment were also spotted to correspond to each concentration of EFNA5/Fc or EPHA5/Fc to control for differences in the number of micrograms of protein spotted at each concentration; however, only the highest Fc concentration is reported as the control in **Figure 2-4**, **Figure 2-5**, **Figure 2-6**, and **Figure 2-7** because no differences in either cell shape (see **Figure 2-4** and **Figure 2-5**) or cell adhesion (**Figure 2-6** and **Figure 2-7**) were observed between the different Fc (IgG) dilutions. Droplets were outlined using fine permanent marker on the underside of the dish to distinguish between treated and untreated areas, and the dish was rinsed twice with 4 mL of ice-cold PBS to remove nonadsorbed EFNA5/Fc or EPHA5/Fc. The dish was then seeded with 1.4 million cells in a 4-mL volume of DMEM/F12 containing 10% FBS. Cells were incubated at 37°C with 5% CO₂ for 2 h to allow the cells to adhere and spread. (The minimum time required to observe maximal cell spreading [i.e., 2 h] had been previously determined experimentally). Cells were then rinsed twice with PBS to remove media and nonadhered cells and fixed in 4% paraformaldehyde in PBS for 10 min at room temperature.

Quantitation of the effects of recombinant EFNA5/Fc on cell spreading. One 100 \times image (1020 \times 768 μm) was taken from the center of each spotted region using an IX70

microscope attached to an DP71 camera (both from Olympus). All cells within one 100× field were visually scored as being “spread” (characterized by the presence of lamellipodia) or “round” (characterized by round morphology and complete absence of lamellipodia). The fraction of spread cells was determined by dividing the number of spread cells in each image of the EFNA5/Fc surface by the number of spread cells in the image from the control Fc (IgG) surface. Three independent experiments were carried out, and the results (**Figure 2-4** and **Figure 2-5**) were analyzed for statistical significance by a one-way ANOVA followed by a Tukey multiple comparison post-hoc test. Quantitation was based, as described, on an image taken from the center of the spotted region (**Figure 2-6A**, asterisk).

Quantitation of the effects of recombinant EPHA5/Fc on cell adhesion. The total number of cells within one 100× field image obtained from the EPHA5/Fc surface was divided by the number of cells on the control Fc (IgG) surface, resulting in a value of one for the Fc-coated plates and fractions of one for the EPHA5/Fc surfaces. Note that the exact images in **Figure 2-6** were not used for quantitation; they are presented to show the dramatic difference in adhesion between EPHA5-coated and noncoated regions. Three independent experiments were carried out, and the results (see **Figure 2-6** and **Figure 2-7**) were analyzed for statistical significance by a one-way ANOVA followed by a Tukey multiple comparison post-hoc test.

2.2.7 Human Phospho-Kinase Array

To screen for potential downstream targets of EFNA5-induced signaling in GCs, such as the phosphorylation of kinases and their protein substrates, we used the Human Phospho-Kinase Array Kit (ARY003B; R&D Systems), which simultaneously detects the relative site-specific phosphorylation of 46 phosphorylated proteins or their targets (**Supplemental Table 6-1**). GFSHR-17 cells were seeded onto tissue-culture surfaces coated with EFNA5/Fc or Fc alone, and lysates were harvested at 15 and 20 min after seeding. We chose 15- and 20-min time points based on a search of the literature, which indicated that many of the signaling elements captured by the array exhibit maximum phosphorylation within 15 min of stimulation. These lysates were applied to the Human Phospho-Kinase Arrays, which were then developed according to the manufacturer's

instructions. Spot intensities were also quantified using ImageJ software (National Institutes of Health, <http://rsb.info.nih.gov/ij/>) according to the manufacturer's directions.

2.2.8 Immunoblot Analysis: Beta-Catenin

The EFNA5/Fc or Fc (IgG) were preclustered before application to tissue-culture surfaces by combining with F(ab')₂ fragment rabbit anti-human IgG antibody (Fc γ fragment specific) at a 5:1 molar ratio followed by gentle agitation at room temperature for 2 h. The preclustered recombinant protein was then used to coat 60-mm tissue-culture dishes and incubated at 37°C for 1.5 h, then rinsed twice with 4 mL of ice-cold PBS. The dish was then seeded with 2.1 million GFSHR-17 cells in a 4-mL volume of DMEM/F12 containing 5% FBS. Cells were incubated at 37°C with 5% CO₂ for 15 and 20 min. At each time point, lysates were generated by placing the dishes on ice, gently rinsing the cells twice with ice-cold PBS, and scraping the cells in 100 μ l of ice-cold RIPA buffer (50 mM Tris-HCl [pH 8.0], 150 mM NaCl, 1% Triton X-100, 0.5% sodium deoxycholate, and 0.1% SDS) supplemented with a protease inhibitor cocktail (1:100; P8340; Sigma) and a phosphatase inhibitor cocktail (1:100; P2850; Sigma). Lysates were then transferred to a 1.5-mL microcentrifuge tube, incubated on ice for 20 min with mild agitation, and then centrifuged at 15000 \times g for 20 min at 4°C. The supernatant was boiled in Laemmli buffer for 5 min and then analyzed using SDS-PAGE. The separated proteins were transferred to a polyvinylidene fluoride membrane at 100 V (constant voltage) for 2 h at 4°C. After blocking for 1 h in Tris-buffered saline and Tween 20 (TBST)/5% nonfat milk, the membrane was probed with rabbit IgG specific to beta-catenin (1:1000 in TBST/5% nonfat milk; D10A8; Cell Signaling). The membrane was then probed with horseradish peroxidase-conjugated donkey IgG against rabbit IgG (1:10000 in TBST/5% nonfat milk) and visualized using ECL Plus (Amersham Biosciences) and Hyperfilm (Amersham). To assess equal protein loading, the membrane was subsequently probed using a rabbit monoclonal IgG against histone deacetylase 4 (HDAC4, sc-11418; Santa Cruz Biotechnology, Inc.). Densitometric analysis of immunoblot data (ImageLab 4.1; Bio-Rad) was then carried out to quantitate the ratio of beta-catenin:HDAC4.

2.3 Results

2.3.1 Identification of FSH-Regulated Ephrin Ligands and Eph Receptors in Mouse GCs

To determine if FSH regulates Eph-ephrin expression in GCs of immature PND 23–28 female mice, we initially screened the mRNA levels of all known mouse ephrin (*Efn*) and Eph receptor (*Eph*) genes in GCs isolated from immature female mice treated for 48 h with either saline or 5.0 IU of eCG (**Supplemental Figure 6-1** and **Supplemental Figure 6-2**). Eph-ephrin gene expression was determined by qRT-PCR. Based on this screening, we chose a subset of *Efn* and *Eph* genes that appeared to be regulated by eCG to further verify and to investigate the possibility of a dose-dependent response to eCG. To do this, we purified mRNA from GCs isolated from immature female mice treated for 48 h with either saline, 3.25 IU of eCG, or 5.0 IU of eCG. Eph-ephrin gene expression was again determined by qRT-PCR. We verified that the mRNA levels of one *Efn* gene and three *Eph* genes were significantly increased by eCG (**Figure 2-1**). At 3.25 IU of eCG, significant increases in the ephrin ligand *Efna5* and the Eph receptors *Epha5* and *Epha3* (**Figure 2-1, A, B, and D**) were observed. At 5.0 IU of eCG, significant increases in *Efna5*, *Epha5*, *Ephb2*, and *Epha3* (**Figure 2-1, A–D**) were observed, along with an apparent increase in *Epha8*, though the effect was not significant ($P = 0.08$ by Student t-test). To demonstrate that these eCG-dependent increases in *Efna5*, *Epha5*, *Ephb2*, and *Epha3* were specific to this subset of Eph-ephrin family members—that is, that eCG did not affect the expression of all Eph-ephrin family members—we also examined the mRNA levels of the ligand *Efna1* and the Eph receptor *Epha2* (**Figure 2-1F**) in response to eCG. *Efna1* mRNA levels did not increase in response to 5.0 IU of eCG; in fact, a significant decrease was observed ($P < 0.01$). In addition, expression of *Epha2* was not significantly changed in response to eCG treatment (**Figure 2-1F**). These results indicate that FSH increases the expression of a subset of ephrin ligands and Eph receptors in GCs of immature mice.

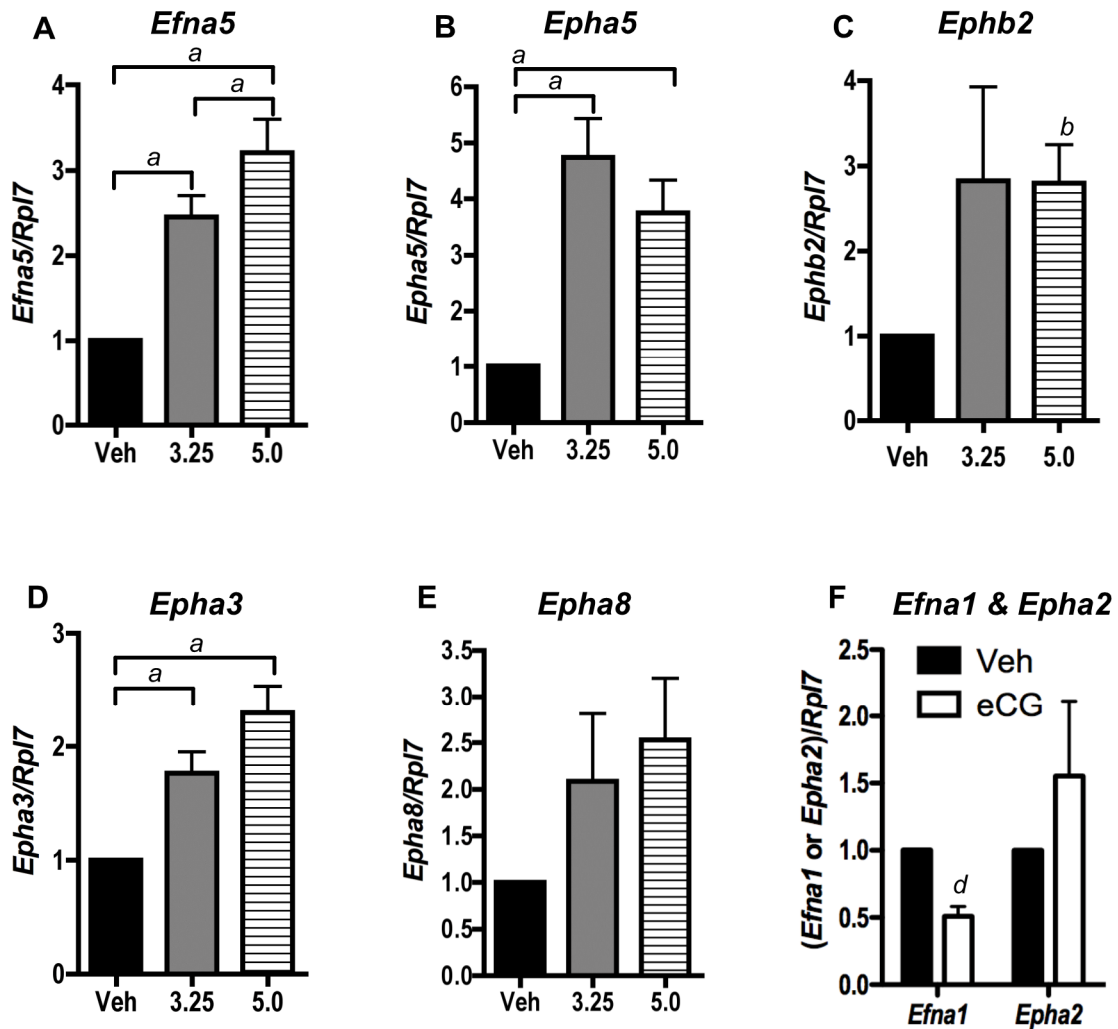


Figure 2-1: Expression of a subset of ephrin ligands and Eph receptors is stimulated by FSH in mouse GCs.

Wild-type PND 23–28 C57Bl/6 mice were treated with saline or eCG (3.25 or 5.0 IU/mouse) for 48 h. GCs were isolated by ovarian puncture and pooled, and then mRNA was isolated. The mRNA levels of *Efnal* (A), *Ephal* (B), *Ephb2* (C), *Ephal3* (D), and *Ephal8* (E) as determined by qRT-PCR were compared to an *Rpl7* control. *Efnal* and *Ephal2* were similarly analyzed (F) to indicate that not all Eph-ephrin ligand and receptor mRNA levels are increased by eCG. Data represent the gene expression compared with the *Rpl7* control and are presented as the average \pm SEM of three independent experiments. Differences in average mRNA levels between vehicle treatment and 3.25 or 5.0 IU of eCG were analyzed by a one-way ANOVA followed by a Tukey multiple

comparison post-hoc test (Tukey test). **A) *Efna5***. A statistically significant difference was found between the three treatments as determined by one-way ANOVA ($F_{2,6} = 18$, $P = 0.003$). Tukey test revealed that statistically significant differences between vehicle and 3.25 IU of eCG ($a: P < 0.05$), between vehicle and 5.0 IU of eCG ($a: P < 0.05$), and between 3.25 and 5.0 IU of eCG ($a: P < 0.05$). **B) *Epha5***. A statistically significant difference was found between the three treatments as determined by one-way ANOVA ($F_{2,6} = 14$, $P = 0.006$). Tukey test revealed statistically significant differences between vehicle and 3.25 IU of eCG ($a: P < 0.05$), between vehicle and 5.0 IU of eCG ($a: P < 0.05$), but not between 3.25 and 5.0 IU of eCG. **C) *Ephb2***. No statistically significant difference was found between the three treatments as determined by one-way ANOVA, but comparison of means between vehicle and 3.25 or 5.0 IU of eCG by a two-tailed unpaired Student *t*-test revealed a statistically significant difference between vehicle and 5.0 IU of eCG ($b: P < 0.02$). **D) *Epha3***. A statistically significant difference was found between the three treatments as determined by one-way ANOVA ($F_{2,6} = 14$, $P = 0.005$). Tukey test revealed statistically significant differences between vehicle and 3.25 IU of eCG ($P < 0.05$), between vehicle and 5.0 IU of eCG ($P < 0.05$), but not between 3.25 and 5.0 IU of eCG. **E) *Epha8***. No statistically significant difference was found between the three treatments as determined by one-way ANOVA. **F) *Efna1* and *Epha2***. Not all Ephrin ligand and receptor mRNA levels are increased by eCG. Data represent the gene expression compared with the *Rpl7* control and are presented as the average \pm SEM of three independent experiments. Differences in average mRNA levels between vehicle treatment and 5.0 IU of eCG were analyzed by a two-tailed unpaired Student *t*-test ($d: P < 0.01$).

2.3.2 FSH and cAMP Regulate *Efna5* and *Epha5* Expression in a Rat GC Line

To determine if FSH increased the expression of *Efna5*, *Epha3*, *Epha5*, *Epha8*, and *Ephb2* in a species other than mouse, we treated GFSHR-17 cells (an immortalized, FSH-responsive cell line derived from primary rat GCs (18)) with human recombinant FSH (50 ng/mL) for 24 or 48 h and determined mRNA levels by qRT-PCR (**Figure 2-2**). Of the five Eph-ephrin family members increased by eCG in primary GCs (**Figure 2-1**), we found that expression of two of these genes, *Efna5* and *Epha5*, increased in response to FSH in GFSHR-17 cells (**Figure 2-2, A and B**). Indeed, *Efna5* mRNA levels were increased after 24 and 48 h of FSH treatment (**Figure 2-2A**), whereas *Epha5* mRNA levels (**Figure 2-2B**) increased only after 24 h of FSH treatment. Because FSH regulates many of its target genes in GCs via the cAMP-dependent protein kinase A (PKA) pathway (27), we next wanted to determine if forskolin, a direct activator of adenylate cyclase, would increase *Efna5* and *Epha5* mRNA levels in GFSHR-17 cells. Again, *Efna5* mRNA levels were increased after 24 and 48 h of forskolin treatment (**Figure 2-2C**), whereas *Epha5* mRNA levels (**Figure 2-2D**) increased only after 24 h of forskolin treatment. We also investigated whether any of the other eCG-responsive Eph-ephrin family members identified in **Figure 2-1** responded to forskolin in GFSHR-17 cells, but only *Efna5* and *Epha5* mRNA levels were affected. These results indicate that *Efna5* and *Epha5* are increased by FSH in both mouse and rat GCs and that this increase is mediated, at least in part, through a cAMP-dependent pathway. Because *Efna5* and *Epha5* were the two Eph-ephrin family members from our screen that were both expressed in both mouse and rat GCs and were regulated by FSH and cAMP in both model systems, we chose to further investigate the localization and function of these genes during the rest of the present study.

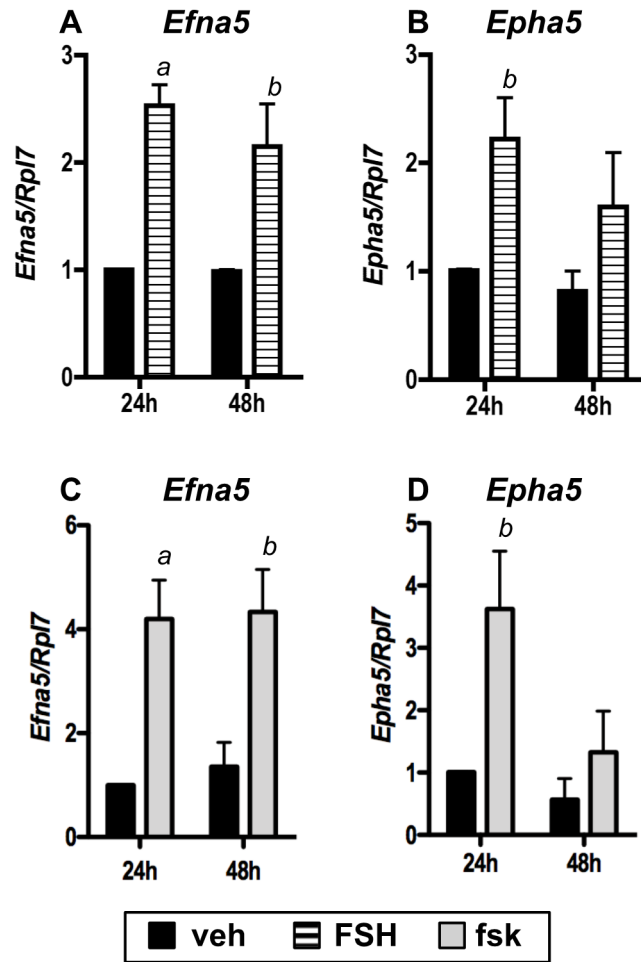


Figure 2-2: FSH and forskolin increase *Efna5* and *Epha5* mRNA levels in the immortalized rat GC line GFSHR-17.

GFSHR-17 cells were treated for 24 and 48 h with recombinant FSH (50 ng/mL; **A** and **B**) or forskolin (fsk; 10 μ M; **C** and **D**), and mRNA levels of *Efna5* and *Epha5* were determined by qRT-PCR and compared to an *Rpl7* control. Data are presented as the mean \pm SEM of three independent experiments. Differences in average mRNA levels between vehicle treatment (veh) and fsk or FSH were analyzed by a two-tailed unpaired Student *t*-test (*a*: $P < 0.01$; *b*: $P < 0.05$).

2.3.3 Localization of EFNA5 and EPHA5 in the Mouse Ovary

Quantitative RT-PCR experiments indicated that *Efna5* and *Epha5* mRNA was present within mouse primary GCs. Therefore, we wanted to investigate EFNA5 and EPHA5 protein localization within the whole mouse ovary using immunofluorescence (**Figure 2-3**). To investigate EFNA5 and EPHA5 localization in follicles of various sizes and in the corpus luteum, immature mice were exposed to one of the following three treatments: saline for 48 h, 5.0 IU of eCG for 48 h, or 5.0 IU of eCG for 48 h followed by 5.0 IU of hCG for 24 h.

EFNA5 (**Figure 2-3, A, C, E, G, and I**) localized to the periphery (**Figure 2-3, G and I**) of GCs in a punctate pattern (**Figure 2-3I**) in follicles ranging in size from primary to preovulatory. Small preantral follicles generally expressed less EFNA5 (**Figure 2-3A**, arrowhead) than larger preantral or antral follicles. In both preantral and antral follicles, we frequently observed that EFNA5 immunoreactivity was higher in mural GCs than in cumulus cells (**Figure 2-3, A and G**), and this difference often appeared as a gradient, with EFNA5 density being highest near the basement membrane and lowest near the antrum (**Figure 2-3G**, arrow). Interestingly, EFNA5 immunoreactivity was lower in corpora lutea (**Figure 2-3E**) than in preantral and antral follicles. Weak EFNA5 staining was also observed in the theca and interstitial cells (**Figure 2-3C**).

Localization of EPHA5 was similar to that of EFNA5, with immunoreactivity localized to the periphery of GCs in follicles ranging in size from primary to preovulatory (**Figure 2-3 B, D, F, H, and I**), again with weaker staining in smaller follicles (**Figure 2-3B**, arrowhead). However, staining appeared to be uniform around the GC periphery, without the punctate appearance that characterized EFNA5 (compare **Figure 2-3, I vs. J**). Finally, EPHA5 immunoreactivity appeared to be weaker in corpora lutea than in preantral or antral follicles (**Figure 2-3F**). Weak EPHA5 staining was also observed in the theca and interstitial cells (**Figure 2-3D**).

To verify that EFNA5 and EPHA5 localized to the GC membrane, we stained ovarian sections with a pan-cadherin antibody (**Figure 2-3, K and L**) to detect the transmembrane cadherin proteins that form adherens junctions between GCs. We

observed similar localization of both EFNA5 and EPHA5 and pan-cadherin (compare **Figure 2-3, A and B vs. K, and G and H vs. L**), indicating that both EFNA5 and EPHA5 are membrane-localized in GCs.

Note that for each primary antibody, no signal was observed in sections stained with secondary antibody alone, indicating the signal we observed was not due to nonspecific binding of the secondary antibody (data not shown).

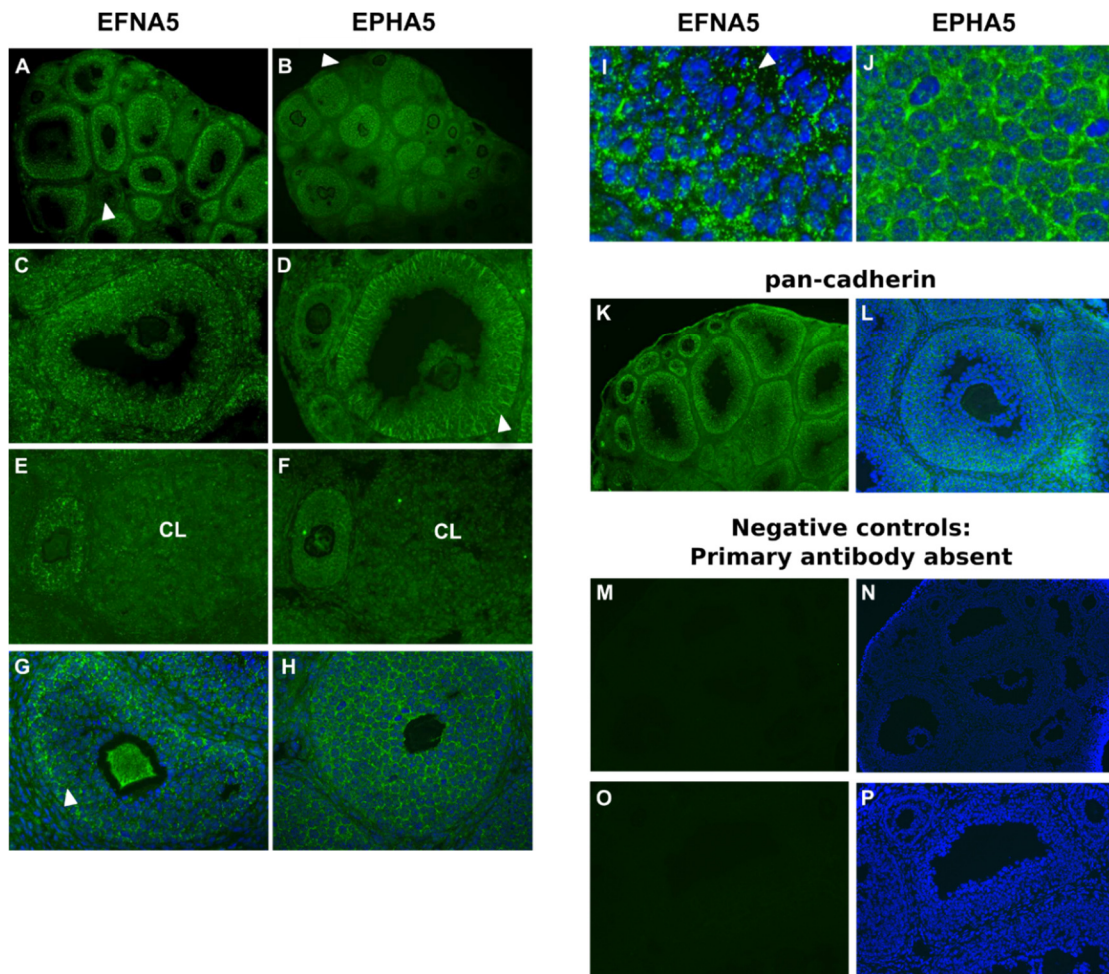


Figure 2-3: Localization of EFNA5 and EPHA5 in the mouse ovary.

Immature mice were treated either with saline for 48 h (**A** and **B**), eCG for 48 h (**C**, **D**, **G**, **H**, **K**, **L**, **M**, **N**, **O**, and **P**), or eCG for 48 h followed by hCG for 24 h (**E** and **F**). Ovaries were isolated and frozen, and EFNA5 and EPHA5 localization was determined by immunofluorescence with anti-EFNA5 and anti-EPHA5 antibodies. A pan-cadherin antibody was also used to detect membrane localization within the ovary (**I** and **J**). EFNA5 was found in the periphery of GCs of small primary to large antral follicles (**A**, **C**, **E**, **G**, and **I**) and often took on a punctate appearance (arrowhead in **I**). Expression was lower in small preantral follicles (arrowhead in **A**) than in larger preantral or antral follicles. EFNA5 expression was reduced in corpora lutea (**E**). We observed similar localization of both EFNA5 (**A** and **B**) and pan-cadherin (**K** and **L**). Weak EFNA5 staining was also observed in the theca and interstitial cells (see, e.g., **A** and **C**). No

EFNA5 signal was observed in sections stained with secondary antibody alone, indicating the EFNA5 signal observed was not due to nonspecific binding of the secondary antibody (FITC: **M and O**) and (FITC + DAPI merge: **N and P**). EPHA5 was localized to the periphery of GCs in follicles from primary to preovulatory (**B, D, F, H, and J**), with weaker staining in small follicles (arrowhead in **B**). EPHA5 expression was weaker in corpora lutea than in larger preantral or preovulatory follicles (**F**). Weak EPHA5 staining was also observed in the theca and interstitial cells. EFNA5 and EPHA5 immunoreactivity was stronger in mural GCs than in cumulus cells of antral follicles (arrowhead in **D and G**). We observed similar localization of both EPHA5 (**B and H**) and pan-cadherin (**K and L**). No EPHA5 signal was observed in sections stained with secondary antibody alone (**M, N, O, P**), indicating the EPHA5 signal observed was not due to nonspecific binding of the secondary antibody. Original magnification $\times 100$ (**A, B, M, and N**), $\times 200$ (**C–H and L, O, and P**), and $\times 400$ (**I and J**).

2.3.4 Inhibition of GC Spreading by EFNA5/Fc

Although ephrins have been previously identified in the ovary, no functional role for ephrins in GCs has been shown. Therefore, we investigated what roles Eph-ephrin signaling may play in GC morphology or function. Because Eph-ephrin signaling inhibits spreading and causes cell rounding in vitro in other cell types (20,28), and because FSH induces GC rounding in both cultured primary cells (1) and GFSHR-17 cells (18), we investigated the effect of EFNA5 on GC morphology using both GFSHR-17 and primary mouse GCs. To do this, we used a cell spreading assay used previously by others (20-23) to study the effects of Eph-ephrin interactions on cell rounding, spreading, and adhesion in other cell types. Specifically, we seeded GFSHR-17 cells onto tissue-culture surfaces spotted with serial dilutions of a recombinant human EFNA5/Fc chimera (74, 37, 18.5, and 9.25 $\mu\text{g}/\text{mL}$) or onto surfaces spotted with Fc alone as a negative control (**Figure 2-4, A and B**). GFSHR-17 cells plated onto the EFNA5/Fc surface were notably rounder and less spread (having fewer lamellipodia) than those on the Fc-coated surface (**Figure 2-4, A and B**). To quantitate the extent of cell spreading, we visually scored each cell as exhibiting either a rounded or a spread morphology (see Materials and Methods for details). We then calculated the ratio of rounded (nonspread) cells to the total number of cells scored (**Figure 2-4A**, bar graph). Spreading was significantly inhibited on EFNA5/Fc-coated surfaces but not on Fc-coated surfaces. The number of rounded cells increased approximately 3-fold on the 74 and 37 $\mu\text{g}/\text{mL}$ of EFNA5/Fc-coated surfaces compared to Fc alone (**Figure 2-4A**, bar graph). To determine if this EFNA5-induced cell rounding could be observed in primary GCs, we conducted an identical experiment with primary GCs isolated from untreated immature mice. Again, EFNA5/Fc significantly inhibited cell spreading and increased cell rounding, although to a lesser extent than GFSHR-17 cells (**Figure 2-5A**, bar graph; compare to **Figure 2-5A** to **Figure 2-4A**). At an EFNA5/Fc concentration of 74 $\mu\text{g}/\text{mL}$, the number of rounded primary GCs was approximately 2-fold higher than when plated onto Fc alone (**Figure 2-5**). Thus, EFNA5 reduces cell spreading of both a rat GC line and primary mouse GCs.

2.3.5 Inhibition of GC-Substrate Adhesion by EPHA5

Given that GCs express both ephrin ligands and Eph receptors, and given that Eph-ephrin signaling regulates cellular adhesion (29), we wanted to determine the effect of EPHA5 signaling on GFSHR-17 and primary mouse GC adhesion (**Figure 2-6** and **Figure 2-7**). The coating/spotting technique in this experiment was similar to that used for the EFNA5/Fc cell spreading experiments (**Figure 2-4** and **Figure 2-5**), with serial dilutions of EPHA5/Fc (83, 42, 21, and 10 $\mu\text{g}/\text{mL}$). GFSHR-17 cells were seeded onto tissue-culture surfaces spotted with dilutions of EPHA5/Fc or Fc alone. We noticed a dramatic and significant reduction in cells adhering to the EPHA5/Fc-coated surface compared to those coated with Fc alone (**Figure 2-6A**) that occurred in an EPHA5/Fc dose-dependent manner (**Figure 2-6B**). We quantified the extent of this reduced adhesion by counting the number of cells in the center of the EPHA5/Fc-coated surface (**Figure 2-6B**) and comparing this to the total number of adherent cells on the Fc-coated surface (EPHA5-Fc:Fc ratio). As the coating density of EPHA5/Fc was reduced, the number of cells adhering to the coated surface increased (**Figure 2-6B**). We were then curious to know if EPHA5 would also inhibit adhesion of primary mouse GCs. Using a similar procedure, primary mouse GCs were plated onto EPHA5/Fc-coated surfaces, and the number of adherent cells was again counted (**Figure 2-7**). As observed for the GFSHR-17 cell line, cell adhesion was significantly reduced by approximately 70% at the highest concentration of EPHA5/Fc (83 $\mu\text{g}/\text{mL}$), resulting in an inverse relationship between cell adhesion and EPHA5/Fc concentration (**Figure 2-7B**). These results suggest that EPHA5, acting through ephrin ligands present on GC membranes, can alter the adhesive properties of both mouse and rat GCs.

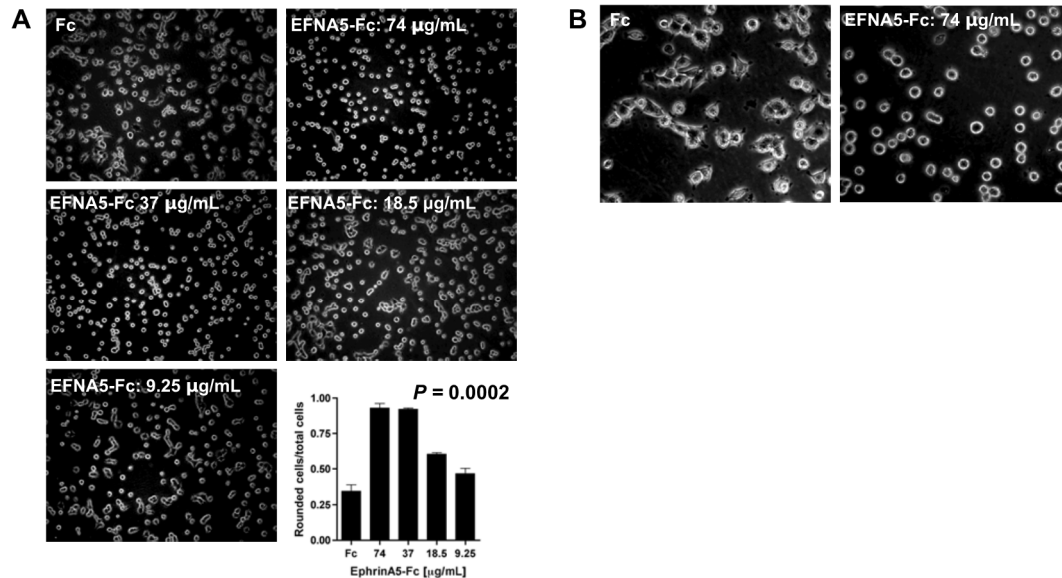


Figure 2-4: EFNA5 inhibits spreading and induces rounding of immortalized rat GCs.

GFSHR-17 cells were seeded onto tissue-culture plates that had been previously spotted with serial dilutions of a recombinant human EFNA5/Fc chimera or the Fc fragment alone (**top left**) as a negative control. GFSHR-17 cells displayed significantly less spreading and a more rounded morphology when plated onto EFNA5/Fc-coated surfaces compared to Fc-coated surfaces, as determined by the absence of lamellipodia (**A**: 9.25–74 µg/mL; **B**: 74 µg/mL only). The fraction of rounded cells was quantified by dividing the number of rounded cells by the total number of cells in the field of vision at $\times 100$ (see *Materials and Methods* for further quantification details). Three independent experiments were conducted, and the difference in the ratio of rounded cells to total cells between Fc-alone and each concentration of EFNA5/Fc was plotted (**A**; bar graph shows average \pm SEM). Differences in the average ratio of rounded cells to total cells were analyzed for all conditions by a one-way ANOVA followed by a Tukey test. A statistically significant difference was found between the five conditions as determined by one-way ANOVA ($F_{4,5} = 64$, $P = 0.0002$). Tukey test revealed numerous statistically significant ($P < 0.05$) differences between many of the conditions. The following comparisons were statistically significant ($P < 0.05$) but are not shown on the bar graph for clarity: Fc versus 74 µg/mL, Fc versus 37 µg/mL, Fc versus 18.5 µg/mL, 74 µg/mL versus 18.5 µg/mL, 74 µg/mL versus 9.25 µg/mL, 37 µg/mL versus 18.5 µg/mL, and 37 µg/mL versus 9.25 µg/mL. Original magnification $\times 100$ (**A**) and $\times 200$ (**B**).

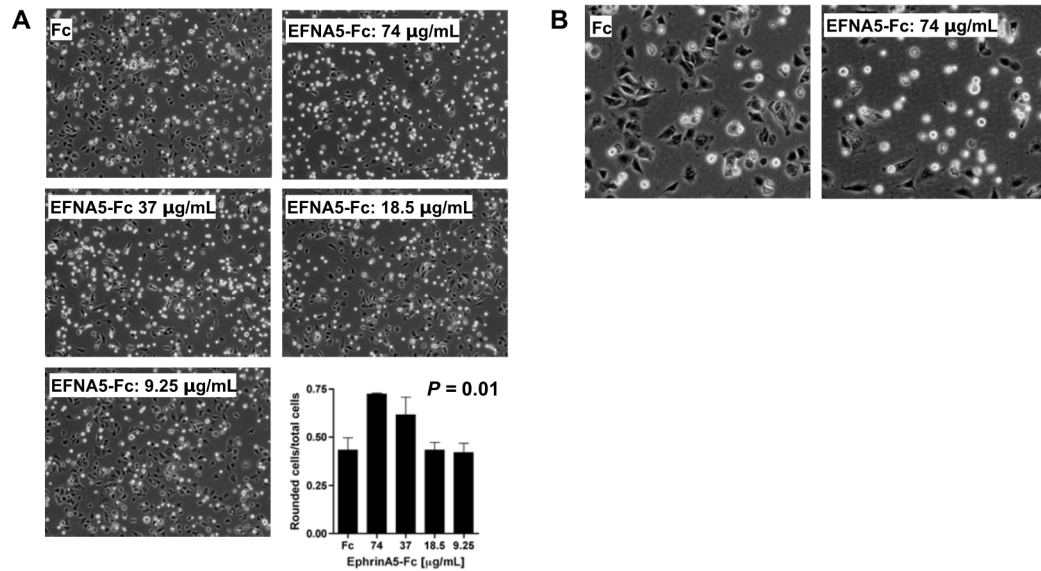


Figure 2-5: EFNA5 inhibits spreading and increases rounding of primary mouse GCs.

GCs isolated from the ovaries of immature mice were seeded onto tissue-culture plates that had been previously spotted with serial dilutions of a recombinant human EFNA5/Fc chimera or the Fc fragment alone (**top left**) as a negative control. Primary mouse GCs displayed significantly less spreading and a more rounded morphology when plated onto EFNA5/Fc-coated surfaces compared to Fc-coated surfaces, as determined by the absence of lamellipodia (**A**: 9.25–74 µg/mL; **B**: 74 µg/mL only). The fraction of rounded cells was quantified by dividing the number of rounded cells by the total number of cells counted in the field of vision at $\times 100$ (see *Materials and Methods* for further quantification details). Three independent experiments were conducted, and the difference in the ratio of rounded cells to total cells between Fc-alone and each concentration of EFNA5/Fc was plotted (**A**; bar graph shows average \pm SEM). Differences in the average ratio of rounded cells to total cells were analyzed for all conditions by a one-way ANOVA followed by a Tukey post-test. A statistically significant difference was found between the five conditions as determined by one-way ANOVA ($F_{4,10} = 6$, $P = 0.01$). Tukey post-test revealed several statistically significant ($P < 0.05$) differences between many of the conditions. The following comparisons were statistically significant ($P < 0.05$) but are not shown on the bar graph for clarity: Fc versus 74 µg/mL, 74 µg/mL versus 18.5 µg/mL, and 74 µg/mL versus 9.25 µg/mL. Original magnification $\times 100$ (**A**) and $\times 200$ (**B**).

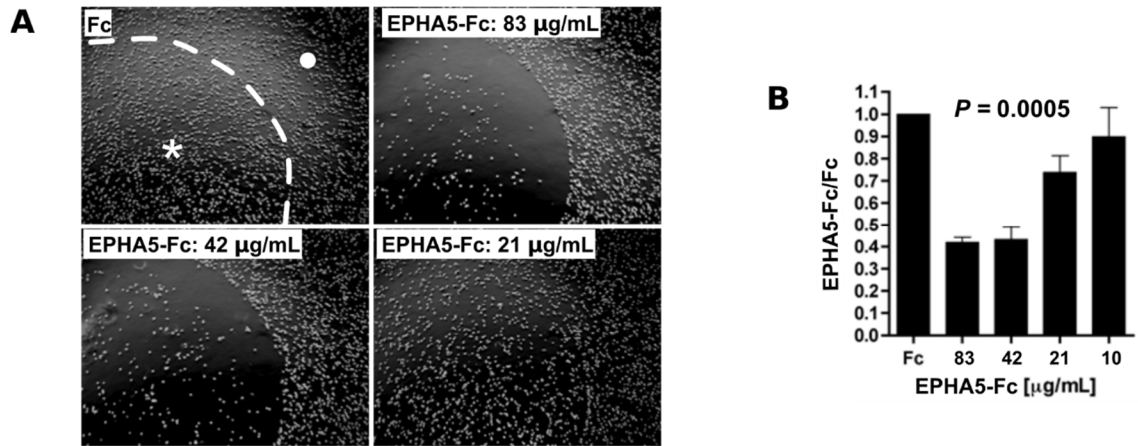


Figure 2-6: EPHA5 receptor inhibits adhesion of immortalized rat GCs to cell culture surfaces.

A) GFSHR-17 cells were plated onto tissue-culture plates previously spotted with serial dilutions of a recombinant rat EPHA5/human Fc chimera or the Fc fragment alone (**top left**) as a negative control. The spotted region is marked by an asterisk and outlined by a dotted line; the uncoated region outside the spotted area is marked by a circle. **B)** The

total number of cells within a single $\times 100$ field image obtained from the EPHA5/Fc surface was divided by the number of cells on the control Fc (IgG) surface, resulting in a value of one for the Fc-coated plates, and fractions of one for the EPHA5/Fc surfaces.

Three independent experiments were carried out, with the results presented as the average \pm SEM for statistical analysis by a one-way ANOVA followed by a Tukey test. A

statistically significant difference was found between the five conditions as determined by one-way ANOVA ($F_{4,10} = 13$, $P = 0.0005$). Tukey test revealed numerous statistically significant ($P < 0.05$) differences between many of the conditions. The following

comparisons were statistically significant ($P < 0.05$) but are not shown on the bar graph for clarity: Fc versus 83 $\mu\text{g/mL}$, Fc versus 42 $\mu\text{g/mL}$, 83 $\mu\text{g/mL}$ versus 10 $\mu\text{g/mL}$, and 42 $\mu\text{g/mL}$ versus 10 $\mu\text{g/mL}$.

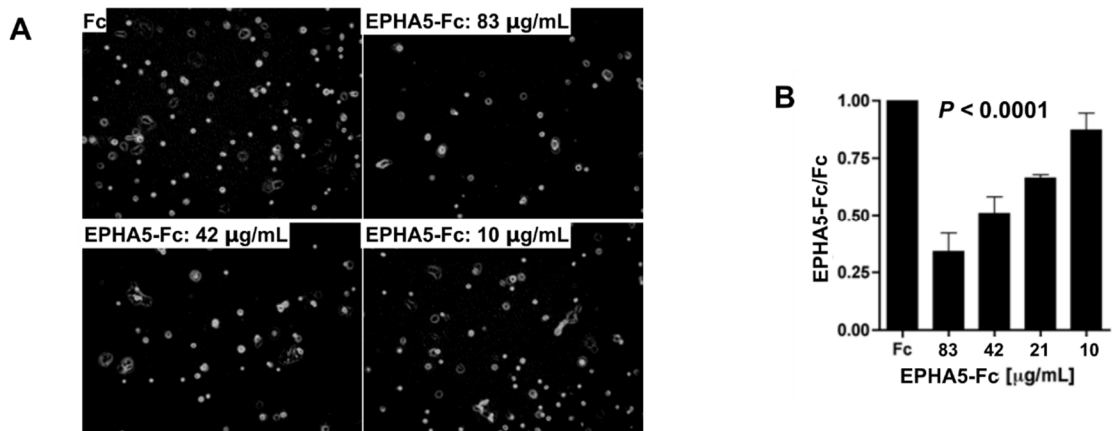


Figure 2-7: EPHA5 inhibits substrate adhesion of mouse primary GCs.

A) Primary GCs were plated onto tissue-culture plates previously spotted with serial dilutions of a recombinant rat EPHA5/human Fc chimera. Mouse primary GCs adhered less to EPHA5/Fc-coated surfaces than Fc-coated surfaces. The total number of cells attached to the EPHA5/Fc surface was divided by the number of cells on the control Fc surface, resulting in a value of one for the Fc-coated plates and fractions of one for the EPHA5/Fc surfaces. **B)** Three independent experiments were carried out, with the results presented as the average \pm SEM for statistical analysis by a one-way ANOVA followed by a Tukey test. A statistically significant difference was found between the five conditions as determined by one-way ANOVA ($F_{4,10} = 20$, $P < 0.0001$). Tukey test revealed numerous statistically significant ($P < 0.05$) differences between many of the conditions. The following comparisons were statistically significant ($P < 0.05$) but are not shown on the bar graph for clarity: Fc versus 83 $\mu\text{g/mL}$, Fc versus 42 $\mu\text{g/mL}$, Fc versus 21 $\mu\text{g/mL}$, 83 $\mu\text{g/mL}$ versus 21 $\mu\text{g/mL}$, 83 $\mu\text{g/mL}$ versus 10 $\mu\text{g/mL}$, and 42 $\mu\text{g/mL}$ versus 10 $\mu\text{g/mL}$.

2.3.6 Beta-Catenin Is a Downstream Target of EFNA5-Induced Signaling in GCs

To screen for potential intracellular targets of EFNA5-induced forward signaling in GCs, we used the Human Phospho-Kinase Array Kit, which simultaneously detects the relative site-specific phosphorylation of 46 phosphorylated proteins and/or their targets. GFSHR-17 cells were seeded onto tissue-culture surfaces coated with EFNA5/Fc (37 $\mu\text{g}/\text{mL}$) or Fc alone, and lysates were harvested at 15 and 20 min after seeding. These lysates were applied to the arrays, and the blots were processed and the spot intensities quantified according to the manufacturer's directions (**Supplemental Figure 6-3**, **Supplemental Table 6-2**, and **Supplemental Table 6-3**). Only two proteins, beta-catenin and phospho-STAT5, were observed at both 15- and 20-min time points at different levels when comparing the blots for Fc (IgG) alone versus EFNA5/Fc. Beta-catenin protein levels were reduced to 0.16 and 0.51 of control values at 15 and 20 min, respectively. Similarly, phospho-STAT5 protein levels were reduced to 0.30 and 0.58 of control values at 15 and 20 min, respectively.

We decided to focus on the observation of reduced beta-catenin levels after exposure to EFNA5 based on beta-catenin's known association with adherens junctions and the actin cytoskeleton (30), which would be relevant to the changes in cell morphology that we observe when GFSHR-17 cells are exposed to EFNA5. Therefore, we verified the reduced beta-catenin levels observed in the array by immunoblot analysis to detect beta-catenin under the same culture conditions used in the array. This analysis revealed that GFSHR-17 cells seeded onto EFNA5/Fc contained lower beta-catenin protein levels at 20 min after seeding (**Figure 2-8**) than cells seeded onto Fc alone, confirming the reduction observed using the Human Phospho-Kinase Array. No differences were observed between EFNA5/Fc and Fc at 15 min after seeding. These results suggest that beta-catenin may be a downstream target of EFNA5 signaling.

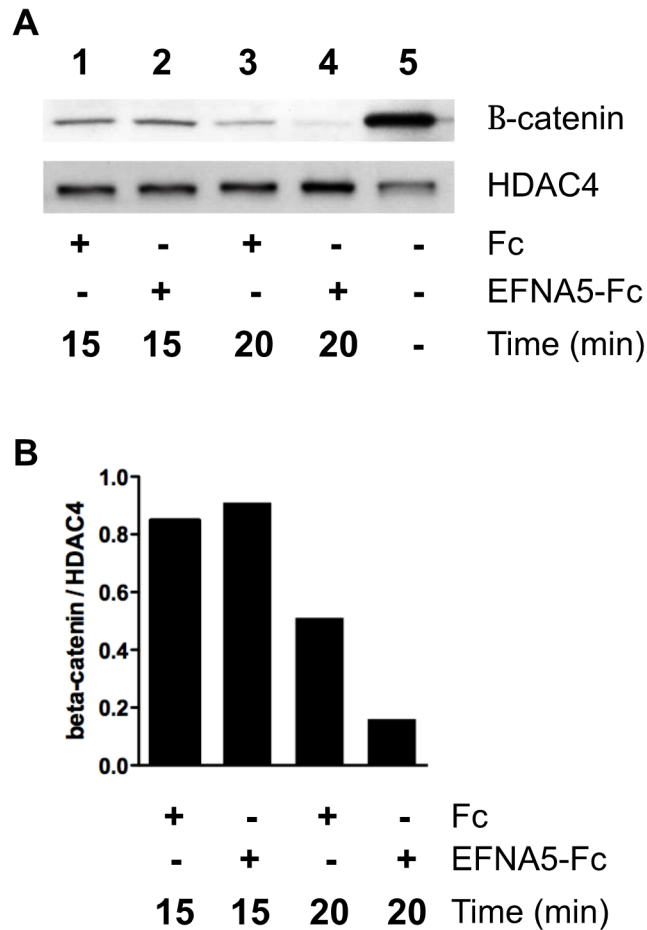


Figure 2-8: Beta-catenin protein levels in GFSHR-17 cells are reduced in response to EFNA5.

A) GFSHR-17 cells were seeded onto 60-mm tissue-culture dishes coated with preclustered ephrinA5-Fc or Fc (37 $\mu\text{g}/\text{mL}$). Lysates were collected 15 min (lanes 1 and 2) and 20 min (lanes 3 and 4) after seeding. Lysate from non-treated HeLa cells (lane 5) was used as a positive control for the beta-catenin antibody. Fifty micrograms of each lysate were separated by SDS-PAGE, and beta-catenin protein levels were assessed by immunoblot analysis. To assess equal protein loading, the membrane was subsequently probed using a rabbit monoclonal IgG against HDAC4. **B)** Densitometric analysis of immunoblot data (ImageLab 4.1) showing the ratio of beta-catenin to HDAC4.

2.4 Discussion

In the present study, we have shown that FSH increases the expression of a subset of ephrin ligands and Eph receptors in primary mouse and immortalized rat (GFSHR-17) GCs and that exposure of GCs to EFNA5 and EPHA5 alters GC morphology and adhesion, respectively. These results suggest that Eph-ephrin signaling may play a role in the changes in GC contact and organization that occur within the follicle during folliculogenesis.

2.4.1 Eph-Ephrin Gene Expression Is Regulated by FSH via the cAMP/PKA Pathway in GCs

We have observed that eCG increases the expression of *Efna5* and several of its receptors (*Epha3*, *Epha5*, *Epha8*, and *Ephb2*) in mouse GCs. Interestingly, all Eph receptors that we observed to be increased in response to eCG bind preferentially to EFNA5 (4) (**Table 2-1** and **Figure 2-1**), the sole ligand increased in response to FSH in our mouse GC model. This coordinate increase of an ephrin and several of its cognate receptors suggests an attractive model in which the expression of an ephrin ligand and its receptors are coordinately increased during the response to FSH, resulting in increased Eph-ephrin signaling that contributes to the formation of the developing follicle. Coordinated increases in Eph receptors and ephrin ligands have been previously observed in mouse skin cells under conditions of hypoxia (31). In theory, this coordinated regulation by FSH would increase Eph-ephrin signaling when cell movement occurs, such as during antrum formation.

We found that treating rat GCs with FSH and forskolin resulted in increased expression of *Efna5* and *Epha5*, suggesting that these genes are activated via the cAMP/PKA pathway (27), as are many FSH target genes. Why only *Efna5* and *Epha5*, but not *Ephb2*, *Epha3*, and *Epha8*, expression increased in response to FSH in GFSHR-17 cells is likely due to differences in species (mouse vs. rat) and in primary GCs compared to an immortalized GC line. To date, little is known about what signaling molecules regulate the expression of ephrin ligand and Eph receptor genes, and to our knowledge, this is the first demonstration that cAMP regulates Eph-ephrin family

members in GCs. Our data indicate that in GCs, cAMP increases *Eph* and *Efn* expression, suggesting that cAMP may similarly regulate *Eph* and *Efn* expression in other model systems.

2.4.2 EFNA5 and EPHA5 Localization During Folliculogenesis

In general, both EFNA5 and EPHA5 were more highly expressed in larger follicles, such as preantral follicles with many layers of GCs or antral follicles, than in smaller ones, such as primary follicles with one or two layers of GCs (**Figure 2-3**). This suggests that expression of EFNA5 and EPHA5 may be driven, at least in part, by FSH. Although primordial and primary follicle development is commonly accepted to be independent of FSH, recent evidence indicates that in immature mice (the model in the present study), primordial follicles respond to FSH (32), suggesting that FSH may regulate GC differentiation and development in small preantral follicles as well, because the FSH receptor is expressed in mouse primary follicles (33). Thus, FSH may be one factor increasing the expression of EFNA5 and EPHA5 in both small preantral and larger antral follicles, which would be consistent with our data that *Efna5* and *Epha5* mRNA levels increase in GCs of mice treated with eCG (**Figure 2-1**) and in GFSHR-17 cells treated with FSH. In addition, the punctate pattern of staining that we observe for EFNA5 (**Figure 2-3, G and I**) has also been observed for other ephrins, notably EFNA3 in glial cells of the hippocampus (34).

An interesting observation was that EFNA5 and EPHA5 immunoreactivity was stronger in mural GCs than in cumulus cells of antral follicles (**Figure 2-3G**), with a gradient of staining between the two. A similar graded pattern of expression has been reported for mRNA of the luteinizing hormone receptor (*Lhcgr*); cytochrome P450, family 11, subfamily A, polypeptide 1 (*Cyp11a1*); and *Cd34* mRNA and is hypothesized to result from an oocyte-stimulated MAD homolog 2/3 (*Smad2/3*) signaling gradient that is strongest in cumulus GCs (35). A mural-to-antral gradient of expression has also been reported for connective tissue growth factor (*Ctgf*) mRNA in rat follicles (36). Therefore, we hypothesize that *EFNA5* and *EPHA5* expression may also be regulated by an oocyte-

derived factor, such as bone morphogenetic protein 15 (BMP15) or growth differentiation factor 9 (GDF9) (35). Although little is known about what factors regulate *EFNA5* or *EPHA5* expression, evidence indicates that *EFNA5* expression is regulated by anti-Müllerian hormone (AMH) and glial cell-derived neurotrophic factor (GDNF) (37), both of which affect the transition from primordial to primary follicles.

Based on our immunofluorescence data, we cannot identify whether individual mouse GCs express *EFNA5* alone, *EPHA5* alone, or *EFNA5* and *EPHA5* simultaneously. Whereas activation of an Eph receptor on one cell by an ephrin ligand on a nearby cell is the most commonly reported interaction, overlapping coexpression of cognate Eph receptor-ligand pairs within the same cell has been frequently observed. For example, *EFNA5* and *EPHA5* are coexpressed in pancreatic beta-cells (38), and *EFNA5* and *EFNA4* are coexpressed in motor neurons of embryonic chick spinal cord (39). Therefore, it is possible that GCs express both *EFNA5* and *EPHA5* and, therefore, that neighboring GCs could activate each other through forward signaling, reverse signaling, or both.

2.4.3 EFNA5 Inhibits Spreading and Increases Rounding of GCs

Our observation that exposure of primary GCs and rat GFSHR-17 cells to *EFNA5* induces cell rounding is consistent with the ability of *EFNA5* to induce cell rounding in a number of other model systems. This cell rounding, often referred to as reduced cell spreading, has been associated with both increased and decreased cell migration, depending on the cell type. For example, spreading of rat primary vascular smooth muscle cells is inhibited on tissue-culture surfaces coated with *EFNA1*, resulting in a rounded cell morphology (20). Similarly, addition of *EFNA5* to cell-culture medium induces rounding of both immortalized human melanoma cells and *EPHA3*-expressing 293T cells (28), which correlates with reduced adhesion. Those authors suggest this reduced adhesion would lead to increased cell motility. Similarly, Foo et al. (40) show that smooth muscle cells lacking *EPHB2* are defective in spreading and show increased motility (40). On the other hand, many reports suggest that reduced spreading (cell

rounding) leads to reduced migration, such as the *EPHA1*-induced rounding and reduced migration observed in Human Embryonic Kidney 293 (HEK293) cells stably transfected with *EPHA1* (41). Thus, in the ovary, changes in GC shape and spreading may regulate migration during folliculogenesis.

In addition to changes in cell shape, “[e]xtensive and intricate changes in the physical arrangement of cells” (p. 6 (42)) occur within a developing follicle during folliculogenesis, and for these rearrangements to occur, GCs must migrate within the follicle. Several stages occur during folliculogenesis when GCs (both mural and cumulus) are thought to migrate within the follicle. GCs migrate to surround the oocyte during the formation of primordial follicles (to form multiple GC layers during proliferation and formation of preantral follicles) and also during the formation of the antrum, which requires a significant creation of space within the follicle. Both older and more recent studies of cultured follicles indicate that on a two-dimensional surface in the absence of FSH, GCs disperse and migrate across tissue-culture plastic away from the oocyte but reorganize to form an antrum when exposed to FSH (43). Three-dimensional culture in hydrogels minimizes the extent of GC migration, yet GC outgrowth still occurs, allowing antrum formation (43). In either model, GC movement clearly is critical to the formation of the antrum. Treatment with hCG enhances cumulus cell migration as determined by in vitro migration assays (44). Finally, during formation of the corpus luteum, luteinizing GCs migrate toward the center of the luteinizing follicle (45) and can be shown to migrate using in vitro migration assays (46). Numerous studies have shown that Eph-ephrin signaling simultaneously induces cell rounding, reduces cell spreading, and enhances cell migration and motility of a number of diverse cell types (22,28,41,47,48). Therefore, the GC rounding we observe in response to *EPHA5* could potentially regulate GC migration in vivo.

2.4.4 *EPHA5* Inhibits Adhesion of GCs

Granulosa cell movement and differentiation during folliculogenesis are thought to require changes in cell-cell adhesion and cellular junctions during this time (49). Not surprisingly, the type of junctions connecting GCs within the follicle change in both number and type during follicle growth (50). Four types of cell-cell junctions have been

identified in the ovary of various species: adherens junctions, gap junctions, desmosomes, and tight junctions (50-52), with adherens and gap junctions being the best characterized. In smaller follicles, gap junctions exist, but adherens junctions and desmosomes predominate (50,53). As the follicle grows under the influence of FSH and other factors, the number of gap junctions increases, whereas the number of desmosomes and adherens junctions decreases (50,53). Gap junction number and size increase dramatically to their maximum frequency in the preovulatory follicle (1), concomitant with a decrease in adherens junctions, and it is believed that this change leads to reduced cell-cell adhesion, allowing the formation of the antrum (54).

In the present study, we observe that primary GCs resist binding when reverse signaling (i.e., signaling into the cell containing the ephrin ligand) is activated through the Eph receptor coated onto tissue-culture surfaces. This suggests that reverse signaling through an EPHA5-compatible ephrin ligand on the GC surface results in reduced adhesion and repulsion. Several recent reports support a role for ephrin ligand-mediated reverse signaling in reducing cell adhesion. In mice lacking *Efna5*, midline fusion occurs in the developing neural tube (55), and those authors propose that this fusion results from loss of Eph-ephrin reverse signaling that would normally promote cell repulsion. In that same study, “an inverse correlation” (p. 203 (55)) was observed “between *Efna5* gene dosage and [cell] adhesion” (p. 203 (55)), and cells from *Efna5*-null mice displayed decreased adhesion compared to wild-type cells. In another study, ephrin-A-expressing retinal neurons avoid EPHA7-Fc surfaces during axonal outgrowth, suggesting that reverse signaling via A-class ephrin ligands promotes repulsion and/or reduced adhesion (56). We speculate that in vivo, this reverse signaling through *Efna5* on GCs could lead to reduced cell-cell contact during, for example, formation of the antrum, when reduced cell-cell adhesion is required for GC migration. This would be similar to the role that Eph-ephrin signaling plays in the repulsive guidance of migrating neurons (29).

Interestingly, Eph-ephrin signaling has been shown to cross-talk with adherens junctions, tight junctions, and gap junctions in other model systems (2). In various tissues, gap junctions are critical for Eph-ephrin function in processes as diverse as cell

sorting, insulin secretion, and osteogenic differentiation (38,57,58). Thus, cross-talk between these junctions and Eph-ephrin signaling may also be occurring in GCs.

Although several published reports have described Eph receptor and ephrin expression in the mouse and human ovaries, none of these demonstrated an effect of ephrin signaling on GC characteristics or function. Gale et al. (14) found that EFNB2 is expressed in the neovasculature of corpora lutea and the theca cell layer of preluteinized follicles. Egawa et al. (15) showed that EFNB1 is expressed in luteal cells of the human corpus luteum. These reports suggest roles for ephrin ligands in the vascularization of the theca and corpora lutea as well as in luteal cells. Xu et al. (16) demonstrated that *EPHA2*, *EPHA4*, *EPHA7*, *EFNA4*, *EFNB1*, and *EFNB2* mRNA are present in cultured human luteinized GCs. In line with the findings of Xu et al., we detected expression of several Eph receptors and ephrins in mouse GCs.

2.4.5 EFNA5 Reduces Beta-Catenin Protein Levels in GCs

We observed a reduction in beta-catenin protein levels in GFSHR-17 cells seeded onto EFNA5/Fc concomitant with rounding/reduced spreading. Beta-catenin has two primary functions in cells. First, in conjunction with alpha-catenin and E-cadherin, it forms a link between adherens junctions and the actin cytoskeleton. Second, it serves as a transcription factor in conjunction with proteins of the T-cell factor (TCF)/lymphoid enhancer-binding factor (LEF) family of transcription factors in the nucleus (59,60). In the cytoplasm, beta-catenin undergoes constant turnover, with phosphorylation, ubiquitination, and then proteasomal degradation (61). We speculate that activation of Eph receptors cognate to EFNA5 in GFSHR-17 cells may regulate adherens junction assembly and/or degradation or lead to transcriptional effects through interactions of beta-catenin with TCF/LEF family members. In the context of the growing follicle, beta-catenin degradation may affect remodeling of adherens junctions, leading to changes in the cytoskeleton, which occur during changes in cell shape (62). In turn, changes in cell shape have been associated with changes in cell migration (28,40,41). Reduced levels of beta-catenin may also influence expression of TCF/LEF target genes in GCs that may influence cellular morphology. Further experiments will be required to fully delineate the relationship between EFNA5 and beta-catenin.

In summary, we have shown that *EFNA5* and *EPHA5* are expressed in mouse GCs, that forward signaling induced by *EFNA5* regulates GC morphology by inhibiting cell spreading, and that reverse signaling induced by *EPHA5* inhibits cell adhesion. The expression of *EPHA5* and *EPHA5* in follicles of various sizes suggests that they may play multiple roles during different stages of folliculogenesis. We speculate that further studies will indicate that these and other members of the Eph-ephrin signaling system play important roles in the development of healthy preovulatory follicles and corpora lutea throughout folliculogenesis.

2.5 Bibliography

1. Amsterdam A, Rotmensch S. Structure-function relationships during granulosa cell differentiation. *Endocr Rev.* 1987;8(3):309-337.
2. Pasquale EB. Eph-ephrin bidirectional signaling in physiology and disease. *Cell.* 2008;133(1):38-52.
3. Pasquale EB. Eph receptors and ephrins in cancer: bidirectional signalling and beyond. *Nat Rev Cancer.* 2010;10(3):165-180.
4. Jensen PL. Eph receptors and ephrins. *Stem Cells.* 2000;18(1):63-64.
5. Himanen JP, Chumley MJ, Lackmann M, Li C, Barton WA, Jeffrey PD, Vearing C, Geleick D, Feldheim DA, Boyd AW, Henkemeyer M, Nikolov DB. Repelling class discrimination: ephrin-A5 binds to and activates EphB2 receptor signaling. *Nat Neurosci.* 2004;7(5):501-509.
6. Luo H, Yu G, Tremblay J, Wu J. EphB6-null mutation results in compromised T cell function. *The Journal of clinical investigation.* 2004;114(12):1762-1773.
7. Feldheim DA, O'Leary DD. Visual map development: bidirectional signaling, bifunctional guidance molecules, and competition. *Cold Spring Harb Perspect Biol.* 2010;2(11):a001768.
8. Andersson L, Westerlund J, Liang S, Carlsson T, Amendola E, Fagman H, Nilsson M. Role of EphA4 receptor signaling in thyroid development: regulation of folliculogenesis and propagation of the C-cell lineage. *Endocrinology.* 2011;152(3):1154-1164.
9. Pitulescu ME, Adams RH. Eph/ephrin molecules--a hub for signaling and endocytosis. *Genes & development.* 2010;24(22):2480-2492.
10. Andres AC, Ziemiecki A. Eph and ephrin signaling in mammary gland morphogenesis and cancer. *J Mammary Gland Biol Neoplasia.* 2003;8(4):475-485.
11. Weiler S, Rohrbach V, Pulvirenti T, Adams R, Ziemiecki A, Andres AC. Mammary epithelial-specific knockout of the ephrin-B2 gene leads to precocious epithelial cell death at lactation. *Dev Growth Differ.* 2009;51(9):809-819.
12. Lin S, Gordon K, Kaplan N, Getsios S. Ligand targeting of EphA2 enhances keratinocyte adhesion and differentiation via desmoglein 1. *Mol Biol Cell.* 2010;21(22):3902-3914.
13. Ting MJ, Day BW, Spanevello MD, Boyd AW. Activation of ephrin A proteins influences hematopoietic stem cell adhesion and trafficking patterns. *Exp Hematol.* 2010;38(11):1087-1098.
14. Gale NW, Baluk P, Pan L, Kwan M, Holash J, DeChiara TM, McDonald DM, Yancopoulos GD. Ephrin-B2 selectively marks arterial vessels and neovascularization sites in the adult, with expression in both endothelial and smooth-muscle cells. *Dev Biol.* 2001;230(2):151-160.

15. Egawa M, Yoshioka S, Higuchi T, Sato Y, Tatsumi K, Fujiwara H, Fujii S. Ephrin B1 is expressed on human luteinizing granulosa cells in corpora lutea of the early luteal phase: the possible involvement of the B class Eph-ephrin system during corpus luteum formation. *The Journal of clinical endocrinology and metabolism*. 2003;88(9):4384-4392.
16. Xu Y, Zagoura D, Keck C, Pietrowski D. Expression of Eph receptor tyrosine kinases and their ligands in human Granulosa lutein cells and human umbilical vein endothelial cells. *Experimental and Clinical Endocrinology and Diabetes*. 2006;114(10):590-595.
17. Forde N, Mihm M, Canty MJ, Zielak AE, Baker PJ, Park S, Lonergan P, Smith GW, Coussens PM, Ireland JJ, Evans AC. Differential expression of signal transduction factors in ovarian follicle development: a functional role for betaglycan and FIBP in granulosa cells in cattle. *Physiol Genomics*. 2008;33(2):193-204.
18. Keren-Tal I, Dantes A, Sprengel R, Amsterdam A. Establishment of steroidogenic granulosa cell lines expressing follicle stimulating hormone receptors. *Mol Cell Endocrinol*. 1993;95(1-2):R1-10.
19. Pfaffl MW. A new mathematical model for relative quantification in real-time RT-PCR. *Nucleic Acids Res*. 2001;29(9):e45.
20. Deroanne C, Vouret-Craviari V, Wang B, Pouyssegur J. EphrinA1 inactivates integrin-mediated vascular smooth muscle cell spreading via the Rac/PAK pathway. *J Cell Sci*. 2003;116(Pt 7):1367-1376.
21. Kaneko M, Nighorn A. Interaxonal Eph-ephrin signaling may mediate sorting of olfactory sensory axons in *Manduca sexta*. *J Neurosci*. 2003;23(37):11523-11538.
22. Stokowski A, Shi S, Sun T, Bartold PM, Koblar SA, Gronthos S. EphB/ephrin-B interaction mediates adult stem cell attachment, spreading, and migration: implications for dental tissue repair. *Stem Cells*. 2007;25(1):156-164.
23. Yin Y, Yamashita Y, Noda H, Okafuji T, Go MJ, Tanaka H. EphA receptor tyrosine kinases interact with co-expressed ephrin-A ligands in cis. *Neurosci Res*. 2004;48(3):285-296.
24. Coate TM, Wirz JA, Copenhaver PF. Reverse signaling via a glycosyl-phosphatidylinositol-linked ephrin prevents midline crossing by migratory neurons during embryonic development in *Manduca*. *J Neurosci*. 2008;28(15):3846-3860.
25. Davis S, Gale NW, Aldrich TH, Maisonpierre PC, Lhotak V, Pawson T, Goldfarb M, Yancopoulos GD. Ligands for EPH-related receptor tyrosine kinases that require membrane attachment or clustering for activity. *Science*. 1994;266(5186):816-819.
26. Palmer A, Klein R. Multiple roles of ephrins in morphogenesis, neuronal networking, and brain function. *Genes & development*. 2003;17(12):1429-1450.

27. Hunzicker-Dunn M, Maizels ET. FSH signaling pathways in immature granulosa cells that regulate target gene expression: branching out from protein kinase A. *Cell Signal*. 2006;18(9):1351-1359.
28. Lawrenson ID, Wimmer-Kleikamp SH, Lock P, Schoenwaelder SM, Down M, Boyd AW, Alewood PF, Lackmann M. Ephrin-A5 induces rounding, blebbing and de-adhesion of EphA3-expressing 293T and melanoma cells by CrkII and Rho-mediated signalling. *J Cell Sci*. 2002;115(Pt 5):1059-1072.
29. Lackmann M, Boyd AW. Eph, a protein family coming of age: more confusion, insight, or complexity? *Sci Signal*. 2008;1(15):re2.
30. Sundfeldt K, Piontkewitz Y, Billig H, Hedin L. E-cadherin-catenin complex in the rat ovary: cell-specific expression during folliculogenesis and luteal formation. *Journal of reproduction and fertility*. 2000;118(2):375-385.
31. Vihanto MM, Plock J, Erni D, Frey BM, Frey FJ, Huynh-Do U. Hypoxia up-regulates expression of Eph receptors and ephrins in mouse skin. *FASEB journal : official publication of the Federation of American Societies for Experimental Biology*. 2005;19(12):1689-1691.
32. Lei L, Jin S, Mayo KE, Woodruff TK. The interactions between the stimulatory effect of follicle-stimulating hormone and the inhibitory effect of estrogen on mouse primordial folliculogenesis. *Biol Reprod*. 2010;82(1):13-22.
33. O'Shaughnessy PJ, Marsh P, Dudley K. Follicle-stimulating hormone receptor mRNA in the mouse ovary during post-natal development in the normal mouse and in the adult hypogonadal (hpg) mouse: structure of alternate transcripts. *Mol Cell Endocrinol*. 1994;101(1-2):197-201.
34. Carmona MA, Murai KK, Wang L, Roberts AJ, Pasquale EB. Glial ephrin-A3 regulates hippocampal dendritic spine morphology and glutamate transport. *Proceedings of the National Academy of Sciences of the United States of America*. 2009;106(30):12524-12529.
35. Diaz FJ, Wigglesworth K, Eppig JJ. Oocytes determine cumulus cell lineage in mouse ovarian follicles. *J Cell Sci*. 2007;120(Pt 8):1330-1340.
36. Harlow CR, Davidson L, Burns KH, Yan C, Matzuk MM, Hillier SG. FSH and TGF-beta superfamily members regulate granulosa cell connective tissue growth factor gene expression in vitro and in vivo. *Endocrinology*. 2002;143(9):3316-3325.
37. Nilsson E, Zhang B, Skinner MK. Gene bionetworks that regulate ovarian primordial follicle assembly. *BMC genomics*. 2013;14:496.
38. Konstantinova I, Nikolova G, Ohara-Imaizumi M, Meda P, Kucera T, Zarbalis K, Wurst W, Nagamatsu S, Lammert E. EphA-Ephrin-A-mediated beta cell communication regulates insulin secretion from pancreatic islets. *Cell*. 2007;129(2):359-370.
39. Marquardt T, Shirasaki R, Ghosh S, Andrews SE, Carter N, Hunter T, Pfaff SL. Coexpressed EphA receptors and ephrin-A ligands mediate opposing actions on

- growth cone navigation from distinct membrane domains. *Cell*. 2005;121(1):127-139.
40. Foo SS, Turner CJ, Adams S, Compagni A, Aubyn D, Kogata N, Lindblom P, Shani M, Zicha D, Adams RH. Ephrin-B2 controls cell motility and adhesion during blood-vessel-wall assembly. *Cell*. 2006;124(1):161-173.
 41. Yamazaki T, Masuda J, Omori T, Usui R, Akiyama H, Maru Y. EphA1 interacts with integrin-linked kinase and regulates cell morphology and motility. *J Cell Sci*. 2009;122(Pt 2):243-255.
 42. Woodruff TK, Shea LD. The role of the extracellular matrix in ovarian follicle development. *Reprod Sci*. 2007;14(8 Suppl):6-10.
 43. Desai N, Alex A, AbdelHafez F, Calabro A, Goldfarb J, Fleischman A, Falcone T. Three-dimensional in vitro follicle growth: overview of culture models, biomaterials, design parameters and future directions. *Reprod Biol Endocrinol*. 2010;8:119.
 44. Akison LK, Alvino ER, Dunning KR, Robker RL, Russell DL. Transient invasive migration in mouse cumulus oocyte complexes induced at ovulation by luteinizing hormone. *Biol Reprod*. 2012;86(4):125.
 45. Smith MF, McIntush EW, Smith GW. Mechanisms associated with corpus luteum development. *J Anim Sci*. 1994;72(7):1857-1872.
 46. Becker S, von Otte S, Robenek H, Diedrich K, Nofer JR. Follicular fluid high-density lipoprotein-associated sphingosine 1-phosphate (S1P) promotes human granulosa lutein cell migration via S1P receptor type 3 and small G-protein RAC1. *Biol Reprod*. 2011;84(3):604-612.
 47. Bochenek ML, Dickinson S, Astin JW, Adams RH, Nobes CD. Ephrin-B2 regulates endothelial cell morphology and motility independently of Eph-receptor binding. *J Cell Sci*. 2010;123(Pt 8):1235-1246.
 48. Miao H, Burnett E, Kinch M, Simon E, Wang B. Activation of EphA2 kinase suppresses integrin function and causes focal-adhesion-kinase dephosphorylation. *Nat Cell Biol*. 2000;2(2):62-69.
 49. Amsterdam A, Aharoni D. Plasticity of cell organization during differentiation of normal and oncogene transformed granulosa cells. *Microscopy research and technique*. 1994;27(2):108-124.
 50. Amsterdam A, Plehn-Dujowich D, Suh BS. Structure-function relationships during differentiation of normal and oncogene-transformed granulosa cells. *Biol Reprod*. 1992;46(4):513-522.
 51. Mora JM, Fenwick MA, Castle L, Baithun M, Ryder TA, Mobberley M, Carzaniga R, Franks S, Hardy K. Characterization and significance of adhesion and junction-related proteins in mouse ovarian follicles. *Biol Reprod*. 2012;86(5):153, 151-114.
 52. Rodewald M, Herr D, Fraser HM, Hack G, Kreienberg R, Wulff C. Regulation of tight junction proteins occludin and claudin 5 in the primate ovary during the

- ovulatory cycle and after inhibition of vascular endothelial growth factor. *Molecular human reproduction*. 2007;13(11):781-789.
53. Kidder GM, Mhawi AA. Gap junctions and ovarian folliculogenesis. *Reproduction*. 2002;123(5):613-620.
 54. Kawagishi R, Tahara M, Morishige K, Sakata M, Tasaka K, Ikeda W, Morimoto K, Takai Y, Murata Y. Expression of nectin-2 in mouse granulosa cells. *European journal of obstetrics, gynecology, and reproductive biology*. 2005;121(1):71-76.
 55. Holmberg J, Clarke DL, Frisen J. Regulation of repulsion versus adhesion by different splice forms of an Eph receptor. *Nature*. 2000;408(6809):203-206.
 56. Rashid T, Upton AL, Blentic A, Ciossek T, Knoll B, Thompson ID, Drescher U. Opposing gradients of ephrin-As and EphA7 in the superior colliculus are essential for topographic mapping in the mammalian visual system. *Neuron*. 2005;47(1):57-69.
 57. Davy A, Bush JO, Soriano P. Inhibition of gap junction communication at ectopic Eph/ephrin boundaries underlies craniofrontonasal syndrome. *PLoS Biol*. 2006;4(10):e315.
 58. Poliakov A, Cotrina M, Wilkinson DG. Diverse roles of eph receptors and ephrins in the regulation of cell migration and tissue assembly. *Dev Cell*. 2004;7(4):465-480.
 59. Korinek V, Barker N, Morin PJ, van Wichen D, de Weger R, Kinzler KW, Vogelstein B, Clevers H. Constitutive transcriptional activation by a beta-catenin-Tcf complex in APC^{-/-} colon carcinoma. *Science*. 1997;275(5307):1784-1787.
 60. Morin PJ, Sparks AB, Korinek V, Barker N, Clevers H, Vogelstein B, Kinzler KW. Activation of beta-catenin-Tcf signaling in colon cancer by mutations in beta-catenin or APC. *Science*. 1997;275(5307):1787-1790.
 61. Aberle H, Bauer A, Stappert J, Kispert A, Kemler R. beta-catenin is a target for the ubiquitin-proteasome pathway. *The EMBO journal*. 1997;16(13):3797-3804.
 62. Homem CC, Peifer M. Diaphanous regulates myosin and adherens junctions to control cell contractility and protrusive behavior during morphogenesis. *Development*. 2008;135(6):1005-1018.

3 Chapter 3: Ephrin-A5 is required for optimal fertility and a complete ovulatory response to gonadotropins in the mouse

This chapter is based on a manuscript submitted to *Endocrinology*:

Buensuceso AV, Son A, Paquet M, Withers BM, Zhou R, and Deroo BJ. (2015) Ephrin-A5 is required for optimal fertility and a complete ovulatory response to gonadotropins in the female mouse. Manuscript ID# EN-15-1216.

3.1 Introduction

Folliculogenesis is a dynamic and carefully-timed process during which a primordial follicle develops into a fully mature preovulatory follicle capable of expelling a fertilizable oocyte. This process requires a tremendous amount of cell proliferation, migration, directional cell growth, extracellular (ECM) synthesis, and changes in cell adhesion and morphology. These dramatic changes are not surprising given that the diameter of a human preovulatory follicle is approximately 600 times larger than a primordial follicle (1). Although changes in cell morphology and migration during folliculogenesis are critical to the production of a healthy preovulatory follicle, the factors regulating these two processes are not well understood.

The Eph-ephrin family of molecules consists of ephrin ligands and their cognate tyrosine kinase receptors, Eph receptors. Eph-ephrin family members regulate both cellular shape and adhesion during development, cancer, and the normal function of many different tissues (2). Since Eph receptors and ephrins are membrane-associated, signaling is initiated exclusively from points of cell-to-cell contact. Eph-ephrin signaling is bidirectional, with signal transduction occurring in both receptor-bearing cells (forward signaling) and in ligand-bearing cells (reverse signaling). Eph receptors and ephrin ligands are both classified into two types, designated A or B, based on receptor-ligand specificity. Receptors and ligands of the same class bind preferentially. In forward signaling, ligand-bound Eph receptors interact with signaling elements via adapter proteins, and may also phosphorylate targets directly. Reverse signaling via B-class ephrins occurs in a similar manner, where the receptor-bound ligand can interact with

intracellular signaling elements via adapter proteins. As well-established regulators of cell positioning, ephrins and Eph receptors are likely candidates for involvement in follicle growth and ovulation. Although members of the Eph-ephrin family have been identified in the ovary, Eph-ephrin signaling and the role it may play during folliculogenesis have not been well-characterized.

We previously reported that FSH increases the expression of a subset of ephrin ligands and Eph receptors in primary mouse and immortalized rat granulosa cells (GCs), and that exposure of GCs to the ligand ephrin-A5 (EFNA5) and its receptor EPHA5 alters GC morphology and adhesion, respectively (3). Expression of ephrins and Eph receptors has also been described in mouse (4), human (5,6), and bovine ovaries (7). Furthermore, in bovine ovaries *Efna5* expression is higher in large antral follicles, ie. with a mean diameter five times higher than small follicles (8). These studies suggest that Eph-ephrin signaling may be required for normal folliculogenesis.

To test the hypothesis that Eph-ephrin signaling regulates folliculogenesis, we characterized the reproductive capacity and characteristics of female mice lacking ephrin-A5. Previous studies of these mice revealed axon guidance defects (9) and disrupted organization of lens cells in the eye (10-12), but have not been previously characterized with respect to reproductive function. We report compromised fertility in adult *Efna5*-null (*Efna5*^{-/-}) females, indicating a novel role for Eph-ephrin signaling in female reproductive function.

3.2 Materials and Methods

3.2.1 Mice and treatments

All mouse experiments described in this study were conducted in accordance with the accepted standards of humane animal care, as outlined in the journal's Ethical Guidelines. Experiments were performed in compliance with the guidelines set by the Canadian Council for Animal Care, and the policies and procedures approved by the University of Western Ontario Council on Animal Care (Protocol Number: 2007-042). The generation of *Efna5*-null (*Efna5*^{-/-}) mice has been described previously (9). Immature *Efna5*^{-/-} female mice and their wildtype (WT) littermates were generated by breeding

heterozygous (*Efna5^{+/-}*) males with heterozygous (*Efna5^{+/-}*) females. All females were weaned at post-natal day (PND) 21 and genotyped as previously described (9).

For studies examining ovulation capacity, serum steroid levels, ovarian gene expression, and histology, mice were treated with: a) 100 μ L saline, b) 5.0 IU equine chorionic gonadotropin (eCG) (Sigma Chemical Co., St. Louis, MO) for 48 hours, or c) 5.0 IU equine chorionic gonadotropin (eCG) for 48 hours followed by 5.0 IU human chorionic gonadotropin (hCG) (Sigma). Whole ovaries were harvested 4, 14, or 24 hours post-hCG treatment.

3.2.2 Continuous breeding study

PND 60 *Efna5^{+/+}* and *Efna5^{-/-}* females were paired with PND 60 *Efna5^{+/+}* males for 6 months. Cages were checked twice weekly for pregnant females, daily thereafter for newborn pups, and the dates of birth and number of pups were recorded. After 6 months, the average litter size and the average number of days between litters was calculated for each female.

3.2.3 Assessment of ovulatory potential in response to gonadotropin treatment

Reproductively immature female mice were subjected to a standard superovulation protocol and counted the number of ovulated oocytes. PND 21 *Efna5^{+/+}* and *Efna5^{-/-}* females were injected subcutaneously (sc) with 5 IU eCG, followed 48 h later by 5 IU hCG. Oviducts were harvested 14 h post-hCG and placed in a 25 μ L drop of saline on a 60 mm tissue culture dish. After harvest was completed, oviducts were transferred to a 25 μ L droplet of M2 medium containing hyaluronidase. Oviducts were then ruptured using a 0.5 inch 30-gauge needle, releasing the ovulated cumulus-oocyte-complexes (COCs) into the surrounding medium. Presence of hyaluronidase resulted in dissociation of oocytes and associated granulosa cells, yielding easily discernible individual oocytes. Upon dissociation, oocytes were counted using a dissecting microscope and a click-counter.

3.2.4 Assessment of serum steroid levels

To determine serum 17 β -estradiol (estradiol) levels, PND 21-22 females were injected sc with 5 IU eCG alone or 5 IU eCG followed by 5.0 IU hCG 48 h later. Blood

was collected from the vena cava 48 h post-eCG for estradiol quantitation and 14 or 24 h post-hCG for progesterone quantitation. Serum was analyzed by the University of Virginia Center for Research in Reproduction Ligand Assay and Analysis Core (Charlottesville, VA) for estradiol (ELISA) and progesterone (RIA) concentrations.

3.2.5 RNA isolation and quantitative RT-PCR

Frozen whole ovaries were homogenized in Trizol (Invitrogen, Carlsbad, CA) and RNA was isolated according to the manufacturer's protocol. RNA was further treated with DNaseI, then reverse-transcribed using Superscript II (Life Technologies, Carlsbad, CA). Complementary DNA (cDNA) levels were detected using quantitative RT-PCR with the ViiA™ 7 Real-Time PCR System (Life Technologies) and SYBR Green I dye or Taqman Gene Expression Analysis probe sets. Primers were generated using Applied Biosystems Primer Express Software version 3.0 or obtained from published literature (**Table 3-1**) and Taqman probe sets were purchased from Life Technologies (**Table 3-2**). Fold changes in gene expression were determined as previously described (3).

Gene	GenBank accession no.	Forward (5' to 3')	Reverse (5' to 3')	Reference
<i>Rpl7</i>	NM_011291	AGCTGGCCTTTGTCATCAGAA	GACGAAGGAGCTGCAGAACCT	
<i>Adams1</i>	NM_009621	CACATGCAAGAAGATGTCAGG	CCCTTTGATTCCGATGTTTC	(13)
<i>Adams4</i>	NM_172845	TCAACACCCCTAACGACTCA	TGCATGGCTTGGAGTTATCA	(14)
<i>Cyp11a1</i>	NM_019779	CCAGTGTCCCATGCTCAAC	TGCATGGTCCTTCCAGGTCT	(15)
<i>Cyp17a1</i>	NM_007809	GATCTAAGAAGCGCTCAGGCA	GGGCACTGCATCACGATAAA	(16)
<i>Hsd17b1</i>	NM_010475	TGTTTCGCCTAGCTTCTGACC	AGCAGCCACAGATTTGGAGT	(15)
<i>Hsd17b7</i>	NM_010476	AATGTGGCTCCTTCGCTTTT	GAGACTCCGGTTTTTGGTGG	
<i>Hsd3b1</i>	NM_008293, NM_00130480 0	CTCAGTTCTTAGGCTTCAGCAATTA C	CCAAAGGCAAGATATGATTTAGG A	(17)
<i>Fshr</i>	NM_013523	ATGTGTTCTCCAACCTACCCA	GCTGGCAAGTGTTTAATGCCTG	(15)
<i>Star</i>	NM_011485	CCGGAGCAGAGTGGTGCA	CAGTGGATGAAGCACCATGC	(15)

Table 3-1: Primer sequences used for quantitative RT-PCR.

Gene	Genbank accession no.	Taqman probe set
<i>Rpl7</i>	NM_011291.5	Mm02342562_gH
<i>Pgr</i>	NM_008829.2	Mm00435628_m1
<i>Ptgs2</i>	NM_011198.3	Mm00478374_m1
<i>Cyp19a1</i>	NM_007810.3	Mm00484049_m1
<i>Lhcgr</i>	NM_013582.2	Mm00442931_m1

Table 3-2: Taqman probe sets used for quantitative RT-PCR in Figure 3-4.

3.2.6 Fixation, sectioning, and preparation of ovaries for histological examination

Immediately after harvest, ovaries were placed into previously weighed 1.5 mL microcentrifuge tubes on ice, and weighed again. The microcentrifuge tubes were filled with 1.4 mL cold fixative solution (paraformaldehyde, 4% v/v in PBS). Microcentrifuge tubes were placed into a 50 mL conical tube which was then placed into a rotisserie rotator for 24 h at 4°C. The fixative solution was aspirated and replaced with 1.4 mL 4°C PBS. The microcentrifuge tubes were rotated for 24 h at 4°C, PBS was aspirated, replaced with 1.4 mL 4°C PBS, and rotated for 24 h at 4°C. The PBS was aspirated and replaced with 1.4 mL ethanol (70% v/v in MilliQ water). Fixed ovaries were then sent to the Molecular Pathology Core Facility (Robarts Research Institute, London, ON, Canada) for paraffin embedding, sectioning, and staining with hematoxylin/eosin (H&E).

3.2.7 Histological quantitation of COCs, corpora lutea, and multi-oocyte follicles

H&E-stained ovary sections were scanned using an Aperio ScanScope slide scanner (Leica Biosystems) at 200x. COCs and corpora lutea (CLs) were counted in every fifth section and multi-oocyte follicles (MOFs) in every third section throughout the entire ovary. When necessary, additional sections were reviewed to ensure that the same COCs, CLs, or MOFs were not counted twice.

3.3 Results

3.3.1 Ephrin-A5 is required for normal female fertility

In order to assess the fertility of female *Efna5*^{-/-} mice, we conducted a continuous breeding study (**Figure 3-1A**). Eight-week old *Efna5*^{+/+} or *Efna5*^{-/-} females were housed individually with 8-week old *Efna5*^{+/+} males for 6 months, and the litter sizes and dates of birth were recorded. *Efna5*^{-/-} females produced 40% smaller litters ($P < 0.001$) than *Efna5*^{+/+} control females (**Figure 3-1A**). Average litter sizes for *Efna5*^{+/+} females were 13.1 (± 0.6 , n=9) pups/litter compared to 8.0 (± 0.9 , n=9) pups/litter for *Efna5*^{-/-} females (**Figure 3-1A**). No difference in litter frequency was observed between genotypes (**Figure 3-1B**). These results indicate that fertility is compromised in female mice lacking ephrin-A5. Therefore, to begin to understand the basis of this decreased fertility, we assessed the ovarian response to gonadotropin stimulation.

3.3.2 *Efna5*^{-/-} females ovulate fewer oocytes than controls

In order to determine the ovulatory potential of *Efna5*^{-/-} females, PND 23-25 *Efna5*^{+/+} and *Efna5*^{-/-} females were hormonally stimulated (superovulated) by treatment with eCG for 48 h, followed by hCG for 14 h, after which the oocyte yield per animal was determined. The oocyte yield for *Efna5*^{-/-} females was 38% lower than for *Efna5*^{+/+} females ($P < 0.01$, **Figure 3-1C**). An average of 49.3 (± 3.4 , $n=11$) COCs/animal was retrieved from *Efna5*^{+/+} females, compared to 30.7 (± 4.3 , $n=12$) oocytes/animal from *Efna5*^{-/-} females (**Figure 3-1C**).

3.3.3 Serum estradiol and progesterone levels are unaffected by loss of ephrin-A5

The circulating levels of 17 β -estradiol (estradiol) and progesterone can be used as parameters for evaluating the ovarian response to gonadotropin stimulation, and can provide insight into the reason for decreased fertility. Therefore, we assessed serum estradiol and progesterone levels in gonadotropin-stimulated, PND 23-28 *Efna5*^{+/+} and *Efna5*^{-/-} females. No significant difference in serum estradiol levels was detected between *Efna5*^{+/+} and *Efna5*^{-/-} females 48 h post-eCG (**Figure 3-2A**). Similarly, no significant difference in serum progesterone levels was detected between *Efna5*^{+/+} and *Efna5*^{-/-} females after either 14 h or 24 h hCG (**Figure 3-2B**).

3.3.4 Ovary to body weight ratio is unaffected by loss of ephrin-A5

In order to determine whether loss of ephrin-A5 alters the ovary-to-body weight ratio in immature or adult mice, ovarian weights from *Efna5*^{+/+} and *Efna5*^{-/-} females were measured at 21, 60, and 120 days of age and normalized to body weight. No differences were detected in the ovary-to-body weight ratio between *Efna5*^{+/+} and *Efna5*^{-/-} females at any of these ages (**Figure 3-3, A-C**).

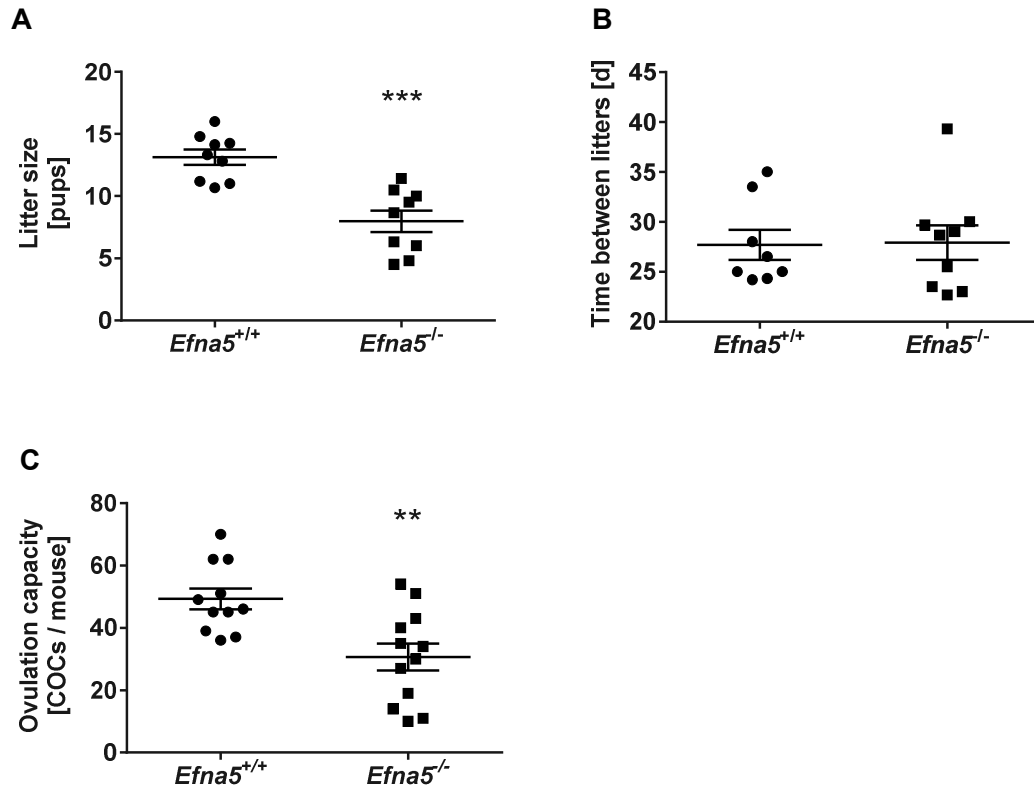


Figure 3-1: Reproductive assessment of *Efn5*^{-/-} females.

Efn5^{+/+} or *Efn5*^{-/-} PND 60 females were paired with an *Efn5*^{+/+} PND 60 male for a 6 month continuous breeding study to determine litter size (mean \pm SEM) (A) and time between births (mean \pm SEM) (B). Released oocytes from superovulated *Efn5*^{+/+} or *Efn5*^{-/-} PND 21-23 females were counted to determine ovulatory capacity (mean \pm SEM) (C). A) “Litter size” and “time between litters” for *Efn5*^{+/+} and *Efn5*^{-/-} genotypes were compared using the Student two-tailed unpaired t-test. A statistically significant difference was found between genotypes for both litter size and time between litters as determined by Student’s unpaired t-test; $t(16)=4.849$. ***, $p=0.0002$. B) “Time between births” for *Efn5*^{+/+} and *Efn5*^{-/-} genotypes was compared using the Student two-tailed unpaired t-test. No statistically significant difference was found between genotypes as determined by Student’s unpaired t-test; $t(15)=0.1008$, $p=0.9211$. C) “Ovulation capacity” for *Efn5*^{+/+} and *Efn5*^{-/-} genotypes was compared using the Student two-tailed unpaired t-test. A statistically significant difference was found between genotypes as determined by Student’s unpaired t-test; $t(21)=3.356$. **, $p=0.0030$.

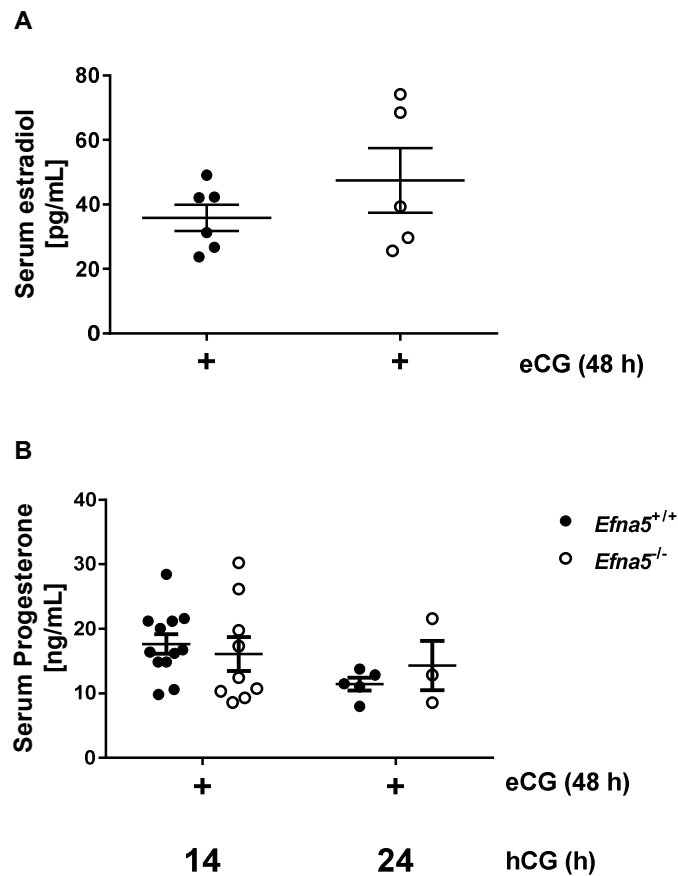


Figure 3-2: Serum estradiol and progesterone concentrations are unaffected by loss of ephrin-A5.

Serum estradiol (mean \pm SEM) (**A**) was measured for eCG-treated *EfnA5*^{+/+} and *EfnA5*^{-/-} females and serum progesterone (mean \pm SEM) (**B**) for superovulated females. **A**) “Serum estradiol” for *EfnA5*^{+/+} and *EfnA5*^{-/-} genotypes was compared using the Student two-tailed unpaired t-test. No statistically significant difference was found between genotypes as determined by Student’s unpaired t-test; $t(9)=1.142$, $p=0.2830$. **B**) “Serum progesterone” for *EfnA5*^{+/+} and *EfnA5*^{-/-} genotypes was compared at 14 h and then at 24 h post-hCG using the Student two-tailed unpaired t-test. At 14 h post-hCG, no statistically significant difference was found between genotypes as determined by Student’s unpaired t-test; $t(19)=0.5520$, $p=0.5874$. At 24 h post-hCG, no statistically significant difference was found between genotypes as determined by Student’s unpaired t-test; $t(6)=0.9392$, $p=0.3839$.

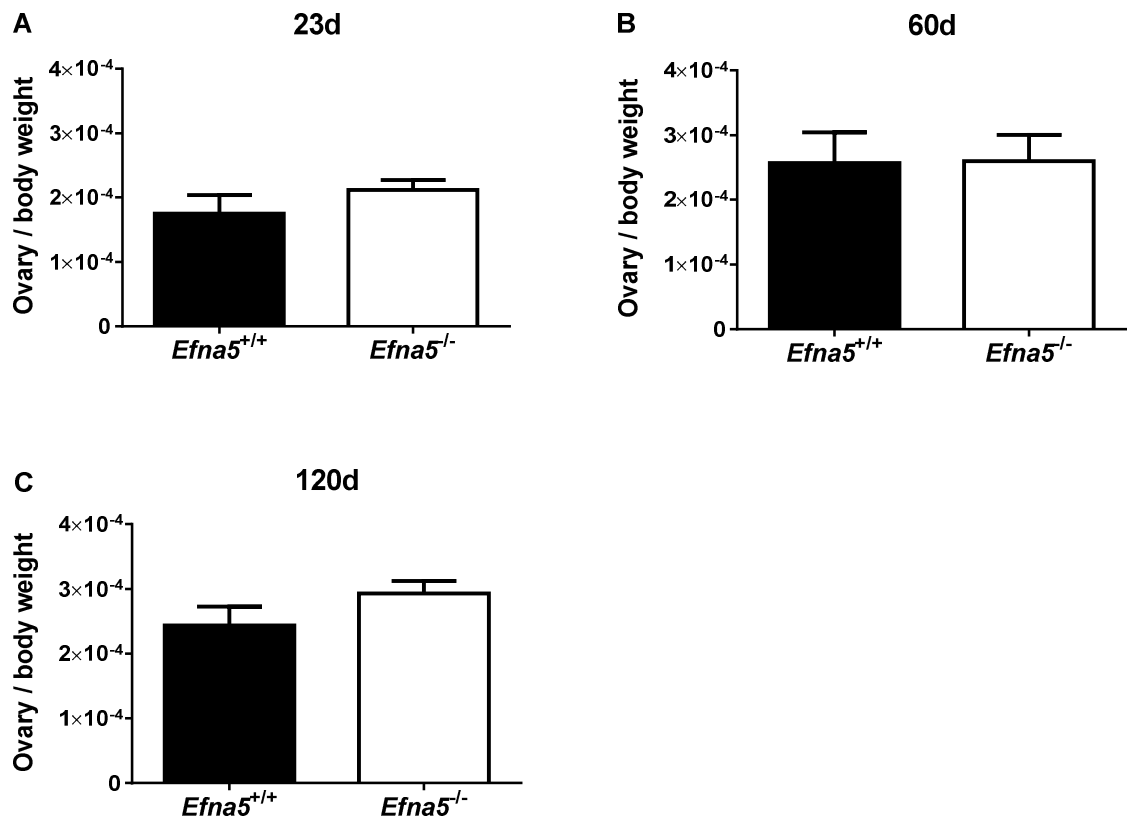


Figure 3-3: Ovary/body weight ratio is normal in *Efna5*^{-/-} females at PND 23, 60, and 120.

Ovaries from *Efna5*^{+/+} and *Efna5*^{-/-} females were harvested, weighed, and normalized to body weight (mean ±SEM) at PND 23 (A), 60 (B) and 120 (C). “Ovary/body weight ratio” for *Efna5*^{+/+} and *Efna5*^{-/-} genotypes was compared using the Student two-tailed unpaired t-test. **A)** At PND 23, no statistically significant difference was found between genotypes as determined by Student’s unpaired t-test; $t(5)=1.212$, $p=0.2795$. **B)** At PND 60, no statistically significant difference was found between genotypes as determined by Student’s unpaired t-test; $t(5)=0.04437$, $p=0.9663$. **C)** At PND 120, no statistically significant difference was found between genotypes as determined by Student’s unpaired t-test; $t(6)=1.460$, $p=0.1946$.

3.3.5 Ovarian gene expression is altered in *Efna5*^{-/-} females after gonadotropin stimulation

Because ovulatory capacity in response to gonadotropin stimulation was impaired in *Efna5*^{-/-} females (**Figure 3-1C**), we determined whether expression of gonadotropin-responsive genes known to be involved in follicle growth and ovulation was altered in *Efna5*^{-/-} ovaries. Immature *Efna5*^{-/-} and *Efna5*^{+/+} females were treated with eCG for 48h +/- hCG for 4, 14, or 24 h, and whole-ovary mRNA levels of known FSH and LH-responsive genes were determined by RT-qPCR. Specifically, we investigated the levels of prostaglandin-endoperoxide synthase 2 (*Ptgs2*), progesterone receptor (*Pgr*), and ADAM metallopeptidase with thrombospondin type 1 motif, 4 (*Adamts4*) (18) to assess the LH response (48h eCG + 4, 14, or 24 h hCG). We quantified the mRNA levels of cytochrome P450, family 19, subfamily A, polypeptide 1 (*Cyp19a1*) and luteinizing hormone/choriogonadotropin receptor (*Lhcgr*) to assess the FSH response (48h eCG).

As expected, hCG treatment increased *Pgr*, *Ptgs2*, and *Adamts4* mRNA levels in *Efna5*^{+/+} ovaries (**Figure 3-4, A-C**). However, in response to the same treatment, *Pgr*, *Ptgs2*, and *Adamts4* mRNA levels in *Efna5*^{-/-} females were 58%, 54%, and 80% lower, respectively, than in *Efna5*^{+/+} controls ($P < 0.0001$, **Figure 3-4, A-C**). To determine if this reduced response to hCG was due to a reduction in LH receptor (*Lhcgr*) gene expression, the mRNA levels of *Lhcgr* were determined after 48h eCG (**Figure 3-4F**). There was no significant difference in *Lhcgr* mRNA levels between genotypes, suggesting that loss of *Lhcgr* in *Efna5*^{-/-} females was not responsible for the attenuated response to hCG.

Since *Lhcgr* is a well-known FSH-responsive gene, this result also suggested that the response to FSH was intact in *Efna5*^{-/-} females. To test this, we investigated the mRNA levels of another well-known FSH-responsive gene, *Cyp19a1*, after 48h eCG treatment. No significant difference in *Cyp19a1* mRNA levels was observed between genotypes (**Figure 3-4D**), which is consistent with the lack of a difference in circulating estradiol levels between genotypes (**Figure 3-2A**). No differences were observed in *Fshr* mRNA levels (**Figure 3-4E**). In total, the results of these gene expression studies suggest that the ovarian response to LH, but not FSH, is disrupted in *Efna5*^{-/-} females.

In order to understand why superovulated *Efna5*^{-/-} females produced fewer oocytes than wildtype controls, we examined the histology of ovaries from superovulated wildtype and *Efna5*^{-/-} females.

3.3.6 *Efna5*^{-/-} ovaries exhibit increased numbers of expanded COCs after gonadotropin stimulation

Since cumulus expansion is necessary for ovulation to occur, we assessed the number of follicles containing expanded COCs in ovaries of superovulated *Efna5*^{+/+} and *Efna5*^{-/-} females. Examination of ovaries from *Efna5*^{-/-} and wildtype control females treated with eCG (48 h) followed by hCG (10 h) revealed a 2.6-fold increase in the number of follicles that had undergone cumulus expansion in *Efna5*^{-/-} females than in controls, with an average of 26 per mouse in *Efna5*^{-/-} females compared to 10 per mouse in *Efna5*^{+/+} females (**Figure 3-5A**). Based on this observation, we wondered if there would be a difference in the number of CLs/mouse between genotypes. However, ovaries from *Efna5*^{+/+} and *Efna5*^{-/-} females treated with eCG (48 h) followed by hCG (14 h) exhibited no significant difference in the total number of corpora lutea/mouse (**Figure 3-5B**). However, *Efna5*^{-/-} females contained a significantly higher number of oocytes aberrantly retained in CLs (1.5 fold) than control females (**Figure 3-5C**).

3.3.7 Abnormal follicle rupture, hemorrhaging, and fibrin thrombus formation in *Efna5*^{-/-} ovaries after gonadotropin stimulation

In ovaries of *Efna5*^{-/-} mice, follicles at all stages of growth were observed (**Figure 3-6, A-J**). However, *Efna5*^{-/-} ovaries exhibited a number of abnormal and fascinating histological features (**Figure 3-6, A-J**) that were not observed or were less pronounced in *Efna5*^{+/+} controls (**Figure 3-6K**). These features included the presence of GCs and COCs in the ovarian interstitium (**Figure 3-6E**, black arrow and **Figure 3-6G**, black arrow) and the presence of GCs in blood vessel lumina (**Figure 3-6C**, black arrow, and **Figure 3-6F**, open arrow). The presence of fibrin thrombi (**Figure 3-6D**, black arrow and **Figure 3-6G**, open pentagon) and hemorrhaging (**Figure 3-6, A-B**, open stars) were also observed. *Efna5*^{-/-} ovaries also exhibited instances of follicles rupturing in abnormal locations, specifically the non-apical rupture of follicles directed towards/into the interstitium as

opposed to the exterior of the ovary (**Figure 3-6D**, open arrow and **Figure 3-6G**, black arrow) and at least one occurrence of possibly premature rupture (**Figure 3-6A**, black arrow). In some cases, follicles exhibiting non-apical rupture contained luteinizing GCs (**Figure 3-6G**, open star). Finally, *Efna5*^{-/-} ovaries also exhibited a significant, 50% increase in oocytes trapped within luteinized follicles compared to *Efna5*^{+/+} controls (**Figure 3-6, H-J**, and **Figure 3-5C**).

3.3.8 Increased number of multi-oocyte follicles in adult *Efna5*^{-/-} mice

Interestingly, we observed that ovaries from 2 month-old *Efna5*^{-/-} females contain over four times more multi-oocyte follicles (MOFs) per ovary than wildtype controls ($P < 0.05$), with an average of 8.8 MOFs (± 2.8 , $n=5$) per *Efna5*^{-/-} female compared to 2.0 MOFs (± 0.70 , $n=5$) per *Efna5*^{+/+} female (**Figure 3-7B**). Having observed this significant increase in MOFs in adult *Efna5*^{-/-} ovaries, we wanted to determine if this increase would also be observed in immature *Efna5*^{-/-} mice, to help understand when and how during folliculogenesis this increase in MOFs might be occurring. In contrast to adult mice, no difference in MOF number was observed between genotypes at PND 21, with an average of 1.5 MOFs (± 1.5 , $n=2$) per *Efna5*^{+/+} female and 2.3 MOFs (± 0.95 , $n=4$) per *Efna5*^{-/-} female (**Figure 3-7A**).

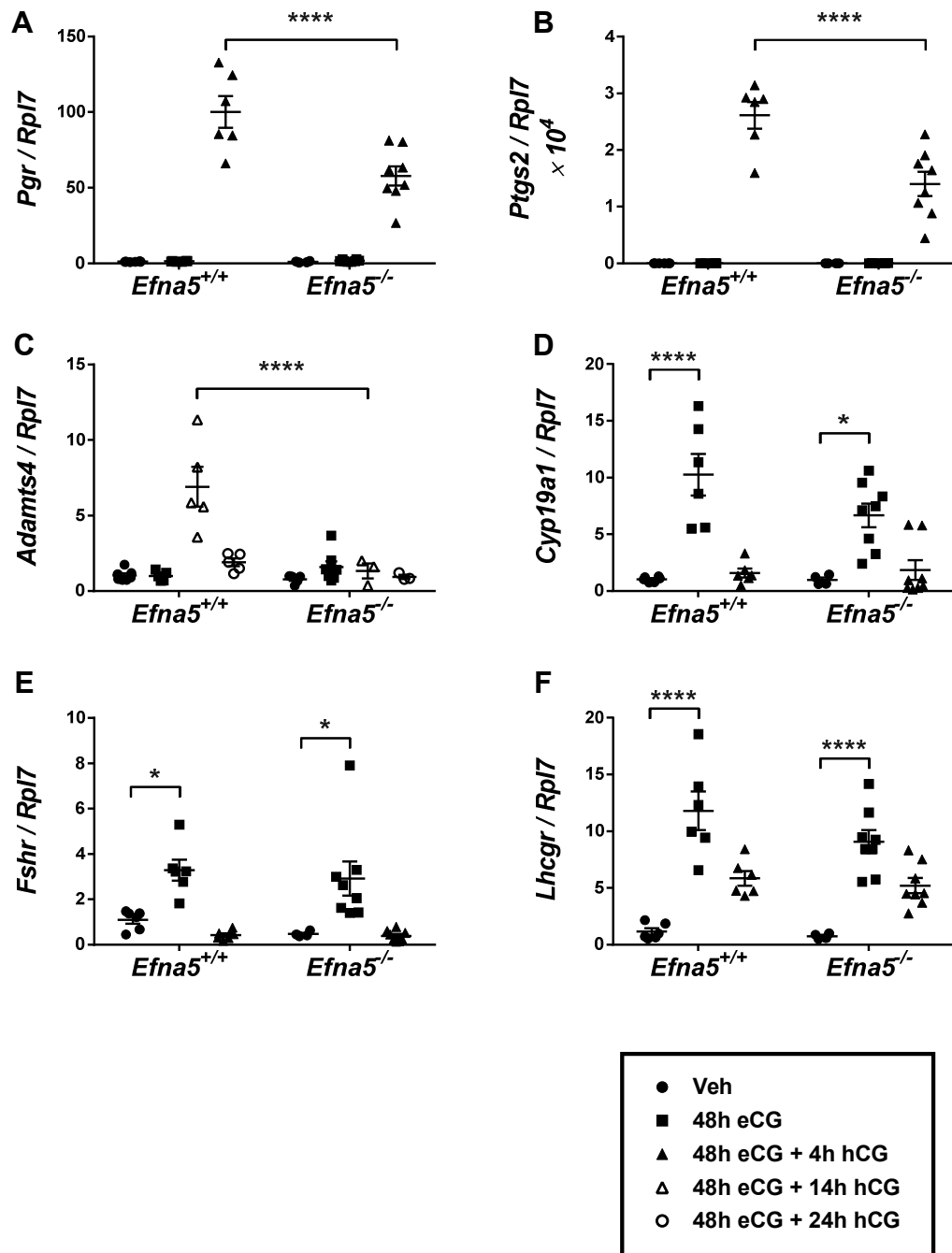


Figure 3-4: hCG-stimulated ovarian expression of *Pgr*, *Ptgs2*, and *Adamts4* is attenuated in *Efna5*^{-/-} mice.

Relative transcript abundance compared to *Rpl7* (mean ±SEM) was determined by qRT-PCR in whole ovaries of superovulated females for *Pgr* (A), *Ptgs2* (B), *Adamts4* (C), *Cyp19a1* (D), *Fshr* (E), and *Lhcgr* (F). A) *Pgr*. A two-way ANOVA found a significant

effect for treatment, $F(2, 32) = 148.7$, $P < 0.0001$; a significant effect for genotype, $F(1, 32) = 10.09$, $P = 0.0033$; and a significant interaction $F(2, 32) = 11.13$, $P = 0.0002$. Tukey's multiple comparisons test revealed a significant difference between genotypes in mice treated with 5.0 IU eCG (48 h) + 5.0 IU hCG (4 h), ****, $P < 0.0001$. **B) *Ptgs2***. A two-way ANOVA found a significant effect for treatment, $F(2, 32) = 132.7$, $P < 0.0001$; a significant effect for genotype, $F(1, 32) = 11.18$, $P = 0.0021$; and a significant interaction $F(2, 32) = 12.09$, $P = 0.0001$. Tukey's multiple comparisons test revealed a significant difference between genotypes in mice treated with 5.0 IU eCG (48 h) + 5.0 IU hCG (4 h), ****, $P < 0.0001$. **C) *Adamts4***. A two-way ANOVA found a significant effect for treatment, $F(3, 32) = 12.44$, $P < 0.0001$; a significant effect for genotype, $F(1, 32) = 15.26$, $P = 0.0005$; and a significant interaction $F(3, 32) = 11.18$, $P = 0.0001$. Tukey's multiple comparisons test revealed a significant difference between genotypes in mice treated with 5.0 IU eCG (48 h) + 5.0 IU hCG (14 h), ****, $P < 0.0001$. **D) *Cyp19a1***. A two-way ANOVA found a significant effect for treatment, $F(2, 32) = 32.83$, $P < 0.0001$; no significant effect for genotype, $F(1, 32) = 1.731$, $P = 0.1976$; and no significant interaction $F(2, 32) = 2.303$, $P = 0.1163$. Tukey's multiple comparisons test revealed a significant difference between *Efna5*^{+/+} mice treated with saline (48 h) or 5.0 IU eCG (48 h), ****, $P < 0.0001$; and a significant difference between *Efna5*^{-/-} mice treated with saline (48 h) or 5.0 IU eCG (48 h), *, $P = 0.0116$. **E) *Fshr***. A two-way ANOVA found a significant effect for treatment, $F(2, 32) = 22.57$, $P < 0.0001$; no significant effect for genotype, $F(1, 32) = 0.8305$, $P = 0.3689$; and no significant interaction, $F(2, 32) = 0.2067$, $P = 0.8143$. Tukey's multiple comparisons test revealed a significant difference between *Efna5*^{+/+} mice treated with saline (48 h) or 5.0 IU eCG (48 h), *, $P = 0.0210$; and a significant difference between *Efna5*^{-/-} mice treated with saline (48 h) or 5.0 IU eCG (48 h), *, $P = 0.0135$. **F) *Lhcgr***. A two-way ANOVA found a significant effect for treatment, $F(2, 32) = 45.02$, $P < 0.0001$; no significant effect for genotype, $F(1, 32) = 2.482$, $P = 0.1250$; and no significant interaction, $F(2, 32) = 0.8808$, $P = 0.4243$. Tukey's multiple comparisons test revealed a significant difference between *Efna5*^{+/+} mice treated with saline (48 h) or 5.0 IU eCG (48 h), ****, $P < 0.0001$; and a significant difference between *Efna5*^{-/-} mice treated with saline (48 h) or 5.0 IU eCG (48 h), ****, $P < 0.0001$.

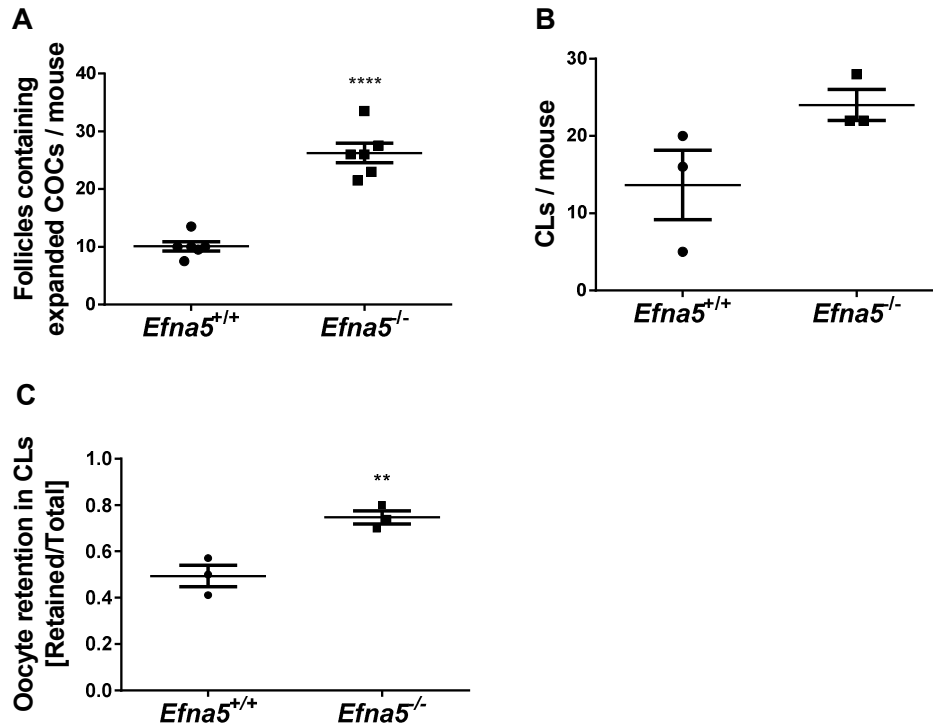


Figure 3-5: Follicles containing expanded COCs and retained oocytes are more numerous in superovulated *Efna5*^{-/-} mice.

Sectioned ovaries from superovulated *Efna5*^{+/+} and *Efna5*^{-/-} mice were stained with hematoxylin/eosin and scanned using an Aperio ScanScope (Leica Biosystems) at a magnification of 200x. Follicles containing expanded COCs (**A**) and corpora lutea (CLs) (mean \pm SEM) (**B**) were counted in every fifth section throughout the entire ovary, noting the fraction of CLs that contained oocytes (mean \pm SEM) (**C**). Additional sections were reviewed when necessary to ensure that CLs were not counted twice. **A**) “Number of follicles containing expanded COCs per mouse” was compared between *Efna5*^{+/+} and *Efna5*^{-/-} genotypes using the Student two-tailed unpaired t-test. A statistically significant difference was found between genotypes as determined by Student’s unpaired t-test; $t(10)=8.597$. ****, $p<0.0001$. **B**) The number of corpora lutea per mouse was compared between *Efna5*^{+/+} and *Efna5*^{-/-} genotypes using the Student two-tailed unpaired t-test. No statistically significant difference was found between genotypes as determined by Student’s unpaired t-test; $t(4)=2.104$, $p=0.1031$. **C**) “Fraction of CLs containing oocytes” was compared between *Efna5*^{+/+} and *Efna5*^{-/-} genotypes using the Student two-tailed unpaired t-test. A statistically significant difference was found between genotypes as determined by Student’s unpaired t-test; $t(4)=4.623$. **, $p=0.0099$.

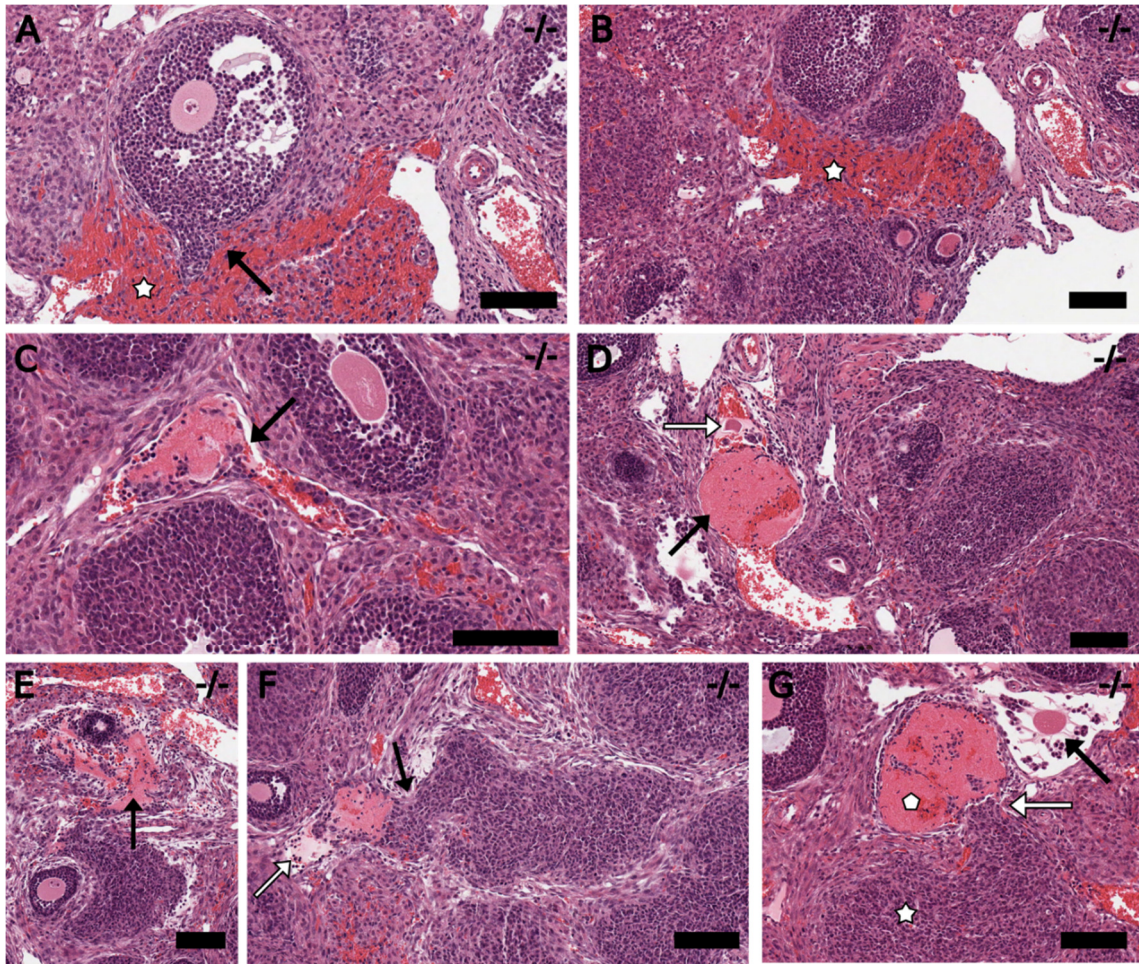


Figure 3-6: Superovulated *Efna5*^{-/-} mice exhibit non-apical follicle rupture and an increased incidence of oocytes trapped within luteinized follicles.

Sectioned ovaries from superovulated *Efna5*^{+/+} and *Efna5*^{-/-} mice were stained with hematoxylin/eosin and scanned using an Aperio ScanScope (Leica Biosystems) at a magnification of 200x. Black bars represent 100 μ m. **A)** Non-apical follicle rupture in the ovarian interstitium (black arrow) associated with hemorrhage near the site of rupture (white star). **B)** Hemorrhaging in the interstitium (open star). **C)** Blood vessel with fibrin thrombus and intraluminal granulosa cells (black arrow). **D)** Fibrin thrombus (black arrow) with the presence of an oocyte in the interstitium (open arrow). **E)** Presence of granulosa cells in the interstitium (black arrow). **F)** Non-apical follicle rupture in interstitium (black arrow) and blood vessel containing fibrin thrombus with granulosa cells. **G)** Fibrin thrombus (open pentagon) with the presence of an oocyte in the interstitium (black arrow), non-basal ovulatory cone indicating follicle rupture (open arrow), and luteinizing granulosa cells (open star).

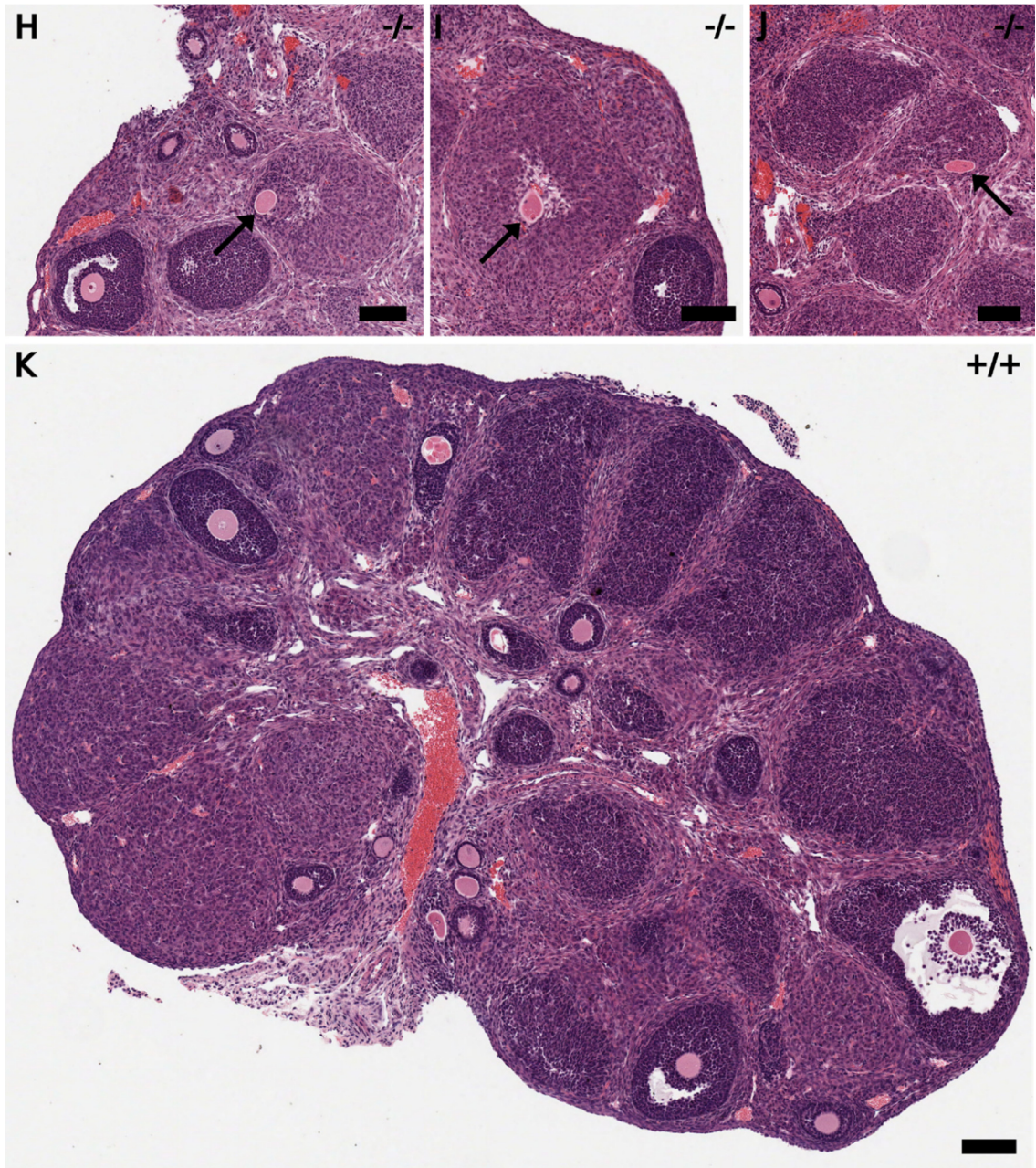


Figure 3-6. Superovulated $Efn5^{-/-}$ mice exhibit non-apical follicle rupture and an increased incidence of oocytes trapped within luteinized follicles.

H, I, J) Oocytes trapped within luteinizing follicles (black arrows). **K)** Representative $Efn5^{+/+}$ ovary.

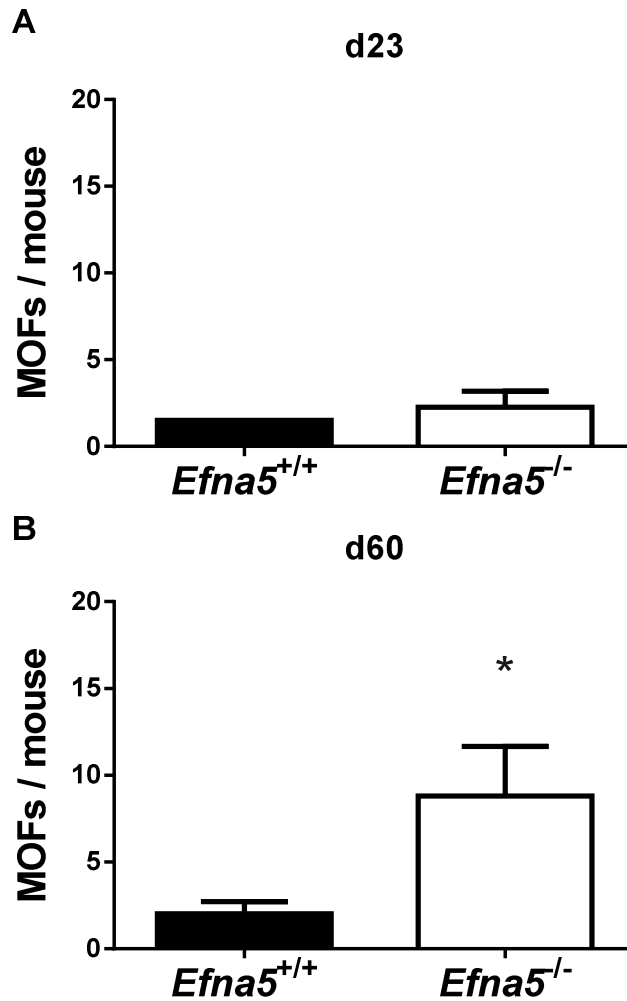


Figure 3-7: *Efna5*^{-/-} adult females exhibit more multi-oocyte follicles than juveniles.

Sectioned ovaries from superovulated *Efna5*^{+/+} and *Efna5*^{-/-} mice were stained with hematoxylin/eosin and scanned using an Aperio ScanScope (Leica Biosystems) at a magnification of 200x. Multi-oocyte follicles (MOFs) were counted in every third section throughout both ovaries of PND 23 (**A**) and PND 60 (**B**) mice. Additional sections were reviewed when necessary to ensure that MOFs were not counted twice. MOF counts were compared between *Efna5*^{+/+} and *Efna5*^{-/-} genotypes using the Student two-tailed unpaired t-test. **A**) At PND 23, no statistically significant difference was found between genotypes as determined by Student's unpaired t-test; $t(4)=0.4435$, $p=0.6803$. **B**) At PND 60 a statistically significant difference was found between genotypes as determined by Student's unpaired t-test; $t(8)=2.313$. *, $p=0.0494$.

3.4 Discussion

To our knowledge, no reproductive assessment has been carried out using the *Efna5*^{-/-} mouse or any other ephrin or Eph receptor knockout animal model. We now report that female mice lacking ephrin-A5 are subfertile and possess a number of ovarian defects that may underlie this reduced fertility.

3.4.1 *Efna5*^{-/-} females produce smaller litters and release fewer oocytes than controls

In a continuous breeding study, *Efna5*^{-/-} females produced litters that were 40% smaller than *Efna5*^{+/+} controls, indicating that ephrin-A5 is important for optimal fertility in female mice. Consistent with this observation, superovulated reproductively immature *Efna5*^{-/-} female mice ovulated 40% fewer COCs than controls, suggesting that ephrin-A5 is required for a maximal response to gonadotropins. This blunted response was not likely due to differences in gonadotropin receptor levels, as both *Lhcgr* and *Fshr* mRNA levels were similar in both genotypes. To further explore the basis of this attenuated ovarian response, we measured the ovarian expression of known FSH and LH responsive genes in *Efna5*^{-/-} females stimulated with eCG and hCG.

3.4.2 *Efna5*^{-/-} females exhibit an attenuated response to hCG but not eCG

After eCG treatment, no differences in the mRNA levels of the FSH-responsive genes *Cyp19a1* and *Lhcgr* were observed between *Efna5*^{+/+} and *Efna5*^{-/-} ovaries, suggesting that *Efna5*^{-/-} ovaries respond normally to FSH. However, we observed attenuated hCG-stimulated expression of the LH-responsive genes *Pgr*, *Ptgs2*, and *Adamts4* in *Efna5*^{-/-} females compared to controls, suggesting that the ovarian response to LH is compromised in *Efna5*^{-/-} females, and may contribute to their reduced ovulatory capacity.

3.4.3 *Efna5*^{-/-} ovaries exhibit numerous histological abnormalities

Ovulation requires extensive tissue remodeling, which involves the dynamic regulation of cell migration and adhesion, and the deposition and degradation of extracellular matrix components. Like all members of the ephrin family, ephrin-A5 is

best known as a regulator of cell positioning and is thus well-suited to be involved in these processes, and ephrin-A5-Fc and EphA5-Fc influence morphology and reduce adhesion, respectively, of mouse GCs in culture (3).

Gonadotropin-stimulated *Efna5*^{-/-} mice possessed ovaries with an increased number of: a) luteinized follicles containing trapped oocytes, b) follicle rupture within the ovary resulting in oocyte release into the interstitium and/or blood vessel lumina, c) GCs present in blood vessel lumina, d) the presence of fibrin thrombi in blood vessels, and e) the presence of extravasated blood near sites of non-apical rupture. These histological features bear a striking resemblance to those observed in several loss-of-function rodent models, specifically for the LH-responsive genes *Pgr*, *Ptgs2*, and *Adamts4*, for which we detected reduced mRNA levels in *Efna5*^{-/-} ovaries.

3.4.4 Progesterone receptor (*Pgr*)

We observed a 58% reduction in ovarian *Pgr* mRNA levels in superovulated *Efna5*^{-/-} mice. While follicle growth and cumulus expansion proceed normally in mice lacking *Pgr*, ovulation fails due to impaired follicle rupture (19). This results in the formation of luteinized follicles containing trapped COCs, suggesting that the primary physiological role of *Pgr* in the ovary is promoting follicle rupture (20). Similar to the *Pgr*^{-/-} ovary (19), *Efna5*^{-/-} ovaries exhibit an increased incidence of oocytes trapped within luteinized follicles. Within the ovary, the PR is expressed primarily in GCs in response to stimulation by LH, and mediates the expression of many genes involved in ovulation. Therefore, attenuated expression of *Pgr* may be responsible, at least in part, for the increased incidence of luteinized follicles containing trapped oocytes that we observed in *Efna5*^{-/-} females.

3.4.5 Prostaglandin-endoperoxide synthase 2 (*Ptgs2*)

We observed a 54% reduction in ovarian *Ptgs2* mRNA levels in superovulated *Efna5*^{-/-} mice. *Ptgs2* is involved in the post-LH rise in prostaglandin synthesis within the preovulatory follicle (21). *Ptgs2*^{-/-} females are infertile, exhibit oocyte retention in CLs, and defective cumulus expansion (22). Rats treated with indomethacin, a PTGS2 inhibitor, are also anovulatory and exhibit follicle rupture defects including oocyte

retention within luteinized follicles and non-apical follicle rupture (23). Similar to *Ptgs2*^{-/-} females, *Efna5*^{-/-} females exhibited COCs trapped within CLs, non-apical follicle rupture resulting in interstitial and intraluminal COC release, and formation of structures reminiscent of follicular fluid emboli reported in ovaries of indomethacin-treated rats (23). Therefore, reduced *Ptgs2* expression may contribute to the reproductive phenotype of *Efna5*^{-/-} females.

3.4.6 ADAM metalloproteinase with thrombospondin type 1 motif, 4 (*Adamts4*)

We observed an 80% reduction in ovarian *Adamts4* mRNA levels in superovulated *Efna5*^{-/-} mice. *Adamts4* encodes a member of the *a disintegrin and metalloproteinase with thrombospondin-like repeats* family. *Adamts4* is expressed in the ovary along with *Adamts1* and *Adamts5* in distinct spatiotemporal patterns, and is thought to be involved in tissue remodeling that occurs prior to, during, and after ovulation (18). However, the specific roles of these proteases in the context of ovulation are not currently known. Interestingly, expression of *Adamts4* is enriched in ovulation cones/stigma, which are highly vascularized. *Adamts4* is also enriched in endothelial cells of the forming CL of superovulated mice 16 h post-hCG (18), suggesting that *Adamts4* plays a role in follicle rupture and neovascularization of the CL. Consistent with these proposed roles for *Adamts4*, *Efna5*^{-/-} females exhibit abnormal follicle rupture and vascular defects such as fibrin thrombi. Although *Adamts4*^{-/-} mice are reported as phenotypically normal (24), suggesting that other proteases may compensate for its loss in the ovary, given the dramatic reduction in *Adamts4* mRNA levels we observe in *Efna5*^{-/-} mice, we speculate that loss of *Adamts4* expression may contribute to the abnormal follicle rupture in *Efna5*^{-/-} females.

3.4.7 Relating LH, *Pgr*, *Ptgs2*, and *Adamts4* to *Efna5*^{-/-} reproductive and ovarian defects

In the *Efna5*^{-/-} ovary, we observed follicles ruptured within the ovary resulting in intraovarian oocyte release, and a higher incidence of CLs containing trapped oocytes. We postulate that in *Efna5*^{-/-} mice, these follicles fail to ovulate normally because they are, to varying degrees, unable to fully respond to LH.

LH triggers a stepwise cascade of events, with cumulus expansion occurring early, leading to ovulation and formation of the CL at a later stage. Therefore, it seems plausible that different follicles may exhibit a range of partial responsiveness to LH. Thus, we might expect to observe an ovulatory defect at any of the LH-triggered stages, with LH able to “push” some preovulatory follicles further along the “ovulation” pathway than others. This idea is supported by the attenuated expression of *Pgr*, *Ptgs2*, and *Adamts4* in *Efna5^{-/-}* females, all of which are proposed to be involved in follicle rupture. Cumulus expansion is normal in *Pgr^{-/-}* mice, and although *Ptgs2^{-/-}* mice exhibit reduced cumulus expansion, *Ptgs2* is reduced by ~50% in *Efna5^{-/-}* females, which may be sufficient for cumulus expansion to occur. Therefore, reduced expression of *Pgr* and *Ptgs2* following hCG treatment could specifically impair follicle rupture, while still allowing cumulus expansion to occur.

Abnormal follicle rupture may also help explain the reduced ovulatory potential of *Efna5^{-/-}* females. A necessary condition of successful ovulation is that follicular rupture occurs on the apical surface of the follicle to facilitate COC release into the oviduct. In *Efna5^{-/-}* mice, COCs released into the interstitium, blood vessel lumina, and retained in corpora lutea, fail to reach the oviduct. Thus, the increased frequency of abnormal follicular rupture, combined with the increased incidence of unruptured follicles, may contribute to the decreased ovulation potential that we observed in *Efna5^{-/-}* females.

3.4.8 Hemorrhaging, fibrin thrombi, and GCs in blood vessel lumina

We observed hemorrhaging and formation of fibrin thrombi in ovaries of superovulated *Efna5^{-/-}* females. These events likely result from non-apically released GCs and follicular fluid, whose proteolytic/invasive properties damage the surrounding tissue, including the vasculature. This vascular damage has been observed in other murine models. In indomethacin-treated rats, release of follicular fluid and GCs into the interstitium results in invasion of the stroma, rupture of blood and lymphatic vessels, hemorrhagia, and the formation of emboli composed of follicular fluid (25). Furthermore, cumulus cells from expanded COCs exhibit transiently increased invasive properties, with increasing migratory and adhesive capacity 4 to 12 h post-hCG (26). Under normal circumstances, these properties may contribute to successful fertilization by promoting

migration of the apically ovulated COC. However, when directed toward the ovarian interstitium during non-apical follicle rupture, these properties may contribute to the ovarian hemorrhaging and formation of fibrin thrombi observed in *Efna5^{-/-}* females.

3.4.9 How does loss of ephrin-A5 result in reduced expression of *Pgr*, *Ptgs2*, and *Adamts4*?

We show that ephrin-A5 is necessary for optimal ovarian expression of *Pgr*, *Ptgs2*, and *Adamts4* in response to gonadotropin stimulation. Since *Pgr* and *Ptgs2* are known LH-responsive genes, and in our study, *Adamts4* is also LH-responsive, it is logical that the reduced mRNA levels of *Pgr*, *Ptgs2*, and *Adamts4* in *Efna5^{-/-}* ovaries are due, at least in part, to an attenuated transcriptional response of GCs to LH. Reduced transcript stabilization is another possible mechanism. How ephrin-A5 might regulate either transcript production or stabilization in the ovary is currently unknown.

Nevertheless, Eph-ephrin signaling has been linked to changes in gene expression in various model systems, although the mechanism(s) by which this occurs are not well understood. Stimulation with A-class ephrins increases expression of epidermal differentiation markers and suppresses expression of genes associated with cell adhesion in human epidermal keratinocytes (27). Furthermore, EphB4^{-/-} embryonic stem cells (ESCs) exhibit impaired differentiation, with many genes dysregulated compared to EphB4^{+/+} ESCs (28). Finally, stimulation of rat epithelial small intestine IEC-6 cells with EphB1 results in upregulation of wound-healing genes via the ERK1/2 pathways (29). Currently, the mechanism by which Eph-ephrin signaling influences ovarian gene expression in GCs is not known. However, several reports indicate that the ERK, beta-catenin, and PKA pathways, which are activated by LH, are influenced by Eph-ephrin signaling, and therefore may be disrupted by loss of ephrin-A5 in the ovary, resulting in reduced expression of LH-responsive genes such as *Pgr* and *Ptgs2*.

In the mouse, extracellular regulated kinases 1 and 2 (ERK1/2) are essential for female fertility. Mice lacking ERK1/2 in GCs exhibit a compromised response to LH, including impaired cumulus expansion, ovulation, luteinization, and induction of many LH-responsive genes, including *Pgr* and *Ptgs2* (30). Several reports in other model

systems indicate that Eph-ephrin signaling regulates phosphorylation of ERK1/2, inhibiting activation in most model systems (31-33) and promoting activation in some (34-37). EPHB4 can inhibit or enhance ERK1/2 activation depending on cell type, due to differences in coupling with downstream signaling elements (38). Therefore, given that ERK1/2 are necessary for LH-stimulated activation of *Ptgs2* and *Pgr* in mouse GCs (30), and that ERK1/2 phosphorylation is elevated for at least 4 h post-LH in cultured rat follicles (39), GCs lacking ephrin-A5 in our model may insufficiently activate ERK1/2 signaling to optimally induce *Ptgs2* and *Pgr* upon stimulation with LH. Determining the molecular mechanism by which loss of ephrin-A5 may attenuate ERK1/2 activation, resulting in suboptimal LH gene activation, requires further investigation.

Second, ephrin-A5 may also influence *Ptgs2* expression by altering beta-catenin levels. We previously reported that stimulation of rat granulosa cells with ephrin-A5 results in decreased beta-catenin levels (3). Beta-catenin serves as both a component of adherens junctions (40) and as a transcriptional activator (41,42). In the ovary, appropriate beta-catenin levels in GCs is critical for fertility, since mice expressing a granulosa cell-specific, dominant-stable form of beta-catenin exhibit impaired ovulation and luteinization, and attenuated hCG-stimulated expression of *Ptgs2* (43). Therefore, FSH-induced expression of ephrin-A5 (3) may promote degradation of beta-catenin in mouse GCs in preparation for the LH surge. In GCs of *Efna5*^{-/-} mice, loss of ephrin-A5 may result in increased beta-catenin levels, contributing to the reduced expression of *Ptgs2*.

Third, Eph-ephrin signaling may cross-talk with the cAMP/PKA pathway. Indirect crosstalk between the Eph-ephrin and cAMP/PKA pathways has been previously described in two model systems. In mouse cortical progenitor cells, stimulation with recombinant ephrin-B1 potentiates activation of the PKA target, cAMP-responsive element binding protein (CREB), by glutamate in an EphB2-dependent manner (44). Furthermore, ephrin-A5 stimulation of cultured mouse hippocampal slices promotes activation of PKA and CREB in an EphA5-dependent manner (45). Therefore, Eph-ephrin signaling may indirectly activate or potentiate PKA in GCs, and loss of ephrin-A5 may result in insufficient PKA activation for optimal induction of *Pgr* and *Ptgs2*.

Finally, it is possible that in *Efna5*^{-/-} females, reduced *Adamts4* expression is a consequence of attenuated induction of *Pgr* by LH. In *Pgr*^{-/-} mice, LH-induced ovarian expression of *Adamts4* is attenuated 12 h post-hCG, suggesting that PR regulates *Adamts4* expression. In *Efna5*^{-/-} ovaries, hCG-induced *Pgr* expression is reduced 4 h post-hCG, and *Adamts4* expression is attenuated 14 h post-hCG, suggesting that the reduction of PR at 4 h may reduce *Adamts4* expression by 14h.

3.4.10 *Efna5* is one of many neuronal guidance genes expressed in the mouse ovary

This study has shown that *Efna5* plays an important role in the mouse ovary, and that its absence has negative consequences for female fertility. However, ephrin-A5 has been characterized primarily in the context of axon guidance during embryonic development; thus, its role in female reproduction and in the mouse ovary are novel. In support of a role for a neuronal guidance gene such as ephrin-A5 in the ovary, it is interesting to note that expression of neuronal cell guidance genes in the ovary is not without precedent. In addition to *Efna5*, expression of several genes associated with neuronal cell guidance is higher in large bovine follicles than in small antral follicles (8). The authors speculate that these genes mediate ovarian tissue remodeling and cell migration in the follicle, resulting in oocyte release facing the ovarian surface (8). In line with this reasoning, we also observed non-apical follicle rupture of follicles in *Efna5*^{-/-} females. Thus, ephrin-A5 may be one of many genes with roles in both neuronal cells and in the ovary.

3.4.11 Experimental Considerations

One limitation of our *Efna5*^{-/-} model is that it is a global knockout, and thus it is possible that abnormal development of the hypothalamus, pituitary, and/or uterus may occur. However, our results suggest that the hypothalamic-pituitary-gonadal (HPG) axis is likely not largely disrupted in *Efna5*^{-/-} females. First, litter frequency was unaffected, suggesting that estrous cyclicity is normal in *Efna5*^{-/-} females, and therefore, as far as its capacity to coordinate the proper timing of follicle growth and ovulation, the HPG axis is intact. An intact HPG axis is also consistent with our observation that gonadotropin-stimulated estradiol and progesterone levels were similar in *Efna5*^{-/-} females and controls.

However, we cannot completely rule out the possibility that the lack of ephrin-A5 in the hypothalamus or pituitary may be in part responsible for the phenotype we observed. To do this, a granulosa cell type-specific, conditional *Efna5* knockout mice would be required.

3.4.12 Unexpected findings

We observed an increased number of multi-oocyte follicles (MOFs) in ovaries of normally-cycling adult *Efna5*^{-/-} females compared to controls. However, we did not detect a difference in MOF numbers in immature mice at 3 weeks of age, suggesting that in *Efna5*^{-/-} females MOF formation is not a result of impaired oocyte nest break-down; otherwise, differences in MOF levels would be expected in immature mice. Instead, our results suggest that the increase in MOF numbers is gonadotropin-dependent, and may occur by gonadotropin-dependent merging of single follicles. Follicle merging has been proposed to increase the incidence of MOFs in mice harboring an oocyte-specific deletion of core-1- β 1,3-galactosyl-transferase (*Clgalt1*) (46,47), due to degradation of the basal lamina and initiation of aberrant granulosa cell invasion. In *Efna5*^{-/-} females, we speculate that MOF formation may be linked to abnormal follicle rupture. Premature rupture of follicles prior to cumulus expansion may result in breaching of the follicle wall and permit joining of adjacent follicles, resulting in MOF formation, as in the oocyte-specific *Clgalt1* knockout mice (46).

3.5 Conclusion

In conclusion, our data indicate that ephrin-A5 is required for optimal reproductive function in female mice. Its absence results in reduced fertility and a partially impaired response to hCG, which includes attenuated ovarian expression of *Pgr*, *Ptgs2*, and *Adamts4*, follicle rupture defects, and reduced ovulatory capacity. Ephrin-A5 plays an important and previously-unidentified role in the normal function of the mouse ovary, and we speculate that defective ovarian ephrin-A5 signaling accounts for some incidences of idiopathic infertility in women.

3.6 Bibliography

1. Gougeon A. Dynamics of follicular growth in the human: a model from preliminary results. *Human reproduction*. 1986;1(2):81-87.
2. Lackmann M, Boyd AW. Eph, a protein family coming of age: more confusion, insight, or complexity? *Sci Signal*. 2008;1(15):re2.
3. Buensuceso AV, Deroo BJ. The ephrin signaling pathway regulates morphology and adhesion of mouse granulosa cells in vitro. *Biol Reprod*. 2013;88(1):25.
4. Gale NW, Baluk P, Pan L, Kwan M, Holash J, DeChiara TM, McDonald DM, Yancopoulos GD. Ephrin-B2 selectively marks arterial vessels and neovascularization sites in the adult, with expression in both endothelial and smooth-muscle cells. *Dev Biol*. 2001;230(2):151-160.
5. Egawa M, Yoshioka S, Higuchi T, Sato Y, Tatsumi K, Fujiwara H, Fujii S. Ephrin B1 is expressed on human luteinizing granulosa cells in corpora lutea of the early luteal phase: the possible involvement of the B class Eph-ephrin system during corpus luteum formation. *The Journal of clinical endocrinology and metabolism*. 2003;88(9):4384-4392.
6. Xu Y, Zagoura D, Keck C, Pietrowski D. Expression of Eph receptor tyrosine kinases and their ligands in human Granulosa lutein cells and human umbilical vein endothelial cells. *Experimental and Clinical Endocrinology and Diabetes*. 2006;114(10):590-595.
7. Forde N, Mihm M, Canty MJ, Zielak AE, Baker PJ, Park S, Lonergan P, Smith GW, Coussens PM, Ireland JJ, Evans AC. Differential expression of signal transduction factors in ovarian follicle development: a functional role for betaglycan and FIBP in granulosa cells in cattle. *Physiol Genomics*. 2008;33(2):193-204.
8. Hatzirodos N, Irving-Rodgers HF, Hummitzsch K, Harland ML, Morris SE, Rodgers RJ. Transcriptome profiling of granulosa cells of bovine ovarian follicles during growth from small to large antral sizes. *BMC genomics*. 2014;15:24.
9. Frisen J, Yates PA, McLaughlin T, Friedman GC, O'Leary DD, Barbacid M. Ephrin-A5 (AL-1/RAGS) is essential for proper retinal axon guidance and topographic mapping in the mammalian visual system. *Neuron*. 1998;20(2):235-243.
10. Pfeiffenberger C, Cutforth T, Woods G, Yamada J, Renteria RC, Copenhagen DR, Flanagan JG, Feldheim DA. Ephrin-As and neural activity are required for eye-specific patterning during retinogeniculate mapping. *Nat Neurosci*. 2005;8(8):1022-1027.
11. Cooper MA, Son AI, Komlos D, Sun Y, Kleiman NJ, Zhou R. Loss of ephrin-A5 function disrupts lens fiber cell packing and leads to cataract. *Proceedings of the National Academy of Sciences of the United States of America*. 2008;105(43):16620-16625.

12. Son AI, Cooper MA, Sheleg M, Sun Y, Kleiman NJ, Zhou R. Further analysis of the lens of ephrin-A5^{-/-} mice: development of postnatal defects. *Molecular vision*. 2013;19:254-266.
13. Genander M, Cook PJ, Ramskold D, Keyes BE, Mertz AF, Sandberg R, Fuchs E. BMP signaling and its pSMAD1/5 target genes differentially regulate hair follicle stem cell lineages. *Cell stem cell*. 2014;15(5):619-633.
14. Bertolin K, Gossen J, Schoonjans K, Murphy BD. The orphan nuclear receptor Nr5a2 is essential for luteinization in the female mouse ovary. *Endocrinology*. 2014;155(5):1931-1943.
15. Chen M, Wang X, Wang Y, Zhang L, Xu B, Lv L, Cui X, Li W, Gao F. Wt1 is involved in leydig cell steroid hormone biosynthesis by regulating paracrine factor expression in mice. *Biol Reprod*. 2014;90(4):71.
16. Chaturvedi G, Arai K, Terranova PF, Roby KF. The Src tyrosine kinase pathway regulates thecal CYP17 expression and androstenedione secretion. *Molecular and cellular biochemistry*. 2008;318(1-2):191-200.
17. Cibois M, Boulanger G, Audic Y, Paillard L, Gautier-Courteille C. Inactivation of the Celf1 gene that encodes an RNA-binding protein delays the first wave of spermatogenesis in mice. *PloS one*. 2012;7(10):e46337.
18. Richards JS, Hernandez-Gonzalez I, Gonzalez-Robayna I, Teuling E, Lo Y, Boerboom D, Falender AE, Doyle KH, LeBaron RG, Thompson V, Sandy JD. Regulated expression of ADAMTS family members in follicles and cumulus oocyte complexes: evidence for specific and redundant patterns during ovulation. *Biol Reprod*. 2005;72(5):1241-1255.
19. Lydon JP, DeMayo FJ, Funk CR, Mani SK, Hughes AR, Montgomery CA, Jr., Shyamala G, Conneely OM, O'Malley BW. Mice lacking progesterone receptor exhibit pleiotropic reproductive abnormalities. *Genes & development*. 1995;9(18):2266-2278.
20. Akison LK, Robker RL. The critical roles of progesterone receptor (PGR) in ovulation, oocyte developmental competence and oviductal transport in mammalian reproduction. *Reproduction in domestic animals = Zuchthygiene*. 2012;47 Suppl 4:288-296.
21. Davis BJ, Lennard DE, Lee CA, Tiano HF, Morham SG, Wetsel WC, Langenbach R. Anovulation in cyclooxygenase-2-deficient mice is restored by prostaglandin E2 and interleukin-1beta. *Endocrinology*. 1999;140(6):2685-2695.
22. Lim H, Paria BC, Das SK, Dinchuk JE, Langenbach R, Trzaskos JM, Dey SK. Multiple female reproductive failures in cyclooxygenase 2-deficient mice. *Cell*. 1997;91(2):197-208.
23. Gaytan F, Tarradas E, Bellido C, Morales C, Sanchez-Criado JE. Prostaglandin E(1) inhibits abnormal follicle rupture and restores ovulation in indomethacin-treated rats. *Biol Reprod*. 2002;67(4):1140-1147.

24. Boerboom D, Lafond JF, Zheng X, Lapointe E, Mittaz L, Boyer A, Pritchard MA, DeMayo FJ, Mort JS, Drolet R, Richards JS. Partially redundant functions of Adamts1 and Adamts4 in the perinatal development of the renal medulla. *Developmental dynamics : an official publication of the American Association of Anatomists*. 2011;240(7):1806-1814.
25. Gaytan M, Bellido C, Morales C, Sanchez-Criado JE, Gaytan F. Effects of selective inhibition of cyclooxygenase and lipooxygenase pathways in follicle rupture and ovulation in the rat. *Reproduction*. 2006;132(4):571-577.
26. Akison LK, Alvino ER, Dunning KR, Robker RL, Russell DL. Transient invasive migration in mouse cumulus oocyte complexes induced at ovulation by luteinizing hormone. *Biol Reprod*. 2012;86(4):125.
27. Walsh R, Blumenberg M. Specific and shared targets of ephrin A signaling in epidermal keratinocytes. *The Journal of biological chemistry*. 2011;286(11):9419-9428.
28. Wang Z, Cohen K, Shao Y, Mole P, Dombkowski D, Scadden DT. Ephrin receptor, EphB4, regulates ES cell differentiation of primitive mammalian hemangioblasts, blood, cardiomyocytes, and blood vessels. *Blood*. 2004;103(1):100-109.
29. Hafner C, Meyer S, Hagen I, Becker B, Roesch A, Landthaler M, Vogt T. Ephrin-B reverse signaling induces expression of wound healing associated genes in IEC-6 intestinal epithelial cells. *World journal of gastroenterology : WJG*. 2005;11(29):4511-4518.
30. Fan HY, Liu Z, Shimada M, Sterneck E, Johnson PF, Hedrick SM, Richards JS. MAPK3/1 (ERK1/2) in ovarian granulosa cells are essential for female fertility. *Science*. 2009;324(5929):938-941.
31. Miao H, Wei BR, Peehl DM, Li Q, Alexandrou T, Schelling JR, Rhim JS, Sedor JR, Burnett E, Wang B. Activation of EphA receptor tyrosine kinase inhibits the Ras/MAPK pathway. *Nat Cell Biol*. 2001;3(5):527-530.
32. Yue X, Dreyfus C, Kong TA, Zhou R. A subset of signal transduction pathways is required for hippocampal growth cone collapse induced by ephrin-A5. *Developmental neurobiology*. 2008;68(10):1269-1286.
33. Petty A, Myshkin E, Qin H, Guo H, Miao H, Tochtrop GP, Hsieh JT, Page P, Liu L, Lindner DJ, Acharya C, MacKerell AD, Jr., Ficker E, Song J, Wang B. A small molecule agonist of EphA2 receptor tyrosine kinase inhibits tumor cell migration in vitro and prostate cancer metastasis in vivo. *PloS one*. 2012;7(8):e42120.
34. Pratt RL, Kinch MS. Activation of the EphA2 tyrosine kinase stimulates the MAP/ERK kinase signaling cascade. *Oncogene*. 2002;21(50):7690-7699.
35. Aoki M, Yamashita T, Tohyama M. EphA receptors direct the differentiation of mammalian neural precursor cells through a mitogen-activated protein kinase-dependent pathway. *The Journal of biological chemistry*. 2004;279(31):32643-32650.

36. Shin J, Gu C, Kim J, Park S. Transient activation of the MAP kinase signaling pathway by the forward signaling of EphA4 in PC12 cells. *BMB reports*. 2008;41(6):479-484.
37. Brantley-Sieders DM, Zhuang G, Hicks D, Fang WB, Hwang Y, Cates JM, Coffman K, Jackson D, Bruckheimer E, Muraoka-Cook RS, Chen J. The receptor tyrosine kinase EphA2 promotes mammary adenocarcinoma tumorigenesis and metastatic progression in mice by amplifying ErbB2 signaling. *The Journal of clinical investigation*. 2008;118(1):64-78.
38. Xiao Z, Carrasco R, Kinneer K, Sabol D, Jallal B, Coats S, Tice DA. EphB4 promotes or suppresses Ras/MEK/ERK pathway in a context-dependent manner: Implications for EphB4 as a cancer target. *Cancer biology & therapy*. 2012;13(8):630-637.
39. Kalma Y, Granot I, Galiani D, Barash A, Dekel N. Luteinizing hormone-induced connexin 43 down-regulation: inhibition of translation. *Endocrinology*. 2004;145(4):1617-1624.
40. Sundfeldt K, Piontkewitz Y, Billig H, Hedin L. E-cadherin-catenin complex in the rat ovary: cell-specific expression during folliculogenesis and luteal formation. *Journal of reproduction and fertility*. 2000;118(2):375-385.
41. Morin PJ, Sparks AB, Korinek V, Barker N, Clevers H, Vogelstein B, Kinzler KW. Activation of beta-catenin-Tcf signaling in colon cancer by mutations in beta-catenin or APC. *Science*. 1997;275(5307):1787-1790.
42. Korinek V, Barker N, Morin PJ, van Wichen D, de Weger R, Kinzler KW, Vogelstein B, Clevers H. Constitutive transcriptional activation by a beta-catenin-Tcf complex in APC^{-/-} colon carcinoma. *Science*. 1997;275(5307):1784-1787.
43. Fan HY, O'Connor A, Shitanaka M, Shimada M, Liu Z, Richards JS. Beta-catenin (CTNNB1) promotes preovulatory follicular development but represses LH-mediated ovulation and luteinization. *Molecular endocrinology*. 2010;24(8):1529-1542.
44. Takasu MA, Dalva MB, Zigmond RE, Greenberg ME. Modulation of NMDA receptor-dependent calcium influx and gene expression through EphB receptors. *Science*. 2002;295(5554):491-495.
45. Akaneya Y, Sohya K, Kitamura A, Kimura F, Washburn C, Zhou R, Ninan I, Tsumoto T, Ziff EB. Ephrin-A5 and EphA5 interaction induces synaptogenesis during early hippocampal development. *PloS one*. 2010;5(8):e12486.
46. Williams SA, Stanley P. Mouse fertility is enhanced by oocyte-specific loss of core 1-derived O-glycans. *FASEB journal : official publication of the Federation of American Societies for Experimental Biology*. 2008;22(7):2273-2284.
47. Su W, Guan X, Zhang D, Sun M, Yang L, Yi F, Hao F, Feng X, Ma T. Occurrence of multi-oocyte follicles in aquaporin 8-deficient mice. *Reprod Biol Endocrinol*. 2013;11:88.

4 Chapter 4: Cyclic AMP stimulates PKA-dependent transcriptional activation of the mouse *Epha5* upstream genomic region in the KGN granulosa cell line

4.1 Introduction

Eph receptors, encoded by *Eph* genes, comprise the largest known family of receptor tyrosine kinases (RTKs) and interact with ligands known as ephrins, which are encoded by *Efn* genes. The entire family of Eph receptors and ephrins is classified into two subclasses, A or B, based on receptor-ligand affinity and amino acid sequence similarity (1). In general, A-class receptors have greater affinity for A-class ephrins than for B-class ephrins, and B-class receptors have greater affinity for B-class ephrins than for A-class ephrins. Receptor-ligand interaction is promiscuous within classes, although inter-class promiscuity has been reported (2). All Eph receptors and ephrins are membrane-associated, and therefore Eph-ephrin signaling is initiated at points of cell-cell contact. Furthermore, as membrane-associated signaling elements, both Eph receptors and ephrins may transmit signals via their cytoplasmic domains and/or by association with other transmembrane signaling proteins. Eph-ephrin signaling has been studied primarily in the context of embryonic development, particularly in axon guidance and tissue segmentation (3,4).

Despite progress in understanding Eph receptor and ephrin function, relatively little is known about regulation of the genes encoding them. Much of the knowledge of *Eph* and *Efn* transcriptional regulation emerged from efforts to understand patterns of expression during embryonic development. As a result, many transcriptional regulators of *Eph* and *Efn* expression identified thus far are well-known regulators in embryonic development. For example, homeobox (*Hox*) genes have been implicated in controlling *Eph* and *Efn* expression during embryonic morphogenesis (5). Chick brain factor 1, encoded by *Cbfl*, regulates expression of *Efna2*, *Efna5*, and *Epha3* during axon guidance in the chick (6), while NFYA (nuclear transcription factor Y, alpha), MEIS1 (myeloid ecotropic viral integration site), and MAZ (Myc-associated zinc finger protein) regulate

Efnb2 expression during prenatal angiogenesis in mice (7). NF- κ B has also been implicated in regulating *EFNA4* expression in human lymphocytes (8).

Furthermore, the expression of numerous *Eph* and *Efn* genes is dysregulated in cancer, where this dysregulation has been associated with tumour-promoting and suppressing activity (9). For example, *Epha2* is upregulated in some human cancers, and its downregulation has been associated with decreased tumour growth and prolonged survival in some animal models (10). Expression of *EFNA1* and *EFNA5* in ovarian tumors negatively correlates with patient survival (11). In contrast, *Ephb4* behaves as a tumor suppressor during intestinal tumorigenesis in a mouse model (12). Moreover, it was recently reported that the Eph receptor complement expressed by a cancer cell can, depending on ephrin expression in the surrounding tissue, determine its invasiveness (13). Therefore, an improved understanding of the mechanisms underlying *Eph* and *Efn* transcriptional regulation has implications for both developmental and cancer biology.

While our knowledge of *Eph* and *Efn* expression in adult ovarian function is sparse, several reports have indicated that expression of *Eph* and *Efn* genes in the adult ovary changes during follicle growth. *Esr2*^{-/-} females, which lack estrogen receptor beta (ER β), exhibit impaired expression of multiple FSH-responsive genes in granulosa cells (GCs), including *Efna5* (14). We previously reported that several genes that encode members of the Eph-ephrin family are upregulated in GCs of female mice treated with equine chorionic gonadotropin (eCG) (15) a horse-derived gonadotropin with FSH receptor (FSHR)-stimulating activity in rodents. Furthermore, expression of *EFNA5* and *EPHB6* is higher in large antral follicles than in small follicles in the cow, suggesting that FSH may also regulate expression of *Eph* and *Efn* genes in other species (16). In addition to suggesting a role for Eph-ephrin signaling in FSH-dependent follicle growth and/or ovulation, these data also provide insight into the transcriptional regulation of *Eph* and *Efn* genes.

We previously reported that *Efna5*, *Epha3*, *Epha5*, *Epha8*, and *Ephb2* are upregulated in mouse GCs following treatment with eCG (15). The FSHR is an integral G_s protein-coupled receptor composed of a FSH-binding extracellular domain, a

membrane-spanning domain composed of 7 transmembrane helices, and a cytoplasmic domain (17). Expressed in GCs of secondary and larger follicles (18), it is one of two gonadotropin receptors in mammals, the other being the luteinizing hormone receptor (LHR). Binding of FSH to the FSHR extracellular domain results in G_s protein activation, which in turn activates adenylate cyclase and catalyzes the hydrolysis of adenosine triphosphate (ATP) to generate the second messenger cyclic adenosine monophosphate (cAMP) (19). In GCs of many species, elevation of cytoplasmic cAMP concentration favours activation of protein kinase A (PKA) and its downstream pathways, including those that modulate gene expression (20). Therefore, activation of many genes downstream of FSHR activation is dependent on cAMP-associated pathways. The promoters of some cAMP-responsive genes are activated by cis-regulatory sequences known as *cAMP-responsive elements* (CREs), which have a consensus sequence of 5'-TGACGTCA-3' (full CRE) or 5'-CGTCA-3' or 5'-TGACG-3' (half CRE) (21).

Estrogen receptors are nuclear hormone receptors, of which there are two forms. Within the ovary in mice, ER α localizes primarily to thecal and interstitial cells and is encoded by the *Esr1* gene. ER β is localized primarily to GCs and is encoded by the *Esr2* gene. That action of estrogens is mediated predominantly by ER α and ER β , which bind estrogens and effect changes in the transcriptional activity of target genes. *Esr2*^{-/-} females exhibit a severe reproductive phenotype that includes subfertility and impaired formation of antral follicles (22). GCs from *Esr2*^{-/-} mice also exhibit suboptimal production of cAMP, a defect thought to contribute to dysregulation of FSH-responsive genes following treatment with FSH (14). Therefore, there is evidence suggesting that *Eph* and *Efn* expression in GCs changes during FSH-dependent follicle growth and is regulated by cAMP. Transcriptional regulation of any *Eph* or *Efn* genes by cAMP-dependent pathways has not been previously described in GCs or in any other model system. Therefore, we investigated the role of cAMP-dependent regulation in regulating *Epha5* transcription in GCs. In particular, we focused on cAMP-dependent regulation of *Epha5* transcription in GCs.

In order to investigate regulation of *Eph* and *Efn* genes by cAMP, we assessed expression of *Efna5*, *Epha3*, *Epha5*, *Epha8*, and *Ephb2* in GCs of *Esr2*^{-/-} mice. In order to

evaluate responsiveness of the *Epha5* putative promoter region to cAMP, we then generated a luciferase reporter construct (Epha5-Luc) containing the mouse genomic sequence from -1589 to +23 relative to the start of the *Epha5* 5' UTR (+1). Using this construct with dibutyryl-cAMP and a PKA inhibitor, we investigated activation of the *Epha5* promoter region in a human tumour-derived GC line. Furthermore, we used site-directed mutagenesis to generate a function-disrupting point mutation in a putative CRE half-site within Epha5-Luc.

4.2 Materials and Methods

4.2.1 Cell culture and transfections

The KGN cell line was derived from a human stage 3 GC carcinoma (23,24). KGN cells were maintained in Dulbecco modified Eagle medium/F-12 (DMEM/F12; Wisent) containing 10% fetal bovine serum (FBS; Wisent) at 37°C in 5% CO₂.

Twenty-four hours prior to transfection, KGN cells were seeded into 24-well plates at a density of 9.5×10^4 cells/well. Eight hours later, the culture medium was replaced with DMEM/F12 containing 10% charcoal-stripped fetal bovine serum (CS-FBS; Wisent). Sixteen hours later, transfections were performed using FuGENE HD (Promega) with a reagent:plasmid ratio of 5:2 (μL FuGENE HD: μg DNA) at 0.5 μg total plasmid per well (490 ng firefly luciferase reporter plasmid and 10 ng Renilla luciferase control plasmid). Transfection mix was prepared according to the manufacturer's instructions (Promega). In all luciferase reporter studies, controls included KGN cells transfected with pGL3-basic (promoter-less vector) to establish that increases in luciferase activity were specific to the Epha5-Luc plasmid (pGL3-basic plasmid containing the mouse genomic sequence -1589 to +23 bp relative to the start of the *Epha5* 5' UTR). Furthermore, controls also included KGN cells transfected with a known cAMP-responsive luciferase plasmid (CRE-Luc) obtained as a gift from Dr. Nathalie di Clemente (Institut National de la Santé et de la Recherche Médicale, Clamart, France).

For qRT-PCR studies with KGN cells, human recombinant FSH was obtained from Dr. A.F. Parlow (National Hormone and Peptide Program, National Institute of Diabetes

and Digestive and Kidney Diseases, USA). Recombinant FSH was reconstituted in sterile water to a concentration of 50 ng/mL and stored at -80°C.

For experiments involving the PKA inhibitor H-89 (Cell Signaling), H-89 was reconstituted in dimethyl sulfoxide (DMSO) to a concentration of 20 mM and stored at -20°C. Cells were pre-treated with H-89 at a final concentration of 20 µM, 1:1000 v/v DMSO, or with an equal volume of DMSO (1:1000 v/v) for 30 minutes. Both H-89- and DMSO-treated KGN cells were treated with dbcAMP at a final concentration of 1.0 mM for 24 hours.

4.2.2 Mice

Experiments were performed in compliance with the guidelines set by the Canadian Council for Animal Care and the policies and procedures approved by The University of Western Ontario Council on Animal Care. Investigations were conducted in accordance with the National Research Council's Guide for Care and Use of Laboratory Animals (Protocol # 2008-047-02). C57BL/6 female mice (Postnatal Day [PND] 23–28) were used in all experiments. For quantitative RT-PCR (qRT-PCR) studies, mice were treated either with saline or with 5.0 IU eCG (Sigma Chemical Co.) for 48 h before isolation of GCs.

4.2.3 Isolation of GCs

48 h after treatment with saline or eCG, mice were euthanized by CO₂ asphyxiation and whole ovaries were harvested into a 100 mm cell culture dish containing cold M199 medium supplemented with 1 mg/mL of bovine serum albumin (BSA), 2.5 µg/mL of amphotericin B, and 50 µg/mL of gentamicin (all reagents from Invitrogen). Ovaries were pooled, and the GCs from each pool were then expressed by manual puncture with 25-gauge needles followed by pressure applied with a sterile spatula. The GC suspension was filtered through a 150-µm Nitex nylon membrane (Sefar America, Inc.) mounted in a Swinnex filter (Millipore). The GCs were then pelleted by centrifugation at 250 × g for 5 min at 4°C followed by two washes in DMEM/F12 medium containing 1%

penicillin/streptomycin solution (Invitrogen). The final cell pellet was frozen at -80°C for qRT-PCR studies.

4.2.4 RNA isolation and qRT-PCR

Frozen pellets of GCs were solubilized in TRIzol (Invitrogen), and RNA was isolated according to the manufacturer's protocol. RNA was further treated with DNase I, then reverse-transcribed using Superscript II (Invitrogen). Complementary DNA (cDNA) levels were detected using qRT-PCR with the ABI PRISM 7900 Sequence Detection System (Applied Biosystems) and SYBR Green I dye (Applied Biosystems). Primers were generated using Primer Express Software (Version 2.0; Applied Biosystems) (**Table 4-1**). Fold-changes in gene expression were determined by quantitation of cDNA from target (treated) samples relative to a calibrator sample (vehicle). The gene for ribosomal protein L7 (*Rpl7* in mouse GCs or *RPL7* in KGN cells) was used as the endogenous control for normalization of RNA levels. Expression ratios were calculated according to the mathematical model described by Pfaffl (25), where ratio = $(E_{\text{target}})^{\Delta\text{Ct}(\text{target})} / (E_{\text{control}})^{\Delta\text{Ct}(\text{control})}$ and E = efficiency of the primer set, calculated from the slope of a standard curve of $\log(\text{ng of cDNA})$ versus cycle threshold (Ct) for a sample that contains the target according to the formula $E = 10^{-(1/\text{slope})}$ and $\Delta\text{Ct} = \text{Ct}_{(\text{vehicle})} - \text{Ct}_{(\text{treated sample})}$. Three independent experiments were carried out for studies using mouse GCs, and the results were averaged for statistical analysis by a two-way ANOVA followed by a Tukey multiple comparison post-hoc test (Tukey test) (**Figure 4-1**). Two independent experiments were carried out for studies using KGN cells, and the results were averaged for statistical analysis by a two-tailed unpaired Student t-test (**Figure 4-4A**).

Table 4-1: Primers used for qRT-PCR in Figure 4-1 and Figure 4-4.

Gene	GenBank accession no.	Forward (5' to 3')	Reverse (5' to 3')
Mouse			
<i>Rpl7</i>	NM_011291	AGCTGGCCTTTGTCATCAGAA	GACGAAGGAGCTGCAGAACCT
<i>Efna5</i>	NM_207654	TCTGCAATCCCAGACAACGGAAGA	TCATGTACGGTGTTCATCTGCTGGT
<i>Epha3</i>	NM_010140	CCGCAGTCAGCATCACAACCT	TTTCTGGAAGTCCGATCTTTCTTAA
<i>Epha5</i>	NM_007937	GCTGGTTCCCATTGGGAAAT	CACATTGGTGACTGGAGAAGGA
<i>Epha8</i>	NM_007939	CTCGGATGAAGAGAAGATGCATT	TGGTTCAAGGGCAAGAAGACA
<i>Ephb2</i>	NM_010142	ACCTCAGTTCGCCTCTGTGAA	GGCTCACCTGGTGCATGAT
Human			
<i>RPL7</i>	NM_000971	AAATTGGCGTTTGTTCATCAGAA	AAGAAGCTGCAACACCTTTTCG
<i>EPHA5</i>	NM_004439	AGGCAGGATATGAAGAGAAAAATGG	ATTGCCGCAGCTCTGGAT
	NM_182472		
	NM_001281765		
	NM_001281766		
	NM_001281767		

4.2.5 Immunoblotting

Protein lysates were generated in a 1.5 mL microcentrifuge tube by homogenizing a GC pellet in ice-cold radioimmunoprecipitation assay (RIPA) buffer (50 mM Tris-HCl [pH 8.0], 150 mM NaCl, 1% Triton X-100, 0.5% sodium deoxycholate, and 0.1% SDS) supplemented with a protease inhibitor cocktail (1:100; P8340; Sigma). Lysates were then centrifuged at $15\,000 \times g$ for 20 min at 4°C. The supernatant was boiled in Laemmli buffer for 5 min and then analyzed using SDS-PAGE. The separated proteins were transferred to a polyvinylidene fluoride membrane at 100 V (constant voltage) for 2 h at 4°C. After blocking for 1 h in Tris-buffered saline and Tween 20 (TBST)/5% nonfat milk, the membrane was probed with a monoclonal IgG specific to ephrin-A5 (1:200 in TBST/5% nonfat milk; ab60705; Abcam). The membrane was then probed with an anti-mouse horseradish peroxidase-conjugated IgG generated in donkey (1:10000 in TBST/5% nonfat milk) and visualized using ECL Plus (Amersham Biosciences) and Hyperfilm (Amersham). To assess equal protein loading, the membrane was subsequently probed using a rabbit monoclonal IgG to detect alpha-tubulin (TUBA1A, T5168; Sigma).

4.2.6 Generation of the Epha5-Luc luciferase reporter plasmid

The genomic sequence upstream of *Epha5* was amplified by PCR using Phusion High-Fidelity DNA Polymerase (New England Biolabs), using the following primer sequences (5' → 3'): *Forward: AGAGGCCACCGAACTGCCCA*, *Reverse: GCTCGCTCGCTCCTGCTGTG*. Amplification was performed using a bacterial artificial chromosome template containing the mouse genomic region of interest (NCBI clone RP23-331O22, Clone ID # 705829) obtained from The Centre for Applied Genomics, The Hospital for Sick Children, Toronto, Canada. This yielded a 1589 bp amplification product that was digested using the KpnI and XhoI restriction enzymes, yielding a 1571 bp digestion product. The pGL3-basic plasmid was also digested using KpnI and XhoI. Both digestion fragments were purified by agarose gel extraction and then ligated, yielding the 6362 bp Epha5-Luc luciferase reporter plasmid. Plasmid minipreps were prepared using 5 mL bacterial cultures grown from transformed colonies, and sent for sequencing (Robarts Research Institute, The University of Western Ontario).

4.2.7 Generation of the mutEpha5-Luc luciferase reporter plasmid by site-directed mutagenesis

In order to assess whether a conserved CRE half-site located at -389 bp relative to the start of the mouse *Epha5* 5' UTR (**Figure 4-2** and **Figure 4-3**) was required for transcriptional activation of Epha5-Luc by cAMP, the QuikChange XL site-directed mutagenesis kit (Agilent) was used to substitute two nucleotides in the CRE half-site to disrupt function (TGACG → TGATC). This strategy has been previously used to disrupt CRE half-site function in a construct containing part of the *Tcl1* mouse promoter (26). QuikChange primers were designed using the QuikChange Primer Design Tool (<http://www.genomics.agilent.com/primerDesignProgram.jsp>).

Forward (5' → 3'): agagcctgtgaatgtgctgttatatgatcacaagggttggtggt.

Reverse: (5' → 3'): accaacaaccttgatcatataacagcacattcacaggctct.

4.2.8 Dual-luciferase assays

KGN cells that had been cultured, transfected, and treated in 24-well plates were washed twice with PBS and then lysed by adding 105 µL Passive Lysis Buffer (Promega) to each well followed by rocking at room temperature for 15 min. 100 µL of each lysate was transferred to 1.5 mL microcentrifuge tubes and centrifuged at 12 000 g for 15 seconds to pellet loose debris. 20 µL of each lysate was transferred to a white, opaque 96-well plate (82050-726; VWR) and assessed for firefly and *Renilla* luciferase activity using the Dual-Luciferase Assay (E1960; Promega). Fluorescence was measured using a Synergy H4 Microplate Reader (Biotek).

4.3 Results

4.3.1 Induction of FSH-responsive *Efn* and *Eph* genes is reduced in GCs of *Esr2*^{-/-} mice

We previously reported that eCG enhances expression of *Efna5*, *Epha3*, *Epha5*, *Epha8*, and *Ephb2* in mouse GCs (15). In order to determine whether eCG-stimulated expression of FSH-responsive *Efn* and *Eph* genes is altered in mice that exhibit impaired production of cAMP, we assessed mRNA transcript levels for these genes in GCs of eCG-treated, reproductively immature *Esr2*^{-/-} mice. PND 23-28 *Esr2*^{+/+} and *Esr2*^{-/-}

females were treated with saline or 5.0 IU eCG (48 h) and GCs were harvested. Relative mRNA transcript abundance was determined by qRT-PCR for *Efna5*, *Epha3*, *Epha5*, *Epha8*, and *Ephb2*. In GCs of eCG-treated *Esr2^{+/+}* females, we observed 3-, 2.5-, 5.2-, 3.7-, and 2.7-fold increases in mRNA levels, respectively, for these genes compared to saline-treated controls. In GCs of eCG-treated *Esr2^{-/-}* females, we did not detect changes in mRNA levels for any of these genes (**Figure 4-1**). Protein levels for ephrin-A5 were lower in GCs from *Esr2^{-/-}* compared to *Esr2^{+/+}* females (**Supplemental Figure 6-4**).

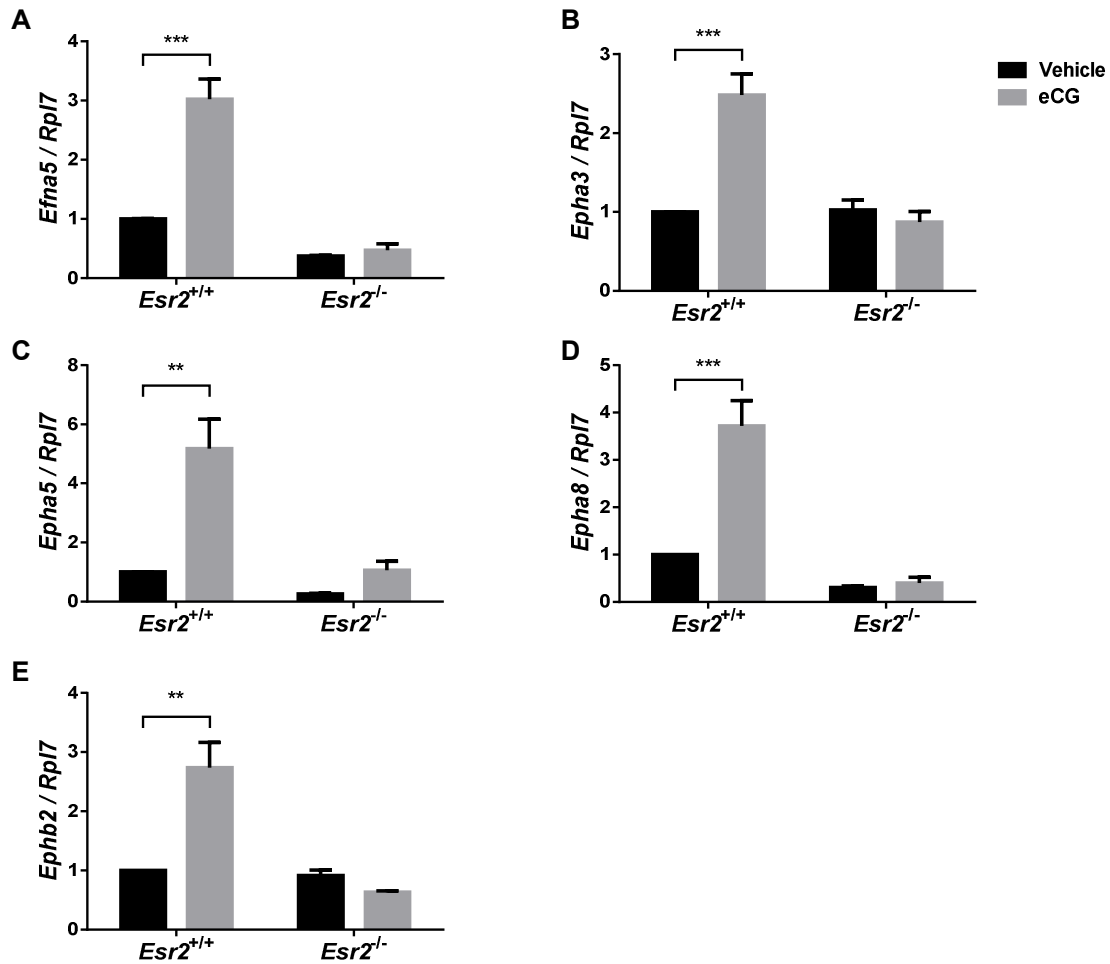


Figure 4-1: Induction of FSH-responsive *Efn* and *Eph* genes by eCG is significantly reduced in *Esr2*^{-/-} GCs.

Relative transcript abundance compared to *Rpl7* (mean \pm SEM) was determined by qRT-PCR in GCs of eCG-treated females for *Efna5* (A), *Epha3* (B), *Epha5* (C), *Epha8* (D), and *Ephb2* (E). **A) *Efna5*.** A two-way ANOVA found a significant effect for treatment, $F(1, 8) = 35.09$, $P = 0.0004$; a significant effect for genotype, $F(1, 8) = 79.47$, $P < 0.0001$; and a significant interaction, $F(1, 8) = 28.92$, $P = 0.0007$. A Tukey test revealed a significant difference between eCG-treated *Esr2*^{+/+} and *Esr2*^{-/-} mice, ***, $P = 0.0002$. **B) *Epha3*.** A two-way ANOVA found a significant effect for treatment, $F(1, 8) = 16.78$, $P = 0.0035$; a significant effect for genotype, $F(1, 8) = 24.03$, $P = 0.0012$; and a significant interaction, $F(1, 8) = 25.43$, $P = 0.0010$. Tukey's multiple comparisons test revealed a significant difference between eCG-treated *Esr2*^{+/+} and *Esr2*^{-/-} mice, ***, $P = 0.0009$. **C)**

Epha5. A two-way ANOVA found a significant effect for treatment, $F(1, 8) = 22.85$, $P = 0.0014$; a significant effect for genotype, $F(1, 8) = 21.82$, $P = 0.0016$; and a significant interaction, $F(1, 8) = 10.57$, $P = 0.0117$. Tukey's multiple comparisons test revealed a significant difference between eCG-treated *Esr2*^{+/+} and *Esr2*^{-/-} mice, **, $P = 0.0021$. **D)** *Epha8*. A two-way ANOVA found a significant effect for treatment, $F(1, 8) = 26.25$, $P = 0.0009$; a significant effect for genotype, $F(1, 8) = 53.72$, $P < 0.0001$; and a significant interaction, $F(1, 8) = 22.95$, $P = 0.0014$. Tukey's multiple comparisons test revealed a significant difference between eCG-treated *Esr2*^{+/+} and *Esr2*^{-/-} mice, ***, $P = 0.0005$. **E)** *Ephb2*. A two-way ANOVA found a significant effect for treatment, $F(1, 8) = 11.00$, $P = 0.0106$; a significant effect for genotype, $F(1, 8) = 24.87$, $P = 0.0011$; and a significant interaction, $F(1, 8) = 21.11$, $P = 0.0018$. Tukey's multiple comparisons test revealed a significant difference between eCG-treated *Esr2*^{+/+} and *Esr2*^{-/-} mice, **, $P = 0.0023$.

4.3.2 Epha5-Luc is transcriptionally activated by cAMP in KGN cells

In order to determine whether the proximal genomic region upstream of *Epha5* is responsive to cAMP, we carried out a promoter-reporter (luciferase) assay. We generated a luciferase reporter construct (Epha5-Luc) containing the mouse genomic sequence from -1589 to +23 bp relative to the start of the *Epha5* 5' UTR, inserted upstream of the luciferase gene (**Figure 4-2**). This plasmid was then transfected into KGN cells, a cell line derived from a human GC tumor (23). In KGN cells treated with FSH, we observed a significant 2.5-fold increase in endogenous *EPHA5* mRNA levels compared to vehicle-treated cells ($p=0.0099$) (**Figure 4-4A**). KGN cells transfected with Epha5-Luc reporter plasmid were co-transfected with the pRL-SV40 *Renilla* luciferase control plasmid, and were treated with 1.0 mM dibutyryl-cAMP (dbcAMP), a cell membrane-permeable form of cAMP, for 24 hours. Cells were then lysed and luciferase activity was measured. In KGN cells treated with dbcAMP, we observed a 56% increase in normalized luciferase activity compared to vehicle-treated cells ($p=0.0461$) (**Figure 4-4B**).

4.3.3 cAMP-stimulated activation of Epha5-Luc is reduced by co-treatment with H-89

Elevated intracellular concentration of cAMP is known to activate several PKA-independent pathways, such as RAPGEF3 (Rap guanine nucleotide exchange factor 3) and RAPGEF4 (Rap guanine nucleotide exchange factor 4) (27,28), as well as PKB (protein kinase B) (29). In order to determine whether activation of Epha5-Luc by dbcAMP in KGN cells was PKA-dependent or PKA-independent, we used the PKA inhibitor H-89. KGN cells transfected with Epha5-Luc were co-treated with 1.0 mM dbcAMP (24 h) and either DMSO (vehicle control, 1:1000 v/v) or 20 μ M H-89 (in DMSO, 1:1000 v/v). In DMSO-treated cells, we observed a 2.3-fold cAMP-induced enhancement of normalized luciferase activity ($p=0.0143$) (**Figure 4-5A**). In the presence of 20 μ M H-89, this enhancement was reduced (**Figure 4-5B**).

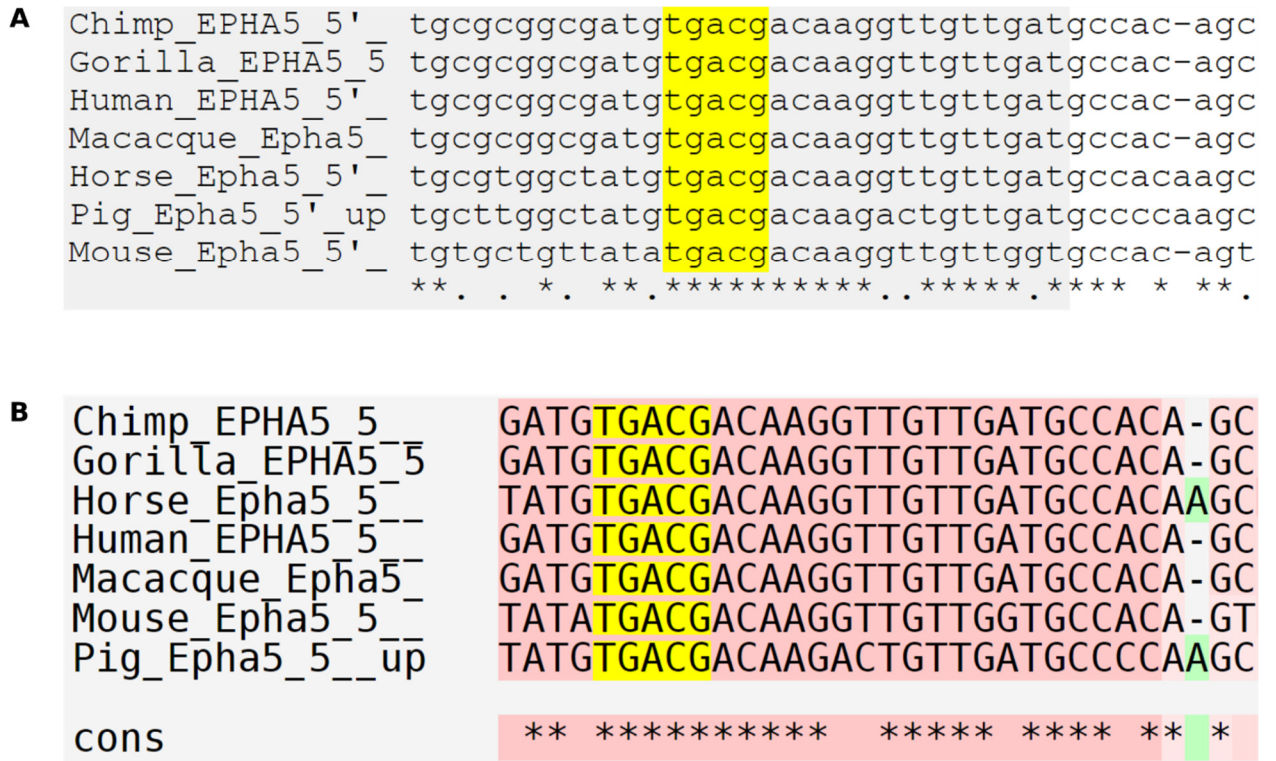


Figure 4-2: A putative consensus CRE half-site upstream of *Epha5* is conserved across several species.

The genomic sequence from -5000 to +1 bp relative to the start of the *Epha5* 5' UTR from several species was aligned using *Multiple Alignment using Fast Fourier Transform* (<http://mafft.cbrc.jp/alignment/software>) (A) and T-Coffee (<http://www.tcoffee.org>) (B). The putative CRE half-site at -389 bp is highlighted in yellow. “cons” = conserved nucleotides.

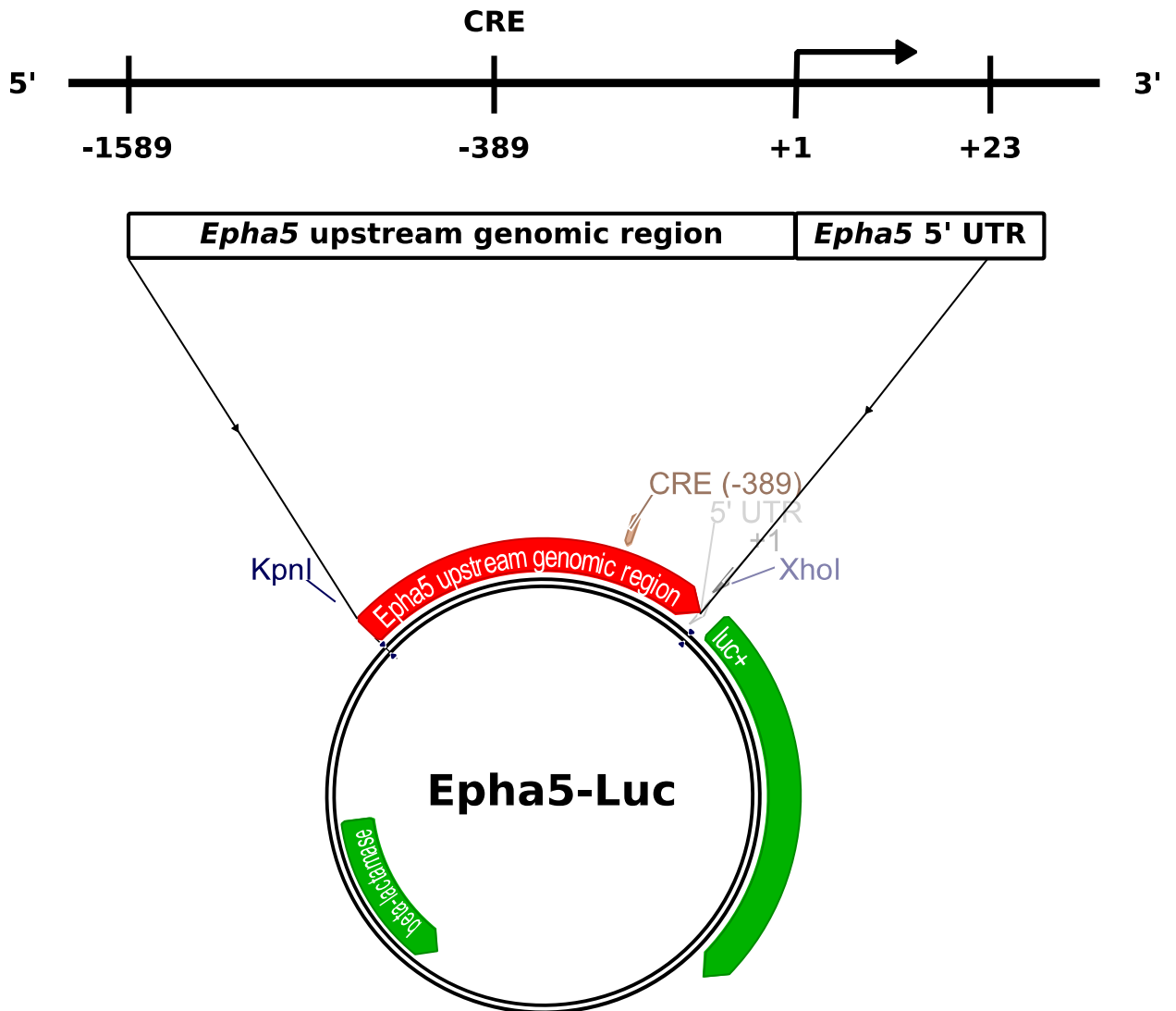


Figure 4-3: Generation of the Epha5-Luc luciferase reporter construct.

The 1589 bp genomic region upstream of the mouse *Epha5* 5' UTR (+1) was amplified, digested with KpnI and XhoI restriction enzymes, and then ligated into the pGL3-basic luciferase reporter plasmid to assess capacity to drive transcription of *luc+* (luciferase). A putative consensus CRE half-site is present (-389). The Epha5-Luc plasmid map was generated using Geneious Pro Trial.

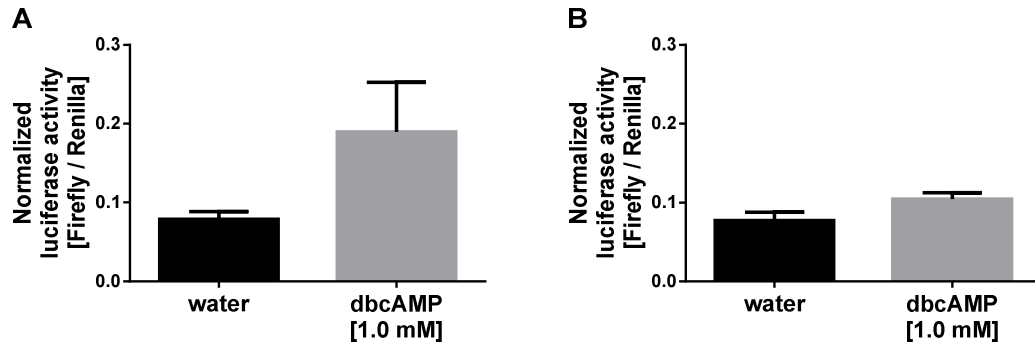


Figure 4-4: Endogenous *EPHA5* is induced by FSH, and *Epha5*-Luc is activated by dbcAMP in KGN cells

Relative transcript abundance for *EPHA5* compared to *RPL7* (mean \pm SEM) was determined by qRT-PCR in FSH-treated (24 h) KGN cells (A). Firefly luciferase activity normalized to *Renilla* luciferase activity (mean \pm SEM) was determined for water- and dbcAMP-treated KGN cells transfected with the *Epha5*-Luc luciferase reporter construct (B). A) A statistically significant difference was found between water- and FSH-treated KGN cells as determined by an unpaired, two-tailed Student's t-test; $t(2)=9.967$. **, $p=0.0099$. B) A statistically significant difference was found between water- and dbcAMP-treated KGN cells as determined by an unpaired, two-tailed Student's t-test; $t(4)=2.857$. **, $p=0.0461$.

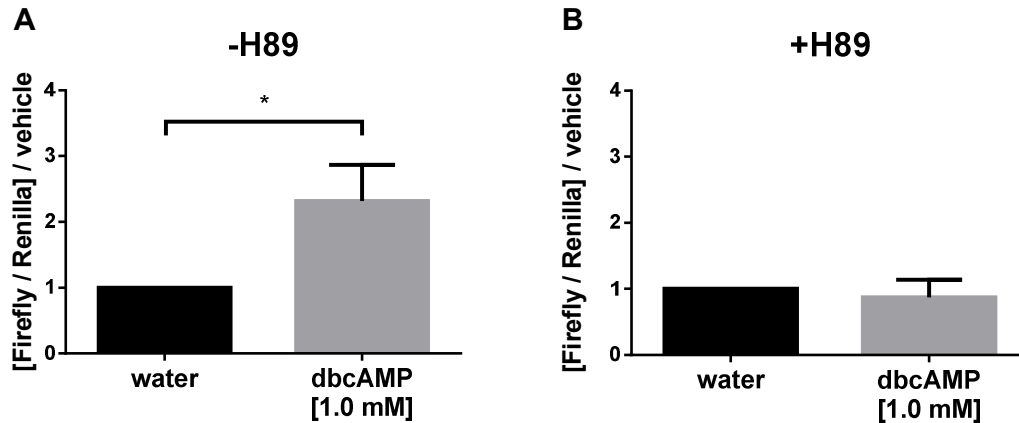


Figure 4-5: Activation of Epha5-Luc by dibutyryl-cAMP is reduced by co-treatment with the PKA inhibitor H-89.

Stimulation of *Renilla*-normalized firefly luciferase activity (mean \pm SEM) was determined for dbcAMP-treated (1.0 mM) KGN cells transfected with Epha5-Luc, in the absence (A) and presence (B) of H-89 (20 μ M). A) A statistically significant difference was found between dbcAMP-treated KGN cells transfected with Epha5-Luc in the absence of H-89 as determined by an unpaired, two-tailed Student's t-test; $t(4)=4.147$. *, $p=0.0143$. B) No statistically significant difference was found between dbcAMP-treated KGN cells transfected with Epha5-Luc in the presence of H-89 as determined by an unpaired, two-tailed Student's t-test; $t(4)=0.8134$. *, $p=0.04616$.

4.4 Discussion

We previously reported that expression of *Efna5*, *Epha3*, *Epha5*, *Epha8*, and *Ephb2* is increased in GCs isolated from mice treated with eCG (15). Furthermore, microarray studies indicate that eCG-stimulated expression of *Efna5* is attenuated in GCs of *Esr2*^{-/-} females, which exhibit impaired cAMP production (14). Since eCG stimulates the FSHR, which in turn activates responsive genes via cAMP-dependent pathways, we investigated the transcriptional regulation of *Eph* and *Efn* genes by cAMP in GCs. Transcriptional regulation of *Eph* and *Efn* genes by cAMP-dependent pathways has not been previously described. Here, we present evidence that stimulation of *Efna5*, *Epha3*, *Epha5*, *Epha8*, and *Ephb2* by eCG is attenuated in GCs of mice with impaired cAMP production. Furthermore, the proximal genomic region upstream of the mouse *Epha5* gene is responsive to dbcAMP in a PKA-dependent manner.

4.4.1 hCG-stimulated induction of *Efna5*, *Epha3*, *Epha5*, and *Ephb2* is significantly reduced in GCs of *Esr2*^{-/-} mice

During our investigation into the roles of Eph receptors and ephrins in the mouse ovary, we assessed expression of *Eph* and *Efn* genes in GCs from eCG-stimulated, reproductively immature *Esr2*^{+/+} and *Esr2*^{-/-} females. *Esr2* encodes estrogen receptor beta (ER β), the predominant form of estrogen receptor in GCs (22). In addition to subfertility and impaired antral follicle formation, eCG-stimulated *Esr2*^{-/-} mice exhibit attenuated expression of *Efna5* in GCs compared to *Esr2*^{+/+} controls. The same study revealed that GCs from these mice also exhibit impaired cAMP production (14).

Since a common mechanism by which FSH enhances expression of its responsive genes occurs via cAMP-dependent pathways (20), we first confirmed that *Efna5* was dysregulated in GCs of eCG-stimulated *Esr2*^{-/-} females, and determine whether other *Efn* and *Eph* genes were similarly dysregulated. We found that eCG enhanced expression of *Efna5*, *Epha3*, *Epha5*, *Epha8*, and *Ephb2* in *Esr2*^{+/+} but not *Esr2*^{-/-} females. This is consistent with the report that GCs from *Esr2*^{-/-} females exhibit attenuated activation of many FSH-responsive genes including *Inhba* (inhibin beta-A) (*Inhba*), *Hsd3b1* (3-beta-hydroxysteroiddehydrogenase 1), and *Comp* (cartilage oligomeric matrix protein) in *Esr2*^{-/-}

⁻ GCs. The same study proposed that a deficiency in cAMP production underlies the reduced induction of FSH-responsive genes. In addition, GCs of *Esr2*^{-/-} females produce 50% less cAMP in response to the adenylate cyclase activator forskolin, and exhibit attenuated phosphorylation of CREB following treatment with FSH, compared to GCs from *Esr2*^{+/+} mice (14). Therefore, impaired production of cAMP is associated with loss of eCG-stimulated *Efna5*, *Epha3*, *Epha5*, *Epha8*, and *Ephb2* expression in mouse GCs.

4.4.2 The 1589 bp region upstream of *Epha5* is transcriptionally activated by cAMP in a PKA-dependent manner in KGN cells

Since FSHR is a G_s protein coupled receptor, its activation results in stimulation of adenylate cyclase and an associated elevation of intracellular cAMP concentration (20). In GCs, the major downstream target of cAMP seems to be PKA, although PKA-independent targets including cAMP-dependent guanine exchange factors (27,28) and protein kinase B (PKB) (29) may also mediate the response to FSH.

PKA is a serine-threonine protein kinase that is composed of two catalytic and two regulatory subunits. In the inactive state, kinase activity of the catalytic subunits is suppressed by the presence of the regulatory subunits. Elevated levels of cAMP favour disengagement of the regulatory subunits, permitting translocation of the catalytic subunits into the nucleus (30) where PKA alters the activity of target proteins by phosphorylation. One target of PKA in the nucleus is cAMP response element binding protein (CREB), a member of the basic region leucine zipper (bZIP) family of DNA-binding proteins. Upon stimulation with cAMP, CREB is activated by phosphorylation at serine 133 (30). Activated CREB then binds to cis-regulatory elements that are associated with cAMP-responsive genes and recruits CREB-binding protein (CBP), a transcriptional coactivator. These cis-regulatory sequences are known as *cAMP-responsive elements* (CREs), and have a consensus sequence of 5'-TGACGTCA-3' (full CRE) or 5'-CGTCA-3' or 5'-TGACG-3' (half CRE) (21). These sequences are typically found near the transcriptional start site, with ~60% of consensus CREs and variants found within 500 bp of the 5' UTR (31). Other transcriptional regulators known to bind CREs include the transcriptional activator *activating transcription factor 1* (ATF1) and the transcriptional

repressor *cAMP responsive element modulator* (CREM). However, the current body of evidence suggests that CREB is the primary CRE-binding protein in most cell types (32).

Among the FSH-responsive genes transcriptionally regulated via CREB in GCs is *Cyp19a1*, which encodes the enzyme CYP19A1 (cytochrome P450, family 19, subfamily A, polypeptide 1), commonly referred to as aromatase. CYP19A1 catalyzes the aromatization of testosterone and androstenedione, and is the rate-limiting step in the synthesis of estradiol in biological systems. Furthermore, increased *Cyp19a1* expression and elevated estradiol production are hallmarks of FSH-induced GC differentiation (33). CREB directly binds the rat promoter region of the rat *Cyp19a1* gene (34). Furthermore, binding of CREB to a CRE in the human *CYP19A1* promoter region is required for cAMP-dependent activation of this region (35). We examined the genomic region upstream of the mouse *Epha5* gene and identified a putative consensus CRE half-site located 389 bp upstream of the 5' UTR that was conserved in multiple species (**Figure 4-2**).

We postulated that this CRE half-site is required for activation of *Epha5* by cAMP via the PKA pathway. In order to test this idea, we cloned 1589 bp of the mouse genomic region upstream of the *Epha5* 5'-UTR into the pGL3-basic luciferase reporter plasmid, generating the *Epha5*-Luc luciferase reporter construct. We then assessed the capacity of this construct to respond to cAMP in KGN cells, a cell line derived from a human GC tumor (23). KGN cells have been previously used as a model system to study the regulation of *CYP19A1* by FSH and cAMP (36). We observed that treatment with FSH increased endogenous expression of *EPHA5* in KGN cells (**Figure 4-4A**), which is consistent with our previous finding that *Epha5* is a FSH-responsive gene in mouse GCs (15). We then found that treatment with dbcAMP increased luciferase activity in KGN cells transfected with *Epha5*-Luc (**Figure 4-4B**), indicating that the 1589 bp genomic region upstream of *Epha5* is responsive to cAMP.

Since cAMP is known to activate several targets other than PKA (27-29), we then determined whether activation of *Epha5*-Luc by dbcAMP was PKA-dependent or PKA-independent. In order to make this distinction, we co-treated KGN cells transfected with

Epha5-Luc with dbcAMP and the PKA inhibitor H-89. Co-treatment with H-89 attenuated activation of Epha5-Luc by dbcAMP (**Figure 4-5**), indicating that activation was PKA-dependent. It should be noted that while H-89 is a widely-used PKA inhibitor, it is known to effectively inhibit at least 7 other kinases (37). Therefore, the possibility that H-89 inhibits other targets should be considered. Future studies investigating regulation of *Eph* and *Efn* genes by cAMP-dependent pathways should include other H-89 specific inhibitors that exhibit reduced cross-inhibition, such as the commercially available molecule Rp-cAMPS (38).

In order to test whether stimulation of the Epha5-Luc construct by dbcAMP was dependent on the CRE half-site 389 bp upstream of the *Epha5* 5' UTR, we used site-directed mutagenesis to introduce two CRE-disrupting base pair substitutions into the site, generating the mutEpha5-Luc luciferase reporter construct, which we will use in future studies of *Epha5* regulation. Current studies (**Supplemental Figure 6-5**) using the mutEpha5-Luc construct have been unsuccessful due to difficulties with transfections that occurred after a change in reagent suppliers. Re-optimization of transfection conditions are ongoing.

Our findings indicate that in GCs, cAMP transcriptionally activates the proximal upstream genomic region of *Epha5* in a PKA-dependent manner. Given the observation that induction of FSH-responsive *Efn* and *Eph* genes by eCG is reduced in GCs of mice that exhibit impaired cAMP production, it is reasonable to speculate that *Efna5*, *Epha3*, *Epha5*, *Epha8*, and *Ephb2* are regulated in a similar manner in GCs. In other tissues, hormones such as thyroid-stimulating hormone (TSH) in the thyroid gland and adrenocorticotrophic hormone (ACTH) in the adrenal cortex stimulate their respective GPCRs, resulting in elevated cAMP concentrations. Activation of these and other G_s protein-associated signaling pathways may stimulate *Efn* and *Eph* expression, and their associated physiological processes may involve Eph-ephrin signaling.

Regulation of *Eph* and *Efn* genes by FSH may also be important in cancer. *FSHR* mRNA has been detected in a large percentage of ovarian epithelial inclusions and ovarian epithelial tumors (OETs) (39), while FSHR protein is detected in endothelial

cells from a wide range of tumors, and may be involved in tumour angiogenesis (40). Furthermore, overexpression of *FSHR* in cultured MCV152 OET cells increases cell proliferation and invasiveness (41). These reports suggest that cAMP-dependent enhancement of *Eph* and *Efn* expression may be involved in the formation, invasiveness, and growth of such FSHR-expressing tumors, particularly in light of the evidence indicating that *Eph* and *Efn* dysregulation is common in cancer (9).

4.4.3 Conclusion

Taken together, our findings indicate that in GCs, *Epha5* expression is induced by FSH via the cAMP-dependent PKA pathway. Our findings in *Esr2^{-/-}* mice suggest the possibility that *Efna5*, *Epha3*, *Epha8*, and *Ephb2* are similarly regulated. Thus, PKA represents a novel upstream regulator of *Epha5*, and potentially other members of the Eph-ephrin family, in GCs.

4.5 Bibliography

1. Himanen JP, Nikolov DB. Eph signaling: a structural view. *Trends in neurosciences*. 2003;26(1):46-51.
2. Himanen JP, Chumley MJ, Lackmann M, Li C, Barton WA, Jeffrey PD, Vearing C, Geleick D, Feldheim DA, Boyd AW, Henkemeyer M, Nikolov DB. Repelling class discrimination: ephrin-A5 binds to and activates EphB2 receptor signaling. *Nat Neurosci*. 2004;7(5):501-509.
3. Cayuso J, Xu Q, Wilkinson DG. Mechanisms of boundary formation by Eph receptor and ephrin signaling. *Dev Biol*. 2014.
4. Laussu J, Khuong A, Gautrais J, Davy A. Beyond Boundaries - Eph:Ephrin Signaling in Neurogenesis. *Cell adhesion & migration*. 2014:0.
5. Arvanitis DN, Davy A. Regulation and misregulation of Eph/ephrin expression. *Cell adhesion & migration*. 2012;6(2):131-137.
6. Takahashi H, Shintani T, Sakuta H, Noda M. CBF1 controls the retinotectal topographical map along the anteroposterior axis through multiple mechanisms. *Development*. 2003;130(21):5203-5215.
7. Sohl M, Lanner F, Farnebo F. Characterization of the murine Ephrin-B2 promoter. *Gene*. 2009;437(1-2):54-59.
8. Munthe E, Aasheim HC. Characterization of the human ephrin-A4 promoter. *The Biochemical journal*. 2002;366(Pt 2):447-458.
9. Pasquale EB. Eph receptors and ephrins in cancer: bidirectional signalling and beyond. *Nat Rev Cancer*. 2010;10(3):165-180.
10. Landen CN, Kinch MS, Sood AK. EphA2 as a target for ovarian cancer therapy. *Expert opinion on therapeutic targets*. 2005;9(6):1179-1187.
11. Herath NI, Spanevello MD, Sabesan S, Newton T, Cummings M, Duffy S, Lincoln D, Boyle G, Parsons PG, Boyd AW. Over-expression of Eph and ephrin genes in advanced ovarian cancer: ephrin gene expression correlates with shortened survival. *BMC cancer*. 2006;6:144.
12. Dopeso H, Mateo-Lozano S, Mazzolini R, Rodrigues P, Lagares-Tena L, Ceron J, Romero J, Esteves M, Landolfi S, Hernandez-Losa J, Castano J, Wilson AJ, Ramon y Cajal S, Mariadason JM, Schwartz S, Jr., Arango D. The receptor tyrosine kinase EPHB4 has tumor suppressor activities in intestinal tumorigenesis. *Cancer research*. 2009;69(18):7430-7438.
13. Astin JW, Batson J, Kadir S, Charlet J, Persad RA, Gillatt D, Oxley JD, Nobes CD. Competition amongst Eph receptors regulates contact inhibition of locomotion and invasiveness in prostate cancer cells. *Nat Cell Biol*. 2010;12(12):1194-1204.
14. Deroo BJ, Rodriguez KF, Couse JF, Hamilton KJ, Collins JB, Grissom SF, Korach KS. Estrogen receptor beta is required for optimal cAMP production in mouse granulosa cells. *Molecular endocrinology*. 2009;23(7):955-965.

15. Buensuceso AV, Deroo BJ. The ephrin signaling pathway regulates morphology and adhesion of mouse granulosa cells in vitro. *Biol Reprod.* 2013;88(1):25.
16. Hatzirodos N, Irving-Rodgers HF, Hummitzsch K, Harland ML, Morris SE, Rodgers RJ. Transcriptome profiling of granulosa cells of bovine ovarian follicles during growth from small to large antral sizes. *BMC genomics.* 2014;15:24.
17. Rajkovic A, Pangas SA, Matzuk MM. Chapter 10 - Follicular Development: Mouse, Sheep, and Human Models. In: Wassarman JDNMPWPRGCMdKSRM, ed. *Knobil and Neill's Physiology of Reproduction (Third Edition)*. St Louis: Academic Press; 2006:383-423.
18. Bianchi E, Barbagallo F, Valeri C, Geremia R, Salustri A, De Felici M, Sette C. Ablation of the Sam68 gene impairs female fertility and gonadotropin-dependent follicle development. *Human molecular genetics.* 2010;19(24):4886-4894.
19. Johnson GL, Dhanasekaran N. The G-protein family and their interaction with receptors. *Endocr Rev.* 1989;10(3):317-331.
20. Hunzicker-Dunn M, Maizels ET. FSH signaling pathways in immature granulosa cells that regulate target gene expression: branching out from protein kinase A. *Cell Signal.* 2006;18(9):1351-1359.
21. Mayr B, Montminy M. Transcriptional regulation by the phosphorylation-dependent factor CREB. *Nature reviews Molecular cell biology.* 2001;2(8):599-609.
22. Kregge JH, Hodgins JB, Couse JF, Enmark E, Warner M, Mahler JF, Sar M, Korach KS, Gustafsson JA, Smithies O. Generation and reproductive phenotypes of mice lacking estrogen receptor beta. *Proceedings of the National Academy of Sciences of the United States of America.* 1998;95(26):15677-15682.
23. Nishi Y, Yanase T, Mu Y, Oba K, Ichino I, Saito M, Nomura M, Mukasa C, Okabe T, Goto K, Takayanagi R, Kashimura Y, Haji M, Nawata H. Establishment and characterization of a steroidogenic human granulosa-like tumor cell line, KGN, that expresses functional follicle-stimulating hormone receptor. *Endocrinology.* 2001;142(1):437-445.
24. Havelock JC, Rainey WE, Carr BR. Ovarian granulosa cell lines. *Mol Cell Endocrinol.* 2004;228(1-2):67-78.
25. Pfaffl MW. A new mathematical model for relative quantification in real-time RT-PCR. *Nucleic Acids Res.* 2001;29(9):e45.
26. Kuraishy AI, French SW, Sherman M, Herling M, Jones D, Wall R, Teitell MA. TORC2 regulates germinal center repression of the TCL1 oncoprotein to promote B cell development and inhibit transformation. *Proceedings of the National Academy of Sciences of the United States of America.* 2007;104(24):10175-10180.
27. Kawasaki H, Springett GM, Mochizuki N, Toki S, Nakaya M, Matsuda M, Housman DE, Graybiel AM. A family of cAMP-binding proteins that directly activate Rap1. *Science.* 1998;282(5397):2275-2279.

28. Chin EC, Abayasekara DR. Progesterone secretion by luteinizing human granulosa cells: a possible cAMP-dependent but PKA-independent mechanism involved in its regulation. *The Journal of endocrinology*. 2004;183(1):51-60.
29. Zeleznik AJ, Saxena D, Little-Ihrig L. Protein kinase B is obligatory for follicle-stimulating hormone-induced granulosa cell differentiation. *Endocrinology*. 2003;144(9):3985-3994.
30. Gonzalez GA, Montminy MR. Cyclic AMP stimulates somatostatin gene transcription by phosphorylation of CREB at serine 133. *Cell*. 1989;59(4):675-680.
31. Konkright MD, Guzman E, Flechner L, Su AI, Hogenesch JB, Montminy M. Genome-wide analysis of CREB target genes reveals a core promoter requirement for cAMP responsiveness. *Molecular cell*. 2003;11(4):1101-1108.
32. Brindle PK. Chapter 253 - Transcriptional Regulation via the cAMP Responsive Activator CREB. In: Dennis RABA, ed. *Handbook of Cell Signaling (Second Edition)*. San Diego: Academic Press; 2010:2077-2081.
33. Couse JF, Hewitt SC, Korach KS. Chapter 15 - Steroid Receptors in the Ovary and Uterus. In: Wassarman JDNMPWPRGCMdKSRM, ed. *Knobil and Neill's Physiology of Reproduction (Third Edition)*. St Louis: Academic Press; 2006:593-678.
34. Fitzpatrick SL, Richards JS. Identification of a cyclic adenosine 3',5'-monophosphate-response element in the rat aromatase promoter that is required for transcriptional activation in rat granulosa cells and R2C leydig cells. *Molecular endocrinology*. 1994;8(10):1309-1319.
35. Michael MD, Michael LF, Simpson ER. A CRE-like sequence that binds CREB and contributes to cAMP-dependent regulation of the proximal promoter of the human aromatase P450 (CYP19) gene. *Mol Cell Endocrinol*. 1997;134(2):147-156.
36. Parakh TN, Hernandez JA, Grammer JC, Weck J, Hunzicker-Dunn M, Zeleznik AJ, Nilson JH. Follicle-stimulating hormone/cAMP regulation of aromatase gene expression requires beta-catenin. *Proceedings of the National Academy of Sciences of the United States of America*. 2006;103(33):12435-12440.
37. Davies SP, Reddy H, Caivano M, Cohen P. Specificity and mechanism of action of some commonly used protein kinase inhibitors. *The Biochemical journal*. 2000;351(Pt 1):95-105.
38. Lochner A, Moolman JA. The many faces of H89: a review. *Cardiovascular drug reviews*. 2006;24(3-4):261-274.
39. Zheng W, Lu JJ, Luo F, Zheng Y, Feng Y, Felix JC, Lauchlan SC, Pike MC. Ovarian epithelial tumor growth promotion by follicle-stimulating hormone and inhibition of the effect by luteinizing hormone. *Gynecologic oncology*. 2000;76(1):80-88.

40. Radu A, Pichon C, Camparo P, Antoine M, Allory Y, Couvelard A, Fromont G, Hai MT, Ghinea N. Expression of follicle-stimulating hormone receptor in tumor blood vessels. *The New England journal of medicine*. 2010;363(17):1621-1630.
41. Zhang Z, Jia L, Feng Y, Zheng W. Overexpression of follicle-stimulating hormone receptor facilitates the development of ovarian epithelial cancer. *Cancer letters*. 2009;278(1):56-64.

5 Chapter 5: Discussion

5.1 Summary

Previous studies have reported detection of numerous *Eph* and *Efn* mRNA transcripts (1-4) and protein (5) in the ovary, suggesting that Eph-ephrin signaling plays a role in ovarian function. The first evidence indicating a functional role in fertility was a microarray screen of genes dysregulated in granulosa cells (GCs) of *Esr2*^{-/-} mice, which are subfertile and exhibit impaired antral follicle growth and ovulation (6). Among the FSH-responsive genes dysregulated in GCs of these mice is *Efna5* (4), suggesting that altered expression of this gene contributes to their ovarian phenotype. Based on these reports, we hypothesized that *Efna5* is required for optimal gonadotropin-dependent follicle growth and ovulation in the mouse.

This thesis presents findings gathered over the course of this investigation, beginning with a characterization of *Eph* and *Efn* expression in mouse GCs and confirmation that these cells are competent to respond to stimulation with recombinant ephrin-A5 and EphA5 in culture, which induce altered morphology and reduced adhesion, respectively. Based on study of a mouse model that lacks ephrin-A5, we present evidence that this ephrin is required for optimal fertility and a complete ovarian response to human chorionic gonadotropin (hCG). Specifically, loss of ephrin-A5 impairs follicle rupture and alters expression of several genes thought to be involved in oocyte release. Furthermore, we use a luciferase reporter system in a GC line to demonstrate that the cAMP-dependent PKA pathway regulates transcription of the mouse *Epha5* gene. We also present evidence indicating that stimulation of FSH-responsive *Eph* and *Efn* genes is attenuated in GCs of *Esr2*^{-/-} mice, which exhibit impaired cAMP production. This suggests that *Efna5*, *Epha3*, *Epha8*, and *Ephb2* are regulated in a similar manner. Therefore, our findings indicate that in the mouse, FSH enhances expression of *Efna5*, *Epha3*, *Epha5*, *Epha8*, and *Ephb2*. *Efna5* is required for a complete response to LH, and its loss results in reduced expression of several genes involved in ovulation and is associated with impaired follicle rupture. The evidence presented in this thesis establishes a place for Eph receptors and ephrins within the current model of gonadotropin-

dependent follicle growth and ovulation in the mouse, and identifies the cAMP-dependent PKA pathway as a novel regulator of *Epha5* transcription.

5.2 Expression of *Efna5*, *Epha3*, *Epha5*, *Epha8*, and *Ephb2* is enhanced in GCs of mice stimulated with equine chorionic gonadotropin (FSH)

Prior to our investigation, several studies reported *Eph* and *Efn* expression in the ovary. *EPHB1*, *EPHB2*, *EPHB4*, *EFNB1*, and *EFNB2* mRNA transcripts were detected in the human corpus luteum by RT-PCR (1) and beta-galactosidase-linked EFNB2 protein was localized to blood vessels of the mouse thecal layer and corpus luteum by X-gal (5-bromo-4-chloro-3-indolyl-beta-D-galactopyranoside) staining (5). Moreover, mRNA transcripts for *Epha1*, *Epha2*, *Ephb1*, and *Ephb3* were reported to be more abundant in dominant follicles compared to subordinate follicles in the cow (3). However, these studies did not investigate *Efn* and *Eph* expression in the context of a fertility-compromised or FSH-stimulated animal model. The report that *Efna5* is dysregulated in GCs isolated from FSH-stimulated (and subfertile) *Esr2*^{-/-} mice (4) suggested that Eph-ephrin signaling contributes to optimal fertility.

Since ephrins initiate signaling upon interaction with cognate Eph receptors, we surmised that GCs are likely to express *Eph* genes, which encode Eph receptors. In Chapter 2, we detected mRNA transcripts for numerous *Eph* and *Efn* genes in GCs of saline-treated mice. Of these genes, expression of a subset of *Eph* and *Efn* genes is enhanced when mice are stimulated with equine chorionic gonadotropin (eCG), a horse-derived gonadotropin that activates the FSH receptor. In GCs, FSH enhances expression of genes that are required for the generation of a preovulatory follicle that is competent to respond to the surge in luteinizing hormone (LH) that triggers ovulation. Chapters 2 and 4 identify *Efna5*, *Epha3*, *Epha5*, *Epha8*, and *Ephb2* as FSH-responsive genes in mouse GCs, and represents the first evidence for gonadotropin-regulated *Efn* and *Eph* expression in GCs. Consistent with our findings, a recently published microarray comparison of gene expression in small and large follicles in the cow ovary found that expression of *Efna5* and *Ephb6* is enhanced 8.6- and 3.8-fold, respectively, in large compared to small follicles (7). Since follicle growth is driven primarily by FSH, this supports the idea that

Eph and *Efn* expression increases under the influence of FSH. Furthermore, it was recently reported that expression of *EFNB2* is enhanced in human luteal cells in response to human chorionic gonadotropin (hCG) (8), a placenta-derived gonadotropin with the capacity to activate the LH receptor. Complemented by our own findings, these studies are adding to a growing body of evidence indicating that Eph receptors and ephrins are part of the ovarian response to gonadotropins, encompassing follicle growth, ovulation, and formation of the corpus luteum.

5.3 *Efna5* is required for a complete response to human chorionic gonadotropin (LH)

To date, no Eph receptor or ephrin knockout mouse has been reported to exhibit altered ovarian function. A partially-penetrant reproductive phenotype has been reported in *Epha7^{-/-}* females, but this was attributed to a developmental uterovaginal defect resulting in complete vaginal obstruction (9). Chapters 2 and 4 of this thesis demonstrate that eCG enhances expression of *Efna5*, *Epha3*, *Epha5*, *Epha8*, and *Ephb2* in mouse GCs. Of these genes, only *Efna5* encodes an ephrin ligand, while the remainder encode Eph receptors that bind ephrin-A5. Therefore, we chose to investigate gonadotropin-dependent follicle growth and ovulation in the *Efna5^{-/-}* mouse, based on the observation that eCG does not enhance expression of other *Efn* genes in GCs that might compensate for the loss of *Efna5*.

In Chapter 3, we present evidence that *Efna5^{-/-}* females are subfertile and exhibit an incomplete response to hCG. The impaired response to hCG included reduced ovulatory potential, attenuated ovarian expression of the LH-responsive genes *Pgr*, *Ptgs2*, and *Adamts4*, as well as impaired follicle rupture. Furthermore, adult *Efna5^{-/-}* females exhibited an increased incidence of multi-oocyte follicles (MOFs).

5.3.1 Morphological and adhesive responses in the context of the *Efna5^{-/-}* phenotype

In Chapter 2, we demonstrated that in a two-dimensional cell culture model system, GCs respond to recombinant ephrin-A5 and EphA5, exhibiting altered morphology and cell-substrate adhesion, respectively. Specifically, seeding primary mouse GCs or rat

GFSHR-17 cells onto an ephrin-A5-coated surface impedes cell spreading, while a surface coated with recombinant EphA5 reduces cell-substrate adhesion. These responses are indicative of repulsion, and it is reasonable to speculate that Eph-ephrin signaling contributes to cell repulsion during ovulation, but whether loss of these morphological and adhesive responses contributes to the ovarian phenotype we observed in *Efna5^{-/-}* mice is unknown. Nevertheless, these findings may provide insight into the way Eph-ephrin-stimulated changes in morphology and adhesion are involved in follicle growth and ovulation.

In the context of the growing follicle, such repulsive responses may contribute to formation of the antrum, which occurs during FSH-dependent follicle growth and requires movement of GCs relative to each other (10). Furthermore, cumulus cells exhibit transiently increased migratory and adhesive properties at the time of ovulation. This is proposed to facilitate adhesion of the COC to follicle wall extracellular matrix (ECM) exposed by thinning of the granulosa layer at the site of rupture (11). Given our observation that stimulation with ephrin-A5 and EphA5 induces a repulsive response in cultured GCs (12), Eph-ephrin signaling may reduce granulosa cell adhesion at the time of ovulation. In *Efna5^{-/-}* mice, GC adhesion may remain sufficiently high as to impede oocyte release. Interestingly, expression of other genes associated with cell repulsion during axon guidance is increased in large compared to small follicles in the cow, such as Slit (*Slitrk1*), roundabout (*Robo1*, *Robo2*), and semaphorin (*Sema6a*) (7). This suggests that multiple pathways may be involved in regulating cell adhesion during follicle growth and/or ovulation.

Given that ephrinA5 and Eph receptor A5 trigger morphological and adhesive changes in granulosa cells in culture, Eph-ephrin signaling may contribute to cell migration during release of the COC from the rupturing follicle. In Chapter 2, our data indicate that in antral follicles of eCG-stimulated mice, immunoreactivity corresponding to both ephrinA5 and Eph receptor A5 protein is stronger in mural granulosa cells than in cumulus cells. This observation is consistent with the idea that FSH and oocyte-stimulated SMAD2/3 signaling establish opposing gradients of gene expression in the follicle, such that expression of FSH-responsive genes is stronger in mural granulosa

cells than in cumulus cells (13). Differential Eph receptor and ephrin expression that gives rise to differences in adhesive affinity has been implicated in the segregation of human colorectal cancer cells (14). In the follicle, differential Eph receptor and ephrin expression in mural granulosa cells and cumulus cells may facilitate COC release through differences in adhesive affinity that contribute to guiding the COC towards the site of follicle rupture. In *Efna5*^{-/-} females, FSH-stimulated expression of ephrinA5 and the resulting gradient would be abolished, potentially altering the capacity of the follicle to facilitate COC release and resulting in an increased likelihood of oocyte retention. Such a scenario would complement the observation that the COC exhibits transiently increased invasive migration at the time of ovulation (11) as well as the idea that in large antral follicles, increased expression of ephrins and other signaling elements with roles in axon guidance promote migration of the oocyte to the site of follicle rupture (7).

5.3.2 A possible role for *Efna5* in follicle atresia

Our investigation yielded the unexpected finding that follicles containing expanded COCs were more numerous in gonadotropin-stimulated (48 h eCG + 10 h hCG) *Efna5*^{-/-} females than in *Efna5*^{+/+} controls. Since the majority of follicles that are recruited for FSH-dependent growth are destined for atresia (15), an increased number of follicles containing expanded COCs may indicate disruption of atresia in *Efna5*^{-/-} mice. The possibility that ephrin-A5 is required for follicular atresia is supported by the observation that expression of *Efna4* and *Efna5* is enhanced 4.2- and 3.3-fold, respectively, in small atretic follicles compared to small healthy follicles in the cow (16). Given our observation that *Efna5* expression in GCs is enhanced by eCG, this is seemingly at odds with the generally accepted idea that FSH serves as a survival signal that rescues follicles from atresia (17). Therefore, enhancement of *Efna5* expression in atretic follicles may occur independently of FSH.

Cell death during atresia occurs by several biological mechanisms, including apoptosis, autophagy, cornification, and necrosis (18). However, apoptosis is thought to be the primary mechanism by which cell death occurs in atretic follicles (16). Eph-ephrin signaling is required for apoptosis in some cell types, supported by the observation that stimulation with recombinant ephrin-A5 promotes apoptosis in *Epha7*-expressing mouse

cortical progenitor cells, while apoptosis is suppressed by loss of *Epha7* (19). Furthermore, *Epha2*^{-/-} mouse embryonic fibroblasts are resistant to UV-induced apoptosis compared to *Epha2*^{+/+} controls (20). Given the observations that expression of *Efna4* and *Efna5* is higher in atretic bovine antral follicles than in healthy follicles (16) and the increased numbers of follicles containing expanded COCs in ovaries of superovulated *Efna5*^{-/-} females, it is reasonable to speculate that Eph-ephrin signaling contributes to follicular atresia. During the follicular phase of the ovarian cycle, a decline in serum FSH concentration is thought to be a key mediator of atresia, resulting in the death of subordinate follicles and selection of the dominant follicle (21). If *Efna5* is required for follicular atresia in the mouse, the absence of ephrin-A5 may permit some fraction of subordinate follicles to acquire some competency to respond to hCG, and achieve cumulus expansion.

5.3.3 Putative Eph-ephrin signaling mechanisms in GCs

One of the most interesting questions raised by our findings pertains to the nature of the signaling mechanisms that act downstream of Eph-ephrin signaling in GCs. Chapter 2 demonstrated that FSH enhances expression of *Efna5* and several genes that encode its cognate receptors, affects GC morphology and adhesion, and identified beta-catenin as a possible downstream signaling target. Chapter 3 provides evidence that ephrin-A5, the sole ephrin ligand upregulated in response to FSH in GCs, is required for a complete ovarian response to LH. Its loss impairs ovulation and attenuates LH-stimulated expression of two genes known to be important for follicle rupture, *Pgr* and *Ptgs2*. However, the molecular mechanism(s) by which activation of Eph-ephrin signaling contributes to GC functions and gene expression is unknown.

5.3.3.1 Crosstalk at the RAF-MEK-ERK pathway

One possibility is that Eph-ephrin signaling in GCs contributes to activation of extracellular regulated kinases 1 and 2 (ERK1/2). Mice that lack ERK1/2 in GCs exhibit a compromised response to LH, including impairment of cumulus expansion, ovulation, luteinization, and abolished expression of many LH-responsive genes, including *Pgr* and *Ptgs2* (22). Therefore, ERK1/2 play a critical role in mediating the response to LH in the

mouse ovary. Consequently, signaling pathways that impinge on ERK1/2 may have the potential to modulate the response to LH in GCs.

Eph-ephrin signaling has been reported to impinge on ERK1/2 signaling, increasing phosphorylation in some cell types and decreasing phosphorylation in others. Eph receptor activation decreases phosphorylation of ERK1/2 in pRNS1-1 and PC-3 human prostatic epithelial cells, mouse embryonic fibroblasts, and primary bovine aortic cells (23). Furthermore, treatment of *EPHB2*-expressing MCF-7 cells with the EphB2 cognate ligand ephrin-B2 or an agonistic EPHB2 antibody results in activation of ERK1/2 (24). However, Eph receptor activation increases phosphorylation of ERK1/2 in MDA-MB-231 breast cancer cells (25), mouse neural progenitor cells (26), and rat PC12 pheochromocytoma cells (27). This suggests the possibility that in follicles growing under the influence of FSH, enhanced expression of *Efna5* and genes encoding its cognate Eph receptors results in increased Eph-ephrin-mediated ERK1/2 activation. Therefore it is reasonable to speculate that in GCs, Eph-ephrin and LH signaling converge at ERK1/2 to promote expression of genes that are important for ovulation. In the *Efna5*^{-/-} mouse, absence of ephrin-A5 may result in ERK1/2 phosphorylation that is insufficient to achieve optimal induction of *Pgr* and *Ptgs2*, which in turn impairs follicle rupture during ovulation.

Another possible mechanism by which ephrin-A5 may impinge on ERK1/2 involves suppression of Eph receptor activation by co-expressed ephrin-A5. The current body of evidence primarily describes interactions between Eph receptors and ephrins *in trans*, that is, between Eph receptors expressed on one cell and ephrins expressed on an adjacent cell. Several reports have described Eph receptor-ephrin interactions *in cis*, that is, co-expressed Eph receptors and ephrins interacting within the same cell membrane, although the body of evidence supporting *cis* as opposed to *trans* interactions is smaller. In *EPHA3*-expressing human embryonic kidney 293 (HEK293) cells, co-expression of *EPHA3* and *EFNA5* abolished activation of *EPHA3* by soluble, recombinant ephrin-A5 (28). The physiological importance of Eph-ephrin interactions *in cis* was demonstrated in a report describing how attenuation of Eph receptor signaling by co-expressed ephrins is required for proper migration of chick spinal motor axons (29). In Chapter 2, we detected

transcripts for a number of *Efn* and *Eph* genes in mouse GCs. Expression of a subset of these genes, which included only one ephrin (ephrin-A5) was enhanced by eCG. This suggests the possibility of a scenario where a basal level of Eph-ephrin signaling suppresses phosphorylation of ERK1/2 in GCs, as has been previously described (23). Increased expression of *Efna5* in response to FSH may then serve to attenuate activation of co-expressed Eph receptors *in cis*, thereby relieving suppression of ERK1/2 signaling. In the *Efna5*^{-/-} mouse, eCG does not enhance expression of *Efna5*, and relief of ERK1/2 suppression by attenuation of Eph receptor forward signaling would not occur. In this scenario, ERK1/2 phosphorylation may be insufficient to achieve optimal expression of *Pgr* and *Ptgs2*, resulting in impaired follicle rupture.

5.3.3.2 Ephrin-A5 alters beta-catenin protein levels in GFSHR-17 cells

In Chapter 2, we reported that ephrin-A5 has the capacity to alter beta-catenin protein levels in the GFSHR-17 rat GC line. Specifically, stimulation with recombinant ephrin-A5 resulted in decreased beta-catenin protein levels. Beta-catenin is known to have dual functions in the cell, serving as a component of adherens junctions (30) and as a transcriptional activator (31,32). Targeting of beta-catenin protein to proteasomal degradation is mediated by a constitutively-active degradation complex that consists of APC (Adenomatous polyposis coli), axin, GSK3 (glycogen synthase kinase 3), and CK1 (casein kinase 1), resulting in constant turnover of beta-catenin. Activation of cell membrane-associated FZD (Frizzled) receptors by WNT (secreted wingless/int1) proteins promotes dissociation of this degradation complex, which results in increased beta-catenin protein levels by accumulation (33). In the context of the ovary, maintenance of appropriate beta-catenin protein levels in GCs is critical for fertility. Mice expressing a dominant-stable (resistant to degradation) form of beta-catenin in GCs exhibit impaired ovulation and luteinization. The same study found that when stimulated with eCG and hCG, these mice exhibit attenuated expression of *Ptgs2* in GCs compared to controls (34). Therefore, in mouse GCs, FSH-stimulated enhancement of *Efna5* expression may serve as a mechanism to promote degradation of beta-catenin. In GCs of *Efna5*^{-/-} mice, loss of ephrin-A5 may result in increased beta-catenin protein levels, contributing to the reduced expression of *Ptgs2* and impairment of ovulation we observed in these mice.

5.3.3.3 Attenuated expression of *Adamts4* in *Efna5*^{-/-} mice

In Chapter 3, we present data indicating that hCG-stimulated enhancement of whole-ovary *A disintegrin and metalloproteinase with thrombospondin-like repeats-4* (*Adamts4*) expression at 14 h post-hCG is 80% lower in *Efna5*^{-/-} than in *Efna5*^{+/+} mice. In the mouse ovary, expression of *Adamts4* exhibits a biphasic pattern of expression following stimulation with hCG, increasing at 4 h and falling by 8 h, and then increasing again at 12-16 h. The same study found that in hCG-treated progesterone receptor (PGR)-null (*Pgr*^{-/-}) mice, ovarian expression of *Adamts4* increases normally at 4 h, but is significantly reduced at 12 h compared to *Pgr*^{+/-} mice, indicating that *Pgr* is required for optimal *Adamts4* induction (35). This is also consistent with the current view that PGR regulates the expression of numerous proteases during the periovulatory period (36). This suggests that in hCG-treated *Efna5*^{-/-} females, attenuated expression of *Pgr* at 4 h contributes to the absence of *Adamts4* induction at 14 h. Previously published immunohistochemistry studies revealed that at 16 h post-hCG, ADAMTS4 protein is substantially enriched at the site of ovulation, suggesting that it is involved in tissue remodeling at this site (35). However, *Adamts4*^{-/-} mice are phenotypically normal and have not been reported to exhibit reproductive defects, suggesting that other proteinases can compensate for its loss (37) or that its contribution to fertility is too small to be detected using reasonable sample sizes. In *Efna5*^{-/-} females, attenuated induction of *Pgr* may result in reduced expression of other proteases that would normally compensate for the loss of *Adamts4*. Therefore, attenuation of *Adamts4* expression in *Efna5*^{-/-} ovaries at 14 h post-hCG may be caused by inadequate ovarian induction of *Pgr* in these mice.

5.3.3.4 Reduced prostaglandin synthesis in follicles of *Efna5*^{-/-} mice may allow non-apical rupture

Our observations suggest that reduced expression of *Pgr* and *Ptgs2* in ovaries of *Efna5*^{-/-} mice contributes to abnormal follicle rupture in these animals. Release of ovulated oocytes into the extraovarian space requires that follicle rupture occurs at the apical surface, which lies closest to the ovarian surface epithelium. Localization of rupture to the apical surface of the follicle has been attributed to the observation that the follicle is thinnest at this region, the apex (38). However, proper localization of rupture

may also be regulated by prostaglandin-stimulated expression of proteolytic inhibitors. In granulosa cells of primate follicles, hCG stimulates expression of *PLAT* (tissue-type plasminogen activator) and *SERPINE1* (plasminogen activator inhibitor, type I) in a prostaglandin-dependent manner (39). Prostaglandin receptor expression in primate follicles differs between GC subtypes, with *PTGER1* (Prostaglandin E receptor 1, subtype EP1) predominant in mural GCs and *PTGER2* (Prostaglandin E receptor 1, subtype EP2) and *PTGER3* (Prostaglandin E receptor 1, subtype EP3) predominant in cumulus cells. The same study demonstrated that while PLAT protein levels are uniform in mural GCs, EP1 and SERPINE1 protein levels are lower in mural GCs at the follicle apex than in non-apex mural GCs. This suggests that follicle rupture is regulated by a balance of activation and inhibition of proteolysis, with reduced inhibition favouring rupture at the apex (40). In *Efna5^{-/-}* females, attenuated *Ptgs2* expression may result in reduced prostaglandin synthesis, such that prostaglandin levels are insufficient to inhibit proteolysis at non-apex follicle sites. This could potentially result in occasional instances of non-apical follicle rupture.

5.3.4 A potential link between abnormal follicle rupture and multi-oocyte follicle formation

Multi-oocyte follicles (MOFs) have been reported in a number of mouse models, most of which exhibit decreased fertility (41). Our observations indicate that at PND 120, MOFs are more numerous in ovaries of adult *Efna5^{-/-}* mice than in *Efna5^{+/+}* controls. However, there is no difference in MOF number between genotypes at PND 21, an age at which mice are reproductively immature. This suggests a gonadotropin-associated mechanism underlying MOF formation, as well as the possibility that MOF formation in these mice occurs by joining of follicles. Incomplete prenatal oocyte nest breakdown during has been proposed to cause MOF formation (42), however the observation that increased MOF number is not seen in immature *Efna5^{-/-}* females but is observed in adults indicates that MOF formation likely occurs by joining of follicles. Breaching of the follicle wall resulting in joining of follicles has been proposed to underlie MOF formation in oocyte-specific *CIgalt1* (core 1 synthase, glycoprotein-N-acetylgalactosamine 3-beta-galactosyltransferase, 1)-deficient mice (41).

In Chapter 3, we present evidence that absence of ephrin-A5 results in non-apical follicle rupture. Furthermore, we observed one occurrence of premature follicle rupture at the antral stage. These observations suggest that ephrin-A5 is involved in localizing follicle rupture to an apical region of the follicle wall, and may also be important for maintaining integrity of the follicle wall. Based on the histological similarity between ovaries of *Efna5*^{-/-} mice and PTGS2 inhibitor (indomethacin)-treated rats, and the observation that enhancement of *Ptgs2* expression is blunted in *Efna5*^{-/-} ovaries, it is reasonable to speculate that reduced PTGS2 activity underlies non-apical rupture in *Efna5*^{-/-} mice. However, premature follicle rupture was not reported in indomethacin-treated rats. This suggests that premature follicle rupture in *Efna5*^{-/-} mice is caused by the absence of ephrin-A5, but by a mechanism that is independent of that which underlies non-apical follicle rupture. If ephrin-A5 is important for maintaining follicle wall integrity, its loss may result in an increased occurrence of follicle wall breaching and merging, resulting in an increased occurrence of MOFs.

5.3.5 cAMP-dependent pathways regulate *Epha5* expression in GCs

In Chapter 2, we demonstrated that FSH enhances expression of *Efna5* and genes encoding several of its cognate Eph receptors, suggesting a role for Eph-ephrin signaling in follicle growth and/or ovulation. However, since the FSH receptor is a G protein coupled receptor (GPCR), this also suggested that expression of these genes is regulated by cAMP-dependent pathways. In Chapter 4, we present evidence that eCG-stimulated enhancement of *Efna5*, *Epha3*, *Epha5*, *Epha8*, and *Ephb2* is attenuated in GCs of *Esr2*^{-/-} mice. *Esr2*^{-/-} mice exhibit impaired cAMP production in GCs, and this defect is the proposed basis of the severely attenuated expression of FSH-responsive genes observed in GCs of these mice. Using reporter assays, we also demonstrated that the 1589 bp genomic sequence upstream of the *Epha5* 5' UTR in the mouse is responsive to cAMP, and that this response is suppressed by co-treatment with an inhibitor of protein kinase A (PKA), H-89. Our findings are consistent with the idea that H-89 inhibits GC differentiation, which is promoted by both FSH and cell-permeable cAMP analogs (43), and with the idea that Eph receptors are part of the response to gonadotropins. Transcriptional regulation of *Eph* and *Efn* genes by cAMP-dependent pathways has not

been previously described. Our studies suggest that regulation by cAMP may also occur in other tissues. Furthermore, GPCRs make up the largest known family of signaling molecules associated with the cell surface, and many GPCRs impinge on cAMP-dependent pathways (44). Therefore, our findings suggest that *Eph* and *Efn* expression may be altered, and Eph-ephrin signaling involved, in GPCR-associated signaling events where Eph-ephrin signaling has not been previously investigated as a potential source of cross-talk.

5.4 Experimental Considerations

5.4.1 Germline *Efna5*^{-/-} mouse model

In Chapter 2, we demonstrated that in GCs, expression of *Efna5* and genes encoding several of its cognate receptors is enhanced by FSH. Based on this finding, we performed a reproductive characterization of the *Efna5*^{-/-} mouse. It should be noted that this mouse model is a germline knockout, and therefore lacks *Efna5* at all stages of development in all cell types. Therefore, we cannot rule out the possibility that loss of ephrin-A5 during embryonic development impairs ovarian function in the adult. Furthermore, non-GC types in the ovary, such as the oocyte, thecal cells, endothelial cells, or the ovarian stroma may require ephrin-A5 for normal function. In future studies, these concerns may be addressed through the use of a Cre/loxP approach to generate a GC-specific *Efna5* knockout mouse. *Cyp19*-Cre transgenic mice have been previously generated (45) and used as a model system to investigate the role of ERK signaling in GCs during FSH-dependent follicle growth (22). To some extent, the breeding and serum steroid concentration data presented in Chapter 3 address these concerns. We detected no difference in litter frequency between *Efna5*^{+/+} and *Efna5*^{-/-} females, suggesting that estrous cyclicity is not affected by loss of ephrin-A5. This in turn suggests that regulation of the hypothalamic-pituitary-gonadal (HPG) axis is normal in *Efna5*^{-/-} females. Furthermore, we detected no difference in serum concentrations of estradiol and progesterone between superovulated *Efna5*^{+/+} and *Efna5*^{-/-} females. This suggests that ovarian production of estradiol and progesterone, steroid hormones that act on the hypothalamus, pituitary, uterus, and other tissues, is normal in *Efna5*^{-/-} females.

5.5 Future Directions

5.5.1 Delineating Eph-ephrin signaling pathways in GCs

In Chapter 3, we demonstrated that loss of ephrin-A5 attenuates hCG-stimulated enhancement of *Pgr* and *Ptgs2* expression in the ovary. While the mechanism by which ephrin-A5 contributes to increased expression of these genes in the ovary is not known, we speculated on the possibility that Eph-ephrin signaling impinges on ERK1/2 in mouse GCs. In order to identify signaling pathways regulated by ephrin-A5, immunoblotting could be used to analyze GC lysates from gonadotropin-stimulated *Efna5^{+/+}* and *Efna5^{-/-}* mice. Proven antibodies against total and phosphorylated forms of candidate targets we have proposed are readily available, such as RAF, MEK, and ERK. Furthermore, commercially available phosphorylated protein kinase detection arrays may reveal additional pathways regulated by ephrin-A5 in GCs. These arrays would permit rapid screening of multiple kinase targets to determine whether other pathways are differentially regulated between *Efna5^{+/+}* and *Efna5^{-/-}* GCs in superovulated mice. Any targets identified by such screens would then be verified by immunoblotting.

If and when ephrin-A5-regulated pathways are identified in GCs of intact mice, a cell culture approach could be used to distinguish between forward (downstream of Eph receptor activation) and reverse (downstream of ephrin activation). In Chapter 2, we stimulated cultured GCs with recombinant ephrin-A5 or EphA5 to demonstrate effects on morphology and adhesion. The same experimental system could be used to specifically stimulate forward or reverse signaling, and immunoblotting would then be used to assess activation of identified signaling targets.

5.6 Conclusion

The work presented in this thesis demonstrates that ephrin-A5 plays an important role in ovarian function. In the mouse, FSH enhances expression of *Efna5*, *Epha3*, *Epha5*, *Epha8*, and *Ephb2* in GCs. Loss of *Efna5* results in subfertility and a partially impaired response to hCG that includes reduced ovulatory potential, attenuated expression of *Pgr*, *Ptgs2*, and *Adamts4* (**Figure 5-1**), as well as abnormal follicle rupture. We also present evidence that cAMP is a transcriptional regulator for genes encoding

several members of the Eph-ephrin family. In the case of *Epha5*, the proximal upstream genomic region is activated by cAMP in a PKA-dependent manner, and contains a conserved, putative consensus CRE half-site. This indicates that *Eph* and *Efn* expression may be regulated by GPCRs in other tissues. The body of evidence indicating the importance of Eph-ephrin signaling in the ovary has only recently begun to grow. Our current knowledge of Eph-ephrin function in the ovary is limited, particularly with respect to the signaling pathways by which these signaling elements influence the ovarian response to gonadotropins. Continued investigation will delineate these mechanisms to generate a more accurate model of ovarian function.

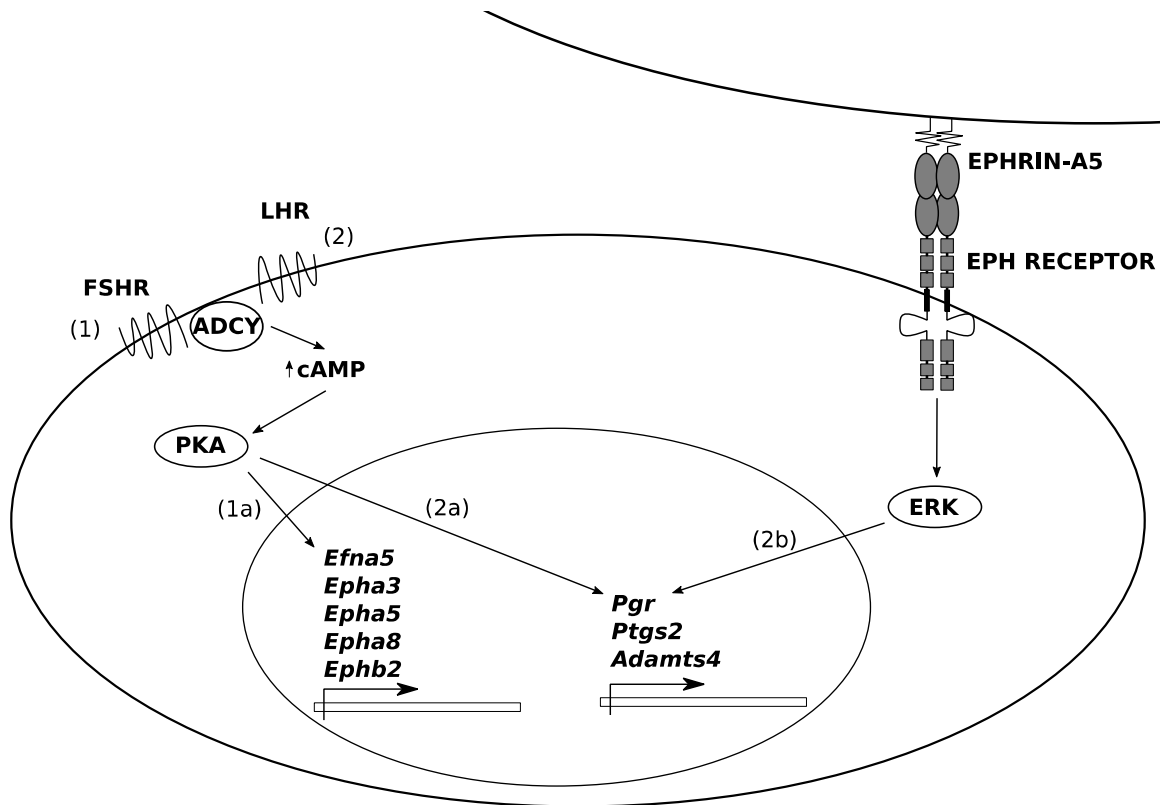


Figure 5-1: Putative model for Eph-ephrin involvement in gonadotropin-stimulated gene expression in mouse granulosa cells.

Activation of FSHR (1) stimulates expression of *Efna5*, *Epha3*, *Epha5*, *Epha8*, and *Ephb2* via the protein kinase A (PKA) signaling pathway (1a). Stimulation of LHR and Eph receptors cognate to ephrinA5 results in activation of the PKA (2a) and extracellular signal regulated kinase (ERK1/2) (2b) signaling pathways, respectively. This results in optimal expression of *Pgr*, *Ptgs2*, and *Adamts4*. *Pgr* and *Ptgs2* are necessary for ovulation, while *Adamts4* may play a role in tissue remodeling at the follicle rupture site.

5.7 Bibliography

1. Egawa M, Yoshioka S, Higuchi T, Sato Y, Tatsumi K, Fujiwara H, Fujii S. Ephrin B1 is expressed on human luteinizing granulosa cells in corpora lutea of the early luteal phase: the possible involvement of the B class Eph-ephrin system during corpus luteum formation. *The Journal of clinical endocrinology and metabolism*. 2003;88(9):4384-4392.
2. Xu Y, Zagoura D, Keck C, Pietrowski D. Expression of Eph receptor tyrosine kinases and their ligands in human Granulosa lutein cells and human umbilical vein endothelial cells. *Experimental and Clinical Endocrinology and Diabetes*. 2006;114(10):590-595.
3. Forde N, Mihm M, Canty MJ, Zielak AE, Baker PJ, Park S, Lonergan P, Smith GW, Coussens PM, Ireland JJ, Evans AC. Differential expression of signal transduction factors in ovarian follicle development: a functional role for betaglycan and FIBP in granulosa cells in cattle. *Physiol Genomics*. 2008;33(2):193-204.
4. Deroo BJ, Rodriguez KF, Couse JF, Hamilton KJ, Collins JB, Grissom SF, Korach KS. Estrogen receptor beta is required for optimal cAMP production in mouse granulosa cells. *Molecular endocrinology*. 2009;23(7):955-965.
5. Gale NW, Baluk P, Pan L, Kwan M, Holash J, DeChiara TM, McDonald DM, Yancopoulos GD. Ephrin-B2 selectively marks arterial vessels and neovascularization sites in the adult, with expression in both endothelial and smooth-muscle cells. *Dev Biol*. 2001;230(2):151-160.
6. Kregel JH, Hodgin JB, Couse JF, Enmark E, Warner M, Mahler JF, Sar M, Korach KS, Gustafsson JA, Smithies O. Generation and reproductive phenotypes of mice lacking estrogen receptor beta. *Proceedings of the National Academy of Sciences of the United States of America*. 1998;95(26):15677-15682.
7. Hatzirodos N, Irving-Rodgers HF, Hummitzsch K, Harland ML, Morris SE, Rodgers RJ. Transcriptome profiling of granulosa cells of bovine ovarian follicles during growth from small to large antral sizes. *BMC genomics*. 2014;15:24.
8. Wissing ML, Kristensen SG, Andersen CY, Mikkelsen AL, Host T, Borup R, Grondahl ML. Identification of new ovulation-related genes in humans by comparing the transcriptome of granulosa cells before and after ovulation triggering in the same controlled ovarian stimulation cycle. *Human reproduction*. 2014;29(5):997-1010.
9. Duffy SL, Coulthard MG, Spanevello MD, Herath NI, Yeadon TM, McCarron JK, Carter JC, Tonks ID, Kay GF, Phillips GE, Boyd AW. Generation and characterization of EphA1 receptor tyrosine kinase reporter knockout mice. *Genesis*. 2008;46(10):553-561.
10. Rodgers RJ, Irving-Rodgers HF. Formation of the ovarian follicular antrum and follicular fluid. *Biol Reprod*. 2010;82(6):1021-1029.

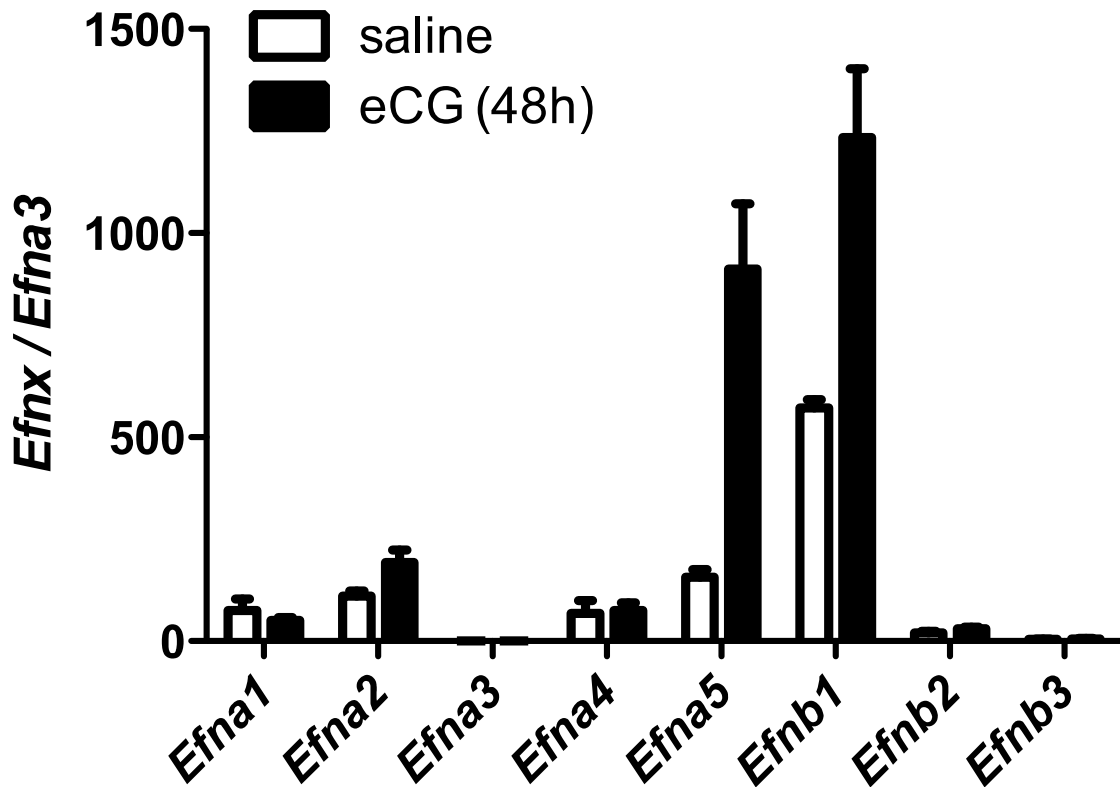
11. Akison LK, Alvino ER, Dunning KR, Robker RL, Russell DL. Transient invasive migration in mouse cumulus oocyte complexes induced at ovulation by luteinizing hormone. *Biol Reprod.* 2012;86(4):125.
12. Buensuceso AV, Deroo BJ. The ephrin signaling pathway regulates morphology and adhesion of mouse granulosa cells in vitro. *Biol Reprod.* 2013;88(1):25.
13. Diaz FJ, Wigglesworth K, Eppig JJ. Oocytes determine cumulus cell lineage in mouse ovarian follicles. *J Cell Sci.* 2007;120(Pt 8):1330-1340.
14. Solanas G, Cortina C, Sevillano M, Batlle E. Cleavage of E-cadherin by ADAM10 mediates epithelial cell sorting downstream of EphB signalling. *Nat Cell Biol.* 2011;13(9):1100-1107.
15. Gougeon A. Dynamics of follicular growth in the human: a model from preliminary results. *Human reproduction.* 1986;1(2):81-87.
16. Hatzirodos N, Hummitzsch K, Irving-Rodgers HF, Harland ML, Morris SE, Rodgers RJ. Transcriptome profiling of granulosa cells from bovine ovarian follicles during atresia. *BMC genomics.* 2014;15:40.
17. Chun SY, Eisenhauer KM, Minami S, Billig H, Perlas E, Hsueh AJ. Hormonal regulation of apoptosis in early antral follicles: follicle-stimulating hormone as a major survival factor. *Endocrinology.* 1996;137(4):1447-1456.
18. Rodgers RJ, Irving-Rodgers HF. Morphological classification of bovine ovarian follicles. *Reproduction.* 2010;139(2):309-318.
19. Depaeppe V, Suarez-Gonzalez N, Dufour A, Passante L, Gorski JA, Jones KR, Ledent C, Vanderhaeghen P. Ephrin signalling controls brain size by regulating apoptosis of neural progenitors. *Nature.* 2005;435(7046):1244-1250.
20. Zhang G, Njauw CN, Park JM, Naruse C, Asano M, Tsao H. EphA2 is an essential mediator of UV radiation-induced apoptosis. *Cancer research.* 2008;68(6):1691-1696.
21. Baerwald AR, Adams GP, Pierson RA. Ovarian antral folliculogenesis during the human menstrual cycle: a review. *Human reproduction update.* 2012;18(1):73-91.
22. Fan HY, Liu Z, Shimada M, Sterneck E, Johnson PF, Hedrick SM, Richards JS. MAPK3/1 (ERK1/2) in ovarian granulosa cells are essential for female fertility. *Science.* 2009;324(5929):938-941.
23. Miao H, Wei BR, Peehl DM, Li Q, Alexandrou T, Schelling JR, Rhim JS, Sedor JR, Burnett E, Wang B. Activation of EphA receptor tyrosine kinase inhibits the Ras/MAPK pathway. *Nat Cell Biol.* 2001;3(5):527-530.
24. Xiao Z, Carrasco R, Kinneer K, Sabol D, Jallal B, Coats S, Tice DA. EphB4 promotes or suppresses Ras/MEK/ERK pathway in a context-dependent manner: Implications for EphB4 as a cancer target. *Cancer biology & therapy.* 2012;13(8):630-637.
25. Pratt RL, Kinch MS. Activation of the EphA2 tyrosine kinase stimulates the MAP/ERK kinase signaling cascade. *Oncogene.* 2002;21(50):7690-7699.

26. Aoki M, Yamashita T, Tohyama M. EphA receptors direct the differentiation of mammalian neural precursor cells through a mitogen-activated protein kinase-dependent pathway. *The Journal of biological chemistry*. 2004;279(31):32643-32650.
27. Shin J, Gu C, Kim J, Park S. Transient activation of the MAP kinase signaling pathway by the forward signaling of EphA4 in PC12 cells. *BMB reports*. 2008;41(6):479-484.
28. Carvalho RF, Beutler M, Marler KJ, Knoll B, Becker-Barroso E, Heintzmann R, Ng T, Drescher U. Silencing of EphA3 through a cis interaction with ephrinA5. *Nat Neurosci*. 2006;9(3):322-330.
29. Kao TJ, Kania A. Ephrin-mediated cis-attenuation of Eph receptor signaling is essential for spinal motor axon guidance. *Neuron*. 2011;71(1):76-91.
30. Sundfeldt K, Piontkewitz Y, Billig H, Hedin L. E-cadherin-catenin complex in the rat ovary: cell-specific expression during folliculogenesis and luteal formation. *Journal of reproduction and fertility*. 2000;118(2):375-385.
31. Morin PJ, Sparks AB, Korinek V, Barker N, Clevers H, Vogelstein B, Kinzler KW. Activation of beta-catenin-Tcf signaling in colon cancer by mutations in beta-catenin or APC. *Science*. 1997;275(5307):1787-1790.
32. Korinek V, Barker N, Morin PJ, van Wichen D, de Weger R, Kinzler KW, Vogelstein B, Clevers H. Constitutive transcriptional activation by a beta-catenin-Tcf complex in APC^{-/-} colon carcinoma. *Science*. 1997;275(5307):1784-1787.
33. Kimelman D, Xu W. beta-catenin destruction complex: insights and questions from a structural perspective. *Oncogene*. 2006;25(57):7482-7491.
34. Fan HY, O'Connor A, Shitanaka M, Shimada M, Liu Z, Richards JS. Beta-catenin (CTNNB1) promotes preovulatory follicular development but represses LH-mediated ovulation and luteinization. *Molecular endocrinology*. 2010;24(8):1529-1542.
35. Richards JS, Hernandez-Gonzalez I, Gonzalez-Robayna I, Teuling E, Lo Y, Boerboom D, Falender AE, Doyle KH, LeBaron RG, Thompson V, Sandy JD. Regulated expression of ADAMTS family members in follicles and cumulus oocyte complexes: evidence for specific and redundant patterns during ovulation. *Biol Reprod*. 2005;72(5):1241-1255.
36. Robker RL, Akison LK, Russell DL. Control of oocyte release by progesterone receptor-regulated gene expression. *Nuclear receptor signaling*. 2009;7:e012.
37. Boerboom D, Lafond JF, Zheng X, Lapointe E, Mittaz L, Boyer A, Pritchard MA, DeMayo FJ, Mort JS, Drolet R, Richards JS. Partially redundant functions of Adamts1 and Adamts4 in the perinatal development of the renal medulla. *Developmental dynamics : an official publication of the American Association of Anatomists*. 2011;240(7):1806-1814.

38. Espey LL, Richards JS. Chapter 11 - Ovulation. In: Wassarman JDNMPWPRGCMdKSRM, ed. *Knobil and Neill's Physiology of Reproduction (Third Edition)*. St Louis: Academic Press; 2006:425-VI.
39. Markosyan N, Duffy DM. Prostaglandin E2 acts via multiple receptors to regulate plasminogen-dependent proteolysis in the primate periovulatory follicle. *Endocrinology*. 2009;150(1):435-444.
40. Harris SM, Aschenbach LC, Skinner SM, Dozier BL, Duffy DM. Prostaglandin E2 receptors are differentially expressed in subpopulations of granulosa cells from primate periovulatory follicles. *Biol Reprod*. 2011;85(5):916-923.
41. Williams SA, Stanley P. Mouse fertility is enhanced by oocyte-specific loss of core 1-derived O-glycans. *FASEB journal : official publication of the Federation of American Societies for Experimental Biology*. 2008;22(7):2273-2284.
42. Jefferson W, Newbold R, Padilla-Banks E, Pepling M. Neonatal genistein treatment alters ovarian differentiation in the mouse: inhibition of oocyte nest breakdown and increased oocyte survival. *Biol Reprod*. 2006;74(1):161-168.
43. Salvador LM, Park Y, Cottom J, Maizels ET, Jones JC, Schillace RV, Carr DW, Cheung P, Allis CD, Jameson JL, Hunzicker-Dunn M. Follicle-stimulating hormone stimulates protein kinase A-mediated histone H3 phosphorylation and acetylation leading to select gene activation in ovarian granulosa cells. *The Journal of biological chemistry*. 2001;276(43):40146-40155.
44. Dorsam RT, Gutkind JS. G-protein-coupled receptors and cancer. *Nat Rev Cancer*. 2007;7(2):79-94.
45. Fan HY, Shimada M, Liu Z, Cahill N, Noma N, Wu Y, Gossen J, Richards JS. Selective expression of KrasG12D in granulosa cells of the mouse ovary causes defects in follicle development and ovulation. *Development*. 2008;135(12):2127-2137.

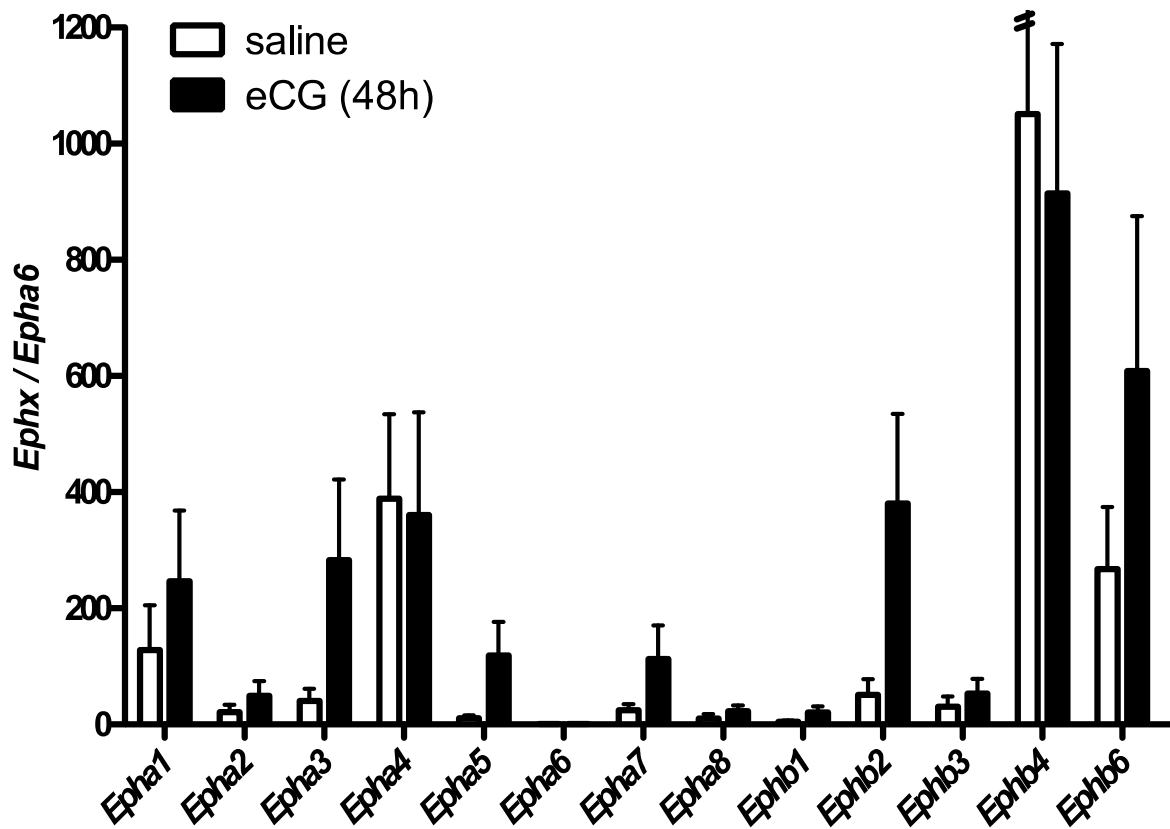
6 Appendix

6.1 Supplementary Material, Chapter 2



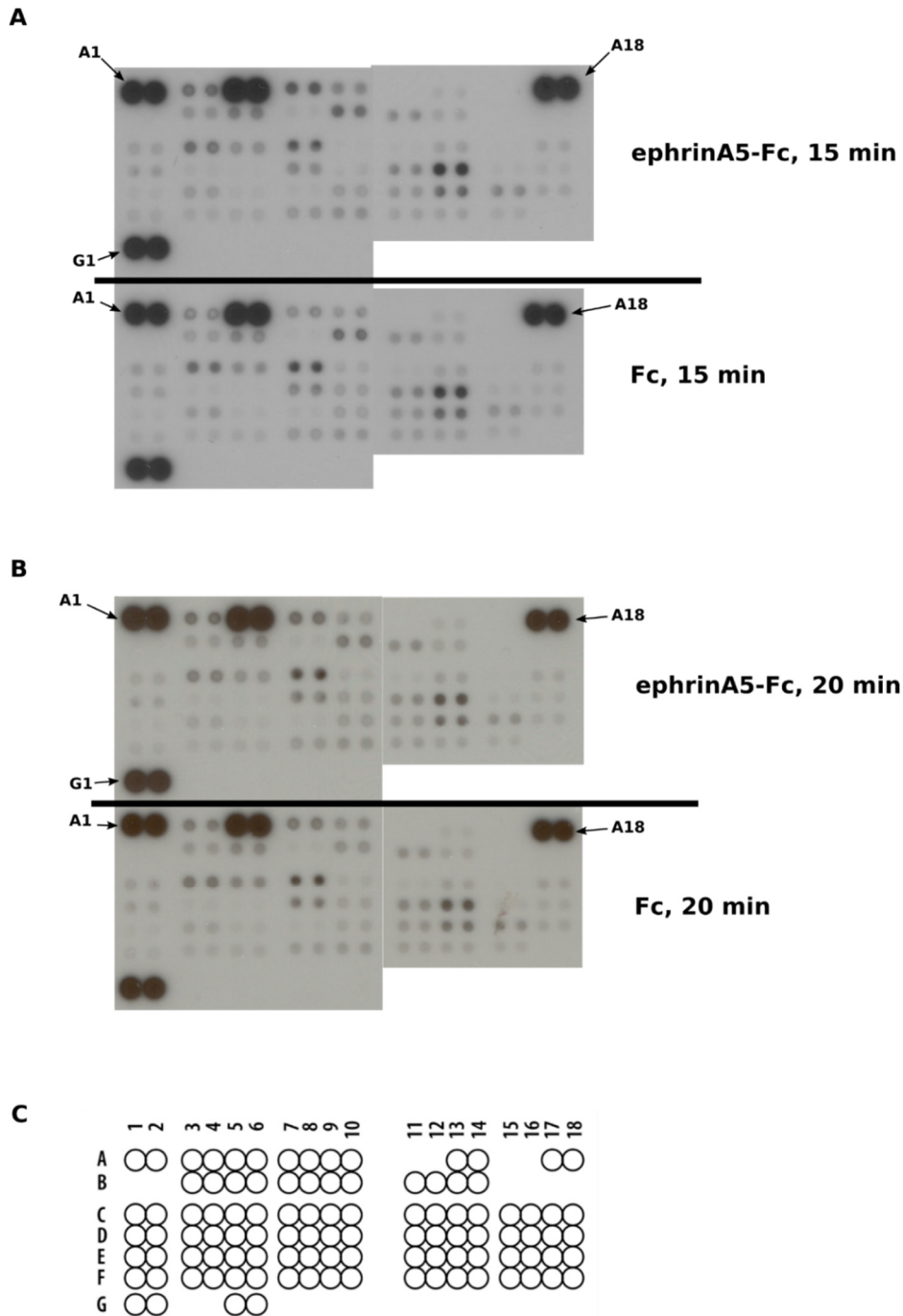
Supplemental Figure 6-1: Screening study to determine mRNA levels of all known mouse ephrin (*Efn*) genes in granulosa cells isolated from immature female mice in response to FSH.

Wild-type postnatal day (PND) 23-28 C57Bl/6 mice were treated with saline or equine chorionic gonadotropin (eCG) (5.0 IU per mouse) for 48 hours. Granulosa cells (GCs) were isolated by ovarian puncture, pooled, and mRNA isolated. mRNA levels were determined by quantitative RT-PCR and compared to an *Rpl7* control. Data are expressed as average gene expression compared with the *Rpl7* control (\pm SEM of three independent experiments). All resulting values were normalized to the *Efna3* vehicle (the *Efn* gene with the lowest expression level) to approximate relative levels of gene expression between *Efn* genes.



Supplemental Figure 6-2: Screening study to determine mRNA levels of all known mouse ephrin receptor (*Eph*) genes in granulosa cells isolated from immature female mice in response to FSH.

Wildtype postnatal day (PND) 23-28 C57Bl/6 mice were treated with saline or equine chorionic gonadotropin (eCG) (5.0 IU per mouse) for 48 hours. Granulosa cells (GCs) were isolated by ovarian puncture, pooled, and mRNA isolated. mRNA levels were determined by quantitative RT-PCR and compared to an *Rpl7* control. Data are expressed as average gene expression compared with the *Rpl7* control (\pm SEM of three independent experiments). All resulting values were normalized to the *Epha6* vehicle (the *Eph* gene with the lowest expression level) to approximate relative levels of gene expression between *Eph* genes.



Supplemental Figure 6-3: Proteome Profiler Phospho-Kinase Arrays.

GFSHR-17 cells were seeded onto tissue culture surfaces coated with ephrinA5-Fc or Fc (control protein). Protein lysates were generated, and analyzed using the Human Phospho-Kinase Array at 15 min (A) and 20 min (B) post-seeding. Capture array layout is represented in (C).

Supplemental Table 6-1: Human Phospho-Kinase Array capture antibodies

Spot	Kinase target
A1, A2	Reference
A3, A4	p38-alpha
A5, A6	ERK1/2
A7, A8	Pan-Jnk
A9, A10	GSK-3-alpha/beta
A13, A14	p53 (S392)
A17, A18	Reference
B3, B4	MEK1/2
B5, B6	MSK1/2
B7, B8	AMPK-alpha-1
B9, B10	Akt (S473)
B11, B12	Akt (T308)
B13, B14	p53 (S46)
C1, C2	TOR
C3, C4	CREB
C5, C6	HSP27
C7, C8	AMPK-alpha-2
C9, C10	beta-catenin
C11, C12	p70 S6 kinase (T389)
C13, C14	p53 (S15)
C15, C16	p27 (T157)
C17, C18	Paxillin
D1, D2	Src
D3, D4	Lyn
D5, D6	Lck
D7, D8	STAT2
D9, D10	STAT5a
D11, D12	p70 S6 kinase (T421/S424)
D13, D14	RSK1/2/3
D15, D16	p27 (T157)
D17, D18	PLC-gamma-1
E1, E2	Fyn
E3, E4	Yes
E5, E6	Fgr
E7, E8	STAT3
E9, 10	STAT5b
E11, E12	p70 S6 kinase (T229)
E13, E14	RSK1/2
E15, E16	c-Jun
E17, E18	Pyk2
F1, F2	Hck

F3, F4	Chk-2
F5, F6	FAK
F7, F8	STAT6
F9, F10	STAT5a/b
F11, F12	STAT1
F13, F14	STAT4
F15, F16	eNOS
F17, F18	Negative control
G1, G2	Reference
G5, G6	Negative control

Supplemental Table 6-2: Phosphorylation of intracellular kinase targets in response to ephrinA5-Fc, 15 min post-seeding.

Target	Phosphorylation Ratio (ephrinA5-Fc / Fc)
Pan-JNK	2.30
p38alpha	1.54
GSK-3alpha/beta	1.46
AMPKalpha1	1.44
MSK1/2	1.21
MEK1/2	1.19
c-Jun	1.15
STAT5a/b	1.09
Fgr	1.08
STAT5b	1.07
Chk-2	1.07
Akt - S473	1.06
Pyk2	1.03
Hck	1.02
Lyn	1.02
RSK1/2/3	1.02
FAK	1.00
Paxillin	1.00
CREB	0.99
Yes	0.98
STAT6	0.98
HSP27	0.95
STAT3	0.94
p53 S15	0.92
Src	0.92
Lck	0.89
Akt	0.88
p53	0.87
eNOS	0.86
p70 S6 kinase T229	0.86
STAT2	0.85
RSK1/2	0.84
PLCgamma-1	0.83
AMPKalpha2	0.81
p70 S6 kinase - T421/S424	0.81
Fyn	0.81
TOR	0.77
p53 S46	0.76
p70 S6 kinase	0.73
STAT4	0.71

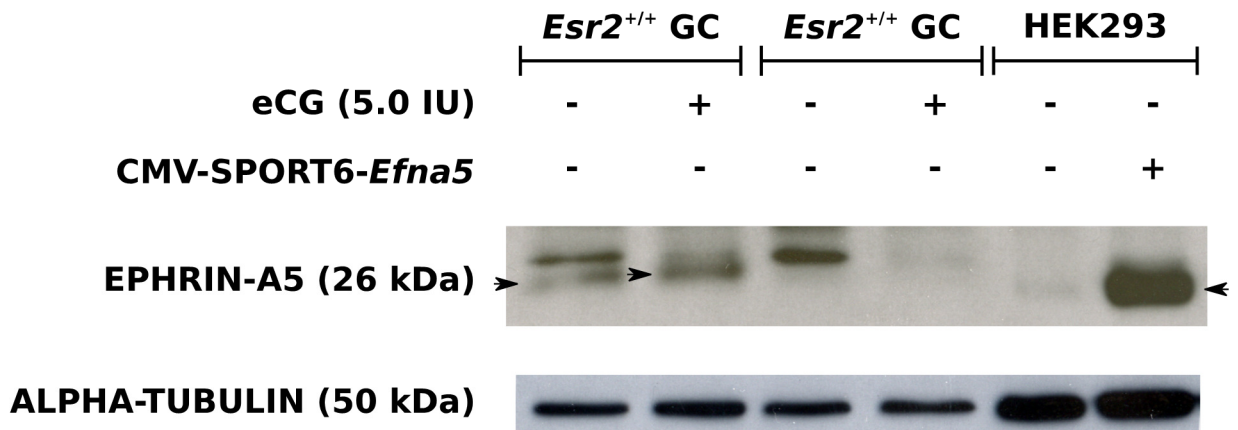
STAT1	0.70
p27 T157	0.65
p27 T198	0.63
STAT5a	0.31
beta-catenin	0.16

Supplemental Table 6-3: Phosphorylation of intracellular kinase targets in response to ephrinA5-Fc, 20 min post-seeding.

Target	Phosphorylation Ratio (ephrinA5-Fc / Fc)
p53 S46	1.35
p53	1.33
HSP27	1.29
Akt	1.23
Chk-2	1.19
CREB	1.16
TOR	1.15
Lyn	1.13
p53 S15	1.12
Fgr	1.11
Yes	1.09
RSK1/2	1.08
STAT1	1.07
MEK1/2	1.07
GSK-3alpha/beta	1.06
p70 S6 kinase	1.06
RSK1/2/3	1.05
STAT4	1.03
FAK	1.02
p27 T198	1.00
p70 S6 kinase T229	0.98
eNOS	0.97
p70 S6 kinase	0.95
Src	0.95
Pyk2	0.91
MSK1/2	0.90
STAT2	0.87
AMPKalpha2	0.83
c-Jun	0.82
PLCgamma-1	0.81
Fyn	0.80
Hck	0.77
p38alpha	0.76
Pan-Jnk	0.75
STAT6	0.64
STAT5a/b	0.59
Paxillin	0.59
STAT5a	0.58
p27 T157	0.58
Akt - S473	0.51

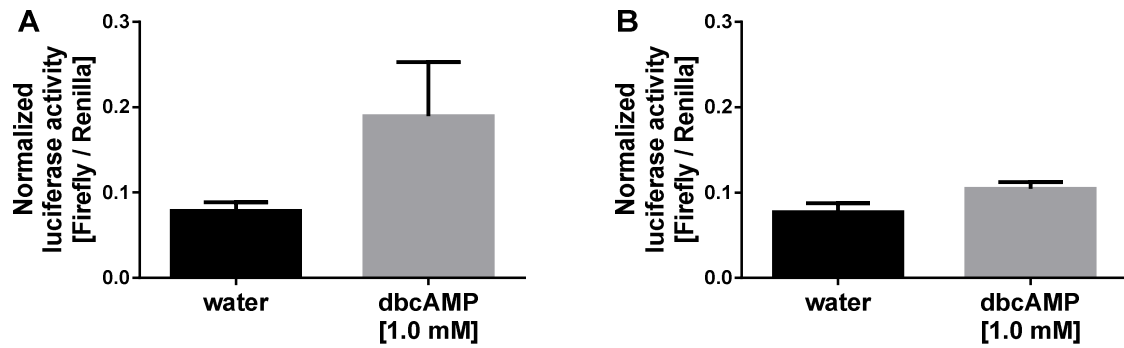
beta-catenin	0.51
AMPKalpha1	0.47
Lck	0.42
STAT5b	0.42
STAT3	0.31

6.2 Supplementary Material, Chapter 3



Supplemental Figure 6-4: EPHRIN-A5 protein levels are lower in granulosa cells of *Esr2*^{-/-} mice compared to *Esr2*^{+/+}.

Immunoblot detection of EPHRIN-A5 in *Esr2*^{+/+} and *Esr2*^{-/-} granulosa cells and in control HEK293 cells overexpressing EPHRINA5 (CMV-SPORT6-*Efna5*, black arrows). Equal protein loading for granulosa cell and HEK293 lysates was confirmed by detection of ALPHA-TUBULIN.



Supplemental Figure 6-5: Stimulation of KGN cells transfected with Epha5-Luc and mutEpha5-Luc with dibutyl cAMP.

Firefly luciferase activity normalized to *Renilla* luciferase activity (mean \pm SEM) was determined for water- and dbcAMP-treated KGN cells transfected with the Epha5-Luc (A) or mutEpha5-Luc (B) luciferase reporter constructs. A) No statistically significant difference was found between vehicle- and dbcAMP-treated KGN cells transfected with Epha5-Luc, as determined by an unpaired, two-tailed Student's unpaired t-test; $t(4)=1.725$. $p=0.1596$. B) No statistically significant difference was found between vehicle- and dbcAMP-treated KGN cells transfected with mutEpha5-Luc, as determined by an unpaired, two-tailed Student's t-test; $t(4)=2.088$. $p=0.1051$.

Curriculum Vitae

Adrian Buensuceso

Education

- 2008 – Present Ph.D. Candidate
Department of Biochemistry, The University of Western Ontario
London, ON
- 2004 – 2007 B.Sc. Biochemistry (Honours)
Department of Chemistry and Biochemistry, Concordia University
Montreal, QC
- 2000 – 2003 DEC Natural Science
John Abbott College
Sainte Anne de Bellevue, QC

Research Experience

- 05-12/2007 **Turnbull Lab, Department of Chemistry and Biochemistry, Concordia University**
Project Title: Investigating the role of His145 in the inhibition of CM-PD by L-tyrosine. Generated and purified a chorismate mutase-prephenate dehydrogenase point mutant to study a residue critical for negative feedback by L-tyrosine. Performed structural and kinetic characterization.
- 05-08/2006 **Phillips Lab, Department of Psychology, Concordia University**
Recruited study subjects and administered tests to investigate lexicon organization in monolingual and bilingual individuals.

01-04/2006

Titorenko Lab, Department of Biology, Concordia University.

Performed viability assays to investigate cellular senescence in a yeast model system. Performed general laboratory duties.

Publications

Rytelewski M, **Buensuceso A**, Leong HS, Deroo BJ, Chambers AF, Koropatnick J. (2015) Evaluating the effectiveness of cancer drug sensitization in vitro and in vivo. *J Vis Exp.* 6:96.

Rytelewski M, Tong JG, **Buensuceso A**, Leong HS, Maleki Vareki S, Figueredo R, Di Cresce C, Wu SY, Herbrich SM, Baggerly KA, Romanow L, Shepherd T, Deroo BJ, Sood AK, Chambers AF, Vincent M, Ferguson PJ, Koropatnick J. (2014) BRCA2 inhibition enhances cisplatin-mediated alterations in tumor cell proliferation, metabolism, and metastasis. *Mol Oncol.* 8:8.

Buensuceso AV and Deroo BJ. (2013) The Ephrin Signaling Pathway Regulates Morphology and Adhesion of Mouse Granulosa Cells In Vitro. *Biol Reprod.* 88:25.

Deroo BJ and **Buensuceso AV**. (2010) Minireview: Estrogen Receptor-(1): Mechanistic Insights from Recent Studies. *Mol Endocrinol.* 24:1703-14.

Submitted Manuscripts

Buensuceso AV, Son A, Paquet M, Withers BM, Zhou R, and Deroo BJ. (2015) Ephrin-A5 is required for optimal fertility and a complete ovulatory response to gonadotropins in the female mouse. Submitted to *Endocrinology*.

Selected Conference Presentations

Buensuceso AV and Deroo BJ. Oral presentation: Transcriptional regulation of *Eph* and *Efn* genes in granulosa cells and a potential role for *Efna5* in mouse ovarian development. *Society for the Study of Reproduction Annual Meeting*, Montreal, Quebec, July 22-26, 2013.

Buensuceso AV, Son A, Zhou R, and Deroo BJ. Poster: Loss of ephrin-A5 reduces fertility in female mice. *London Health Research Day*, London, ON, March, 2014.

Buensuceso AV and Deroo BJ. Poster: Ephrins: novel estrogen receptor beta transcriptional targets that influence morphology and adhesion in granulosa cells. *Paul Harding Research Day*, London, ON, April 27, 2011. Second prize in poster category (graduate students).

Buensuceso AV and Deroo BJ. Poster: Eph-ephrin signaling during folliculogenesis and its potential dysregulation in estrogen receptor β -null mice. *The Endocrine Society Annual Meeting*, San Diego, CA, June 19-22, 2010.

Buensuceso AV and Deroo BJ. Oral Presentation: Eph-ephrin signaling during folliculogenesis and its potential dysregulation in estrogen receptor β -null mice. *Paul Harding Research Day*, London, ON, May 19, 2010.

Buensuceso AV and Deroo BJ. Oral Presentation: Eph-ephrin signaling during folliculogenesis and its potential dysregulation in estrogen receptor β -null mice. *Southern Ontario Reproductive Biology Meeting*, Waterloo, ON, Canada. May 2009.